Tehnički institut / Technical Institute of Bijeljina

ZBORNIK RADOVA / BULLETIN OF
Godina / Year XV – No. 28.

DOI: 10.59456

ISSN 1840-4855
e-ISSN 2233-0046

A R H I V

ZA TEHNIČKE NAUKE

Archives for Technical Sciences

B i j e l j i n a 2023

Tehnički institut / Technical Institute of Bijeljina

ZBORNIK RADOVA / BULLETIN OF
Godina / Year XV – No. 28.

DOI: 10.59456

ISSN 1840-4855
e-ISSN 2233-0046

Founder and publisher:

Technical Institute of Bijeljina
Republic of Srpska - Bosnia and Herzegovina

Editor in Chief:

Academician Prof. Ph.D. Neđo Đurić
Academy of Sciences and Arts of the Republic of Srpska,
Bosnia and Herzegovina

Technical Editor:

Dr. sci. Dijana Đurić

Lector for English

School of Foreign Languages "Cerovac" Bijeljina

Address:

Technical Institute Bijeljina, Starine Novaka Street 25
76 300 Bijeljina
Republic of Srpska - Bosnia and Herzegovina
Tel./fax +387 (55) 203 – 022, 211 – 701
Mob: +38765511772
E. mail: tehnicki@tehnicki-institut.com
arhiv@arhivzatehnickenauke.com
nedjo@arhivzatehnickenauke.com
www.arhivzatehnickenauke.com

Press:

Mojić d.o.o. Bijeljina

Circulation:

300 copies

Tehnički institut / Technical Institute of Bijeljina

ZBORNIK RADOVA / BULLETIN OF
Godina / Year XV – No. 28.

DOI: 10.59456

ISSN 1840-4855
e-ISSN 2233-0046

Tehnički institut / Technical Institute of Bijeljina

ZBORNIK RADOVA / BULLETIN OF
Godina / Year XV – No. 28.

DOI: 10.59456

ISSN 1840-4855
e-ISSN 2233-0046

TABLE OF CONTENTS

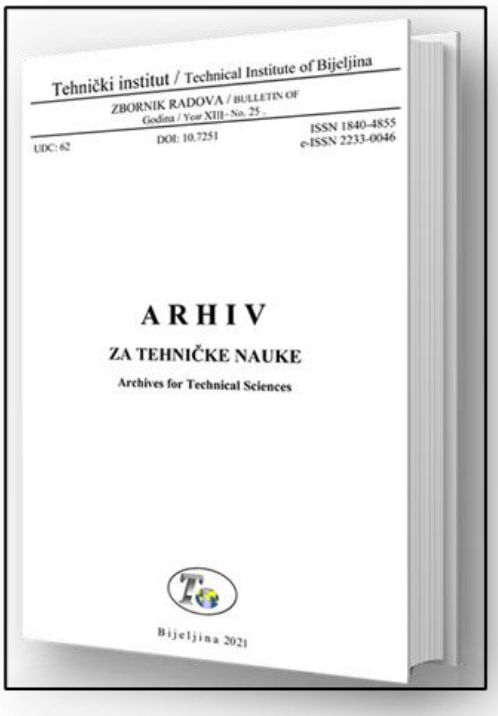

ENVIRONMENT

MINING

Methods of mining ore deposits

Editors

Prof. Ph.D. Božo Kolonja
Prof. Ph.D. Mirko Ivković

Review paper
http://dx.doi.org/10.59456/afts.2023.1528.001M

CHOICE OF EXCAVATION METHOD OF THE ORE DEPOSITS

Majstorović Slobodan[1], Tošić Dražana[1], Torbica Duško[1]

[1]*University of Banja Luka, Faculty of Mining Prijedor, slobodan.majstorović@rf.unibl.com*

ABSTRACT

The paper defines choice of the optimal excavation method for ore deposits, which are characterized by general irregularity due to their origin, occurrence and different content of the usable minerals. In such complex conditions, the choice of the excavation method is defined according to: the natural characteristics of the deposit and according to the techno - economic parameters of the comparison methods and the methods of multi-criteria optimization.

Keywords: *excavation method, natural characteristics, multicriteria optimization, AHP method*

INTRODUCTION

The choice of the optimal manner of excavating ore deposits is the most important phase when designing the future of underground mine. From the selected manner of excavation (methods of excavation) depend on [1]:

- the economic indicators of mine operation, (the cost of deposit exploitation is 60% of the total costs of the underground mine)
- work safety of employees and equipment
- use of certain mining mechanization

The choice of the excavation method of ore deposits is a complex and very responsible procedure when designing the underground exploitation of a deposit, and the selection process itself is done in two basic manners:

- the choice of the excavation method according to the natural characteristics of the deposit is a rational manner of choosing the excavation method
- optimal manner of choosing the method of excavation, which is done on the basis of technical and economic parameters by economic comparison of variants of excavation methods, i.e. by the method of multi-criteria optimization

CHOICE OF EXCAVATION METHOD ACCORDING TO THE NATURAL CHARACTERISTICS OF DEPOSIT

The choice of the excavation method for a certain non-layered (ore) mineral deposit is made according to certain mining and geological characteristics of that deposit, whereby these characteristics can be divided into two groups:

1. The basic or constant factors:
   - stability of the ore and the surrounding rock
   - capacity (thickness) of the ore body (deposits)
   - dip angle

2. The variable factors:
   - deposit size per strike and dip
   - ore body morphology
   - value of ore
   - the character of the useful minerals distribution in the ore body
   - tendency of ore to compaction (hardening), oxidation or self-ignition
   - the hydrogeological characteristics
   - the need to preserve the surface of the terrain above deposit

The basic or constant factors are taken into account in each case, while variable factors are taken as limitations in certain cases [2].

The stability of ores and surrounding rocks defines the possibility of applying excavation methods with gape excavated areas, methods with support or methods with caving [3]. Depending on the stability of the ore and surrounding rocks, the excavation method is chosen (Table 1), as well as the parameters of the roof control system that provide safe working conditions [4,5,6].

Table 1. Mining methods according to the stability of the ore and the surrounding rock

Stability combination of cases ores and surrounding rocks	The possible groups or subgroups of excavation methods.
Stable ore and surrounding rocks	All groups of excavation methods are acceptable, except for excavation methods with caving.
Stable ore and unstable surrounding rocks	From the group of excavation methods with backfilling, a subgroup of methods with the horizontal levels is acceptable, it is also possible to use the subgroups of excavation methods in sloped levels. Acceptable group of excavation methods with caving, except for block caving methods.
Unstable ore and stable surrounding rocks	Subgroups of excavation methods with support of excavation, then with support and backfilling of stopes are acceptable.
Unstable ore and souronding rocks	Subgroups of excavation methods with stope support are acceptable.

Table 2 gives the choice of the excavation method depending on the dip angle and the thickness (capacity) of the deposit.

Table 2. Excavation methods according to the capacity and dip angle

Possibility and dip angle of deposits	Methods with natural maintenance of open stope (open stope methods)	Methods with ore and surrounding rock caving	Methods with artificial support of stope (methods with support)
The deposits are steep	The chamber excavation system - at any thinkness. Shrinkage stoping where the thickness must not be less than 1 - 1.3 m to avoid ore bind.	Block caving methods for thick deposits. Sublevel caving methods at deposit thickness less than 3 m.	Excavation methods with backfilling in horizontal and inclined levels - at any deposit thickness. Self-filling methods of narrow deposit. Methods with support and backfilling at every deposit thickness.
The deposits with slightly slope	Frontal and room- pillar excavation methods at medium and low thickness. Chamber methods with ore shrinkage in more thick deposits.	Block caving methods in thick deposits. Methods with caving of thick deposits.	Methods of excavation horizontally and inclined with backfilling. Support methods. Methods with support and backfilling of stopes.

Table 3. presents systematized basic or constant factors and their influence for certain groups and subgroups of ore mining methods.

Table 3. Influential natural parameters on the choice of excavation method

Group	Subgroup		Layer thickness (m)	Dip angle (^{0})	Ore stability	Stability of hanging wall / floor
I AND OPEN EXCAVATION METHODS	1. Frontal excavation methods		1,5 – 4	$\leq 30^0$	stable	stable / stable
	2. Room and pillar methods		2 – 30	$\leq 45^0$	stable	stable / stable
	3. Sublevel caving methods		$\geq$30	$\geq 60^0$	stable	stable / stable
	4. Shrinkage stope methods		0,6 – 5	$\geq 60^0$	stable	stable / stable
II EXCAVATION METHODS WITH BUILDING	1. Excavation methods with backfilling of stopes	1.1. Roof excavations in horizontal levels	≥ 1	$\geq 60^0$	stable	any/ any
		1.2. Roof excavations in sloping levels	0,7 – 4	$\geq 60^0$	stable	stable / stable
		1.3. Self-backfilling excavation methods	0,1- 0,8	$\geq 60^0$	stable	any/ any
	2. Excavation method with substructure and backfilling of excavated areas	2.1. Excavation methods in horizontal levels	> 4	$\geq 50^0$	unstable	any/ any
		2.2. Excavation methods by square set	> 4	0 - 90^0	unstable	any/ any
	3. Excavation methods with subdivision of excavated areas	3.1. Excavation methods in horizontal levels	> 4	0 - 90^0	unstable	any
		3.2. Frontal excavation methods	> 3	$\leq 30^0$	unstable	moderately firm
		3.3. Excavation methods per dip of deposit	< 3	$\leq 45^0$	unstable	moderately firm
III METHODS OF EXCAVATION WITH CAVING	1. Excavation methods by the immediate roof caving		< 4	< 40^0	stable	moderately firm
	2. Excavation method by roof caving in the levels		> 3	≥ 45	stable	unstable/ unstable
	3. Sublevel caving methods		> 15	≥ 45	any	unstable/ unstable
	4. Excavation methods with block cutting		> 25	≥ 75	unstable	moderately firm

On the example of one deposit of irregular contours, with stable ore and unstable sides. The deposit has an average capacity of about 2 m, with dip angle of about 50° and a depth of about 300 m. The value of the ore in the deposit is average, and the distribution of useful minerals is uneven in such a way that the rich parts of the ore are mixed with the poor parts. Based on the known characteristics, Table 4. is compiled with a list of factors and their characteristics.

Table 4. Choice of the excavation method based on the natural characteristics of the deposit (Example)

Characteristic	Value	Possible method of excavation
Dip angle	50^0	I-3,4; II-1.1.,1.2.,1.3.,1.4. ,2,1.,2.2.,3.1, III-2,3,4
Deposit thickness	2 m	I-1,2,4;II-1.1,1.2,1.3,3.1,3.2;III-1,2
Strength 1. Ore 2. Surrounding rocks	 Stable Unstable	II-1.1,1.3;III-2,3
Deposit contours Contact of ore and surrounding rocks	Incorrect contour Clear contact	 I - III
Metal distribution in the deposit	Rich ore alternates with poor ore and waste	I – III with selective excavation
Disturbance of the terrain surface	No limit	I - III
Depth of exploitation	300 m	I - III

Table 4. shows that the following excavation methods are suitable for a specific ore deposit:

- Method of roof directional excavation with backfilling in horizontal levels
- Sub-level caving method
- Excavation methods with backfilling and backfilling in horizontal levels
- Excavation methods with supporting in the horizontal levels

The final decision on the choice of excavation method will be made by optimizing of the selected excavation methods, which can be done on the basis of technical and economic parameters by economic comparison of variants of the excavation methods or by the method of multi-criteria optimization [7,8,9].

CHOICE OF EXCAVATION METHOD BY MULTICRITERIA ANALYSIS

The method of analytical hierarchical processes (AHP) was developed by Thomas Saaty in the early 1970s and it represents one tool in decision analysis. The area of method application is multi-criteria decision, where based on the defined set of criteria and attribute values for each alternative, the most acceptable solution is selected, i.e. the complete schedule of the importance of the alternative in the model is shown. Four phases of application of the method can be distinguished [10]:

1) structuring the problem
2) data collection
3) estimation of the relative weights
4) determining the solution to the problem

Problem structuring consists of decomposing a certain complex decision problem into a series of hierarchies, where each level represents a smaller number of the managed attributes. A graphical representation of the structuring of the problem is presented in Figure 1.

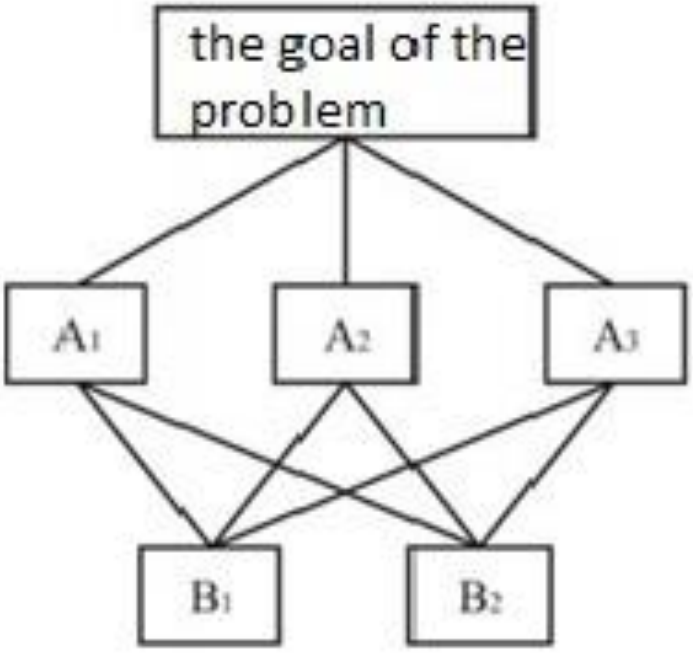

Figure 1. Structuring of the problem

By collecting data and measuring them, the second phase of the AHP method begins. The decision maker assigns the relative ratings to pairs of attributes of one hierarchical level, for all levels of the entire hierarchy. The Saaty scale of nine points, presented in Table 5, is used.

Table 5. Saaty scale

Impotance intensity	Definition	Explanation
1	Equally important	It is used when both factors act equally on the final result.
3	Somewhat more important	It is used when there is a small difference on the side of one factor in relation to another.
5	Much more important	It is used when one factor is much more important than another factor.
7	Significantly more important	It is used where one factor is significantly more important than another.
9	Absolutely more important	It is used in the case when one instance is absolutely more important than another instance, without any doubt.
2,4,6,8	Intermediate values	They are used when a compromise between two values is needed. That is, when it is difficult to decide between two odd intensities of importance.

At the end of this phase, an appropriate matrix of comparisons by pairs corresponding to each level of the hierarchy is obtained.

Estimation of relative weights is the third phase of application of the AHP method. The comparison matrix will be "translated" in pairs into problems of determining of own values, in order to obtain normalized and unique own vectors, as well as weights for all attributes at each level of the hierarchy $A_{1}, A_{2}, ..., A_{n}$, with the weight vector $m_{1}, m_{2}, ..., m_{n}$, [10].

Determining the solution of the problem is the last phase of the AHP method, and it involves finding the so-called composite normalized vector. Once the vector of the sequence of activity of the criteria in the model is determined, in the next round it is necessary, within each observed criterion, to determine the sequence of importance of the alternative in the model [11].

Finally, the overall synthesis of the problem is performed as follows: the participation of each alternative is multiplied by the weight of the certain criterion, and then these values are summed for each alternative separately. The obtained data represents the weight of the certain alternative in the model. In the same way, the weight is determined for all other alternatives, after which the final sequence of alternatives in the model can be determined.

The AHP method belongs to the group of popular methods, because it has the possibility of identifying and analyzing the consistency of the decision maker in the process of comparing elements from the hierarchy. Since the comparison of the alternative is based on a subjective assessment by the decision maker, it is necessary to constantly monitor it, in order to ensure the necessary accuracy [12]. The AHP method makes it possible to monitor the consistency of estimates at any time in the process of comparing the alternative pairs.

Using the consistency index:
$C.I. = (\lambda_{max} - n)/(n-1)$

the consistency ratio is calculated: $C.R. = \frac{C.I.}{R.I.}$

R.I.- random index (matrix consistency index of size *n* randomly generated pair comparisons).

Table 6. Random index value R.I.

n	1	2	3	4	5	6	7	8	9	10
R.I.	0	0	0,52	0,89	1,11	1,25	1,35	1,40	1,45	1,49

The coefficient λ_{max} is the maximum and main characteristic of the value of the comparison matrix, while *n* is the size of the comparison matrix. In this case, it is valid that $\lambda \geq n$, and the difference λ_{max} - *n* is used in measuring the consistency of the estimation. In case of inconsistency, if λ_{max} is closer to *n*,

the estimate is more consistent. If the comparison matrix is *C. R.* ≤ 0,10, estimates of the relative importance of the criteria (alternative priorities) are considered as acceptable. Otherwise, the reasons why the inconsistency of the assessment is unacceptably high need to be found.

The choice of the excavation method according to the natural characteristics of the deposit always precedes to the final choice, which means that in this way the variants of the excavation method are defined which according to the natural characteristics meet the set conditions [13]. For example, for the appropriate deposit the following excavation methods are selected that could be applied in Table 7.

Table 7. The variants of excavation methods selected according to the natural characteristics of the deposit

Serial number	Excavation method
1	Roof directional excavation method with backfilling in horizontal levels
2	Sublevel caving method
3	Methods of excavation with support and backfilling in horizontal levels
4	Excavation methods with support in horizontal levels

Attributes at the second level (decision criteria) are marked as follows (Table 8):

Table 8. Criteria for choice of excavation method

S.N.	Criterion	Mark
1	Value of excavated ore	$K_1 \rightarrow max$
2	Safety of excavation work	$K_2 \rightarrow max$
3	Processing coefficient (k_p)	$K_3 \rightarrow min$
4	Recovery of deposit (i)	$K_4 \rightarrow max$
5	Dilution of the obtained ore (r)	$K_5 \rightarrow min$
6	Production price of 1 t of ore (C_{pr})	$K_6 \rightarrow min$
7	Excavation effect (U_o)	$K_7 \rightarrow max$
8	Surface impact and other environmental impacts	$K_8 \rightarrow min$

Criteria such as coefficient of processing, recovery, dilution of ore, excavation effect for individual groups and subgroups of excavation methods of non-layered (ore) deposits are given in Table 9.

Table 9. Influential techno-economic parameters for the choice of the excavation method

Group	Subgroup		U_o t/shift	k_p m/1000 t	i %	r (%)	C_{pr} (€/t)
I OPEN STOPE METHODS	1. Frontal excavation methods		30 - 70	0,5 - 3	70 - 90	5 - 15	17,5 – 25
	2. Chamber-pillar methods		30 - 70	2- 14	60- 80	5 - 15	20 - 30
	3. Sublevel caving methods		60 - 90	3 - 16	80 - 95	5 - 15	18 - 25
	4. Shrinkage methods		25 - 40	2 - 17	75 - 90	3 - 15	25 - 32
II EXCAVATION METHODS WITH BUILDING	1. Excavation methods with backfilling of stopes	1.1. Roof excavations in horizontal levels	10 - 25	3 - 9	95 - 99	1 - 5	27 - 40
		1.2. Roof excavations in sloping levels	9 - 18	4 - 14	94 - 98	2 - 8	25 - 40
		1.3. Self-backfilling excavation methods	2 - 8	5 - 20	88 - 98	5 - 20	15 - 30
	2. Excavation method with support and backfilling of stopes	2.1. Methods of excavation in horizontal levels	5 - 20	2 - 12	85 - 95	5 - 15	20 - 40
		2.2. Methods of excavation by square set support	2 - 15	5 - 12	90 - 95	5 - 15	34 - 45
		3.1. Excavation methods	2 - 15	5 - 12	95 - 98	2 - 10	28 - 35

	3. Excavation methods with subdivision of excavated areas	in horizontal levels					
		3.2. Frontal excavation methods	4 - 15	5 - 12	90 - 95	5 - 15	25 - 35
		3.3. Excavation methods per dip of deposit	2 - 15	7 - 12	90 - 95	2 - 13	25 - 32
III METHODS WITH CAVING	1. Excavation methods by caving of the immediate hanging wall		10 - 20	3 - 8	85 - 95	2 - 15	15 - 28
	2. Excavation method by roof caving		15 - 35	4 - 6	95 - 98	1 - 8	12 - 30
	3. Sublevel caving methods		40 - 90	3 - 15	80 - 95	5 - 25	15 - 25
	4. Excavation methods with block cutting		5 - 130	2 - 10	75 - 95	10 - 25	15 - 30

The next step of the AHP method is pairwise comparison, Saaty's scale of relative importance is used when comparing in pairs.

Table 10. Comparison of attributes at the level of decision criteria

	K_1	K_2	K_3	K_4	K_5	K_6	K_7	K_8	Weights
K_1	1,000	3,000	4,000	3,000	5,000	2,000	7,000	8,000	0,2792
K_2	0,333	1,000	2,000	0,333	4,000	0,200	3,000	5,000	0,0967
K_3	0,250	0,500	1,000	0,333	4,000	0,166	3,000	5,000	0,0799
K_4	0,333	3,000	3,000	1,000	5,000	0,166	4,000	6,000	0,1417
K_5	0,200	0,250	0,250	0,200	1,000	0,143	0,500	3,000	0,0359
K_6	0,500	5,000	6,000	6,000	7,000	1,000	7,000	8,000	0,3016
K_7	0,143	0,333	0,333	0,250	2,000	0,143	1,000	4,000	0,0454
K_8	0,125	0,200	0,200	0,166	0,133	0,125	0,250	1,000	0,0195
Total	2,884	13,283	16,783	11,282	28,130	3,943	25,750	40,00	

$\square$ *=8,77 ;* $C.I. = \frac{\lambda_{max} - n}{n-1} = \frac{8,77-8}{7} = 0,11$; $C.R. = \frac{C.I.}{R.I.} = \frac{0,11}{1,4} = 0,079 < 0,10$

Analogous to the previous one, the attributes of the alternative level can be marked as follows (Table 11):

Table 11. Alternative level attributes

Roof directional excavation method with backfilling in horizontal levels	A_1
Excavation method with roof caving	A_2
Methods of excavation with support and backfilling in horizontal levels	A_3
Excavation methods with support in horizontal levels	A_4

The corresponding alternative comparison matrices for each criterion attribute and their priorities are shown in the following tables (12 – 19.).

Table 12. Matrices of relevant importance of the alternative in relation to attribute K_1 (Value of exc. ore)

	A_1	A_2	A_3	A_4	Weights
A_1	1,000	5,000	3,000	3,000	0,5050
A_2	0,200	1,000	0,500	0,333	0,0868
A_3	0,333	2,000	1,000	3,000	0,2441
A_4	0,333	3,000	0,333	1,000	0,1641
Σ	1,866	11,000	4,833	7,333	

$$\lambda = 4{,}25\ ;\ C.I. = \frac{\lambda_{max} - n}{n-1} = \frac{4{,}25-4}{3} = 0{,}084\ ;\ C.R. = \frac{C.I.}{R.I.} = \frac{0{,}084}{0{,}89} = 0{,}094 < 0{,}10$$

Table 13. Matrices of relevant importance of the alternative in relation to attribute K_2 (Work safety)

	A_1	A_2	A_3	A_4	Weights
A_1	1,000	7,000	3,000	5,000	0,5769
A_2	0,143	1,000	0,333	0,500	0,0716
A_3	0,333	3,000	1,000	3,000	0,2399
A_4	0,200	2,000	0,333	1,000	0,1125
Σ	1,676	13,000	4,666	9,500	

$$\lambda = 4{,}06\ ;\ C.I. = \frac{\lambda_{max} - n}{n-1} = \frac{4{,}06-4}{3} = 0{,}02\ ;\ C.R. = \frac{C.I.}{R.I.} = \frac{0{,}02}{0{,}89} = 0{,}022 < 0{,}10$$

Table 14. Matrices of relevant importance of the alternative in relation to attribute K_3 (Processing coefficient)

	A_1	A_2	A_3	A_4	Weights
A_1	1,000	5,000	3,000	2,000	0,4658
A_2	0,200	1,000	0,333	0,200	0,0691
A_3	0,333	3,000	1,000	0,500	0,1679
A_4	0,500	5,000	2,000	1,000	0,2973
Σ	2,033	14,000	6,333	3,700	

$$\lambda = 4{,}058\ ;\ C.I. = \frac{\lambda_{max} - n}{n-1} = \frac{4{,}058-4}{3} = 0{,}019\ ;\ C.R. = \frac{C.I.}{R.I.} = \frac{0{,}019}{0{,}89} = 0{,}022 < 0{,}10$$

Table 15. Matrices of relevant importance of the alternative in relation to attribute K_4 (Recovery of deposit)

	A_1	A_2	A_3	A_4	Weights
A_1	1,000	7,000	5,000	4,000	0,6256
A_2	0,143	1,000	0,200	0,333	0,0614
A_3	0,200	5,000	1,000	0,500	0,1659
A_4	0,250	3,000	2,000	1,000	0,1988
Σ	1,593	16,000	8,200	4,833	

$$\lambda = 4{,}236\ ;\ C.I. = \frac{\lambda_{max} - n}{n-1} = \frac{4{,}236-4}{3} = 0{,}079\ ;\ C.R. = \frac{C.I.}{R.I.} = \frac{0{,}079}{0{,}89} = 0{,}088 < 0{,}10$$

Table 16. Matrices of relevant importance of the alternative in relation to the attribute K_5 (Dilution of the obtained ore)

	A_1	A_2	A_3	A_4	Weights
A_1	1,000	0,143	0,333	0,200	0,0568
A_2	7,000	1,000	5,000	4,000	0,5917
A_3	3,000	0,200	1,000	0,500	0,1302
A_4	5,000	0,250	2,000	1,000	0,2212
Σ	16,000	1,593	8,333	5,700	

$$\lambda = 4{,}124\ ;\ C.I. = \frac{\lambda_{max} - n}{n-1} = \frac{4{,}124-4}{3} = 0{,}041;\ C.R. = \frac{C.I.}{R.I.} = \frac{0{,}041}{0{,}89} = 0{,}045 < 0{,}10$$

Table 17. Matrices of relevant importance of the alternative in relation to attribute K_6 (Production price of 1t of ore)

	A_1	A_2	A_3	A_4	Weights
A_1	1,000	5,000	3,000	2,000	0,4583
A_2	0,200	1,000	0,333	0,200	0,0691
A_3	0,333	3,000	1,000	2,000	0,2372
A_4	0,500	5,000	0,500	1,000	0,2247
Σ	2,033	14,000	4,833	5,200	

$$\lambda = 4{,}225 \; ; \; \text{C.I.} = \frac{\lambda_{max} - n}{n-1} = \frac{4{,}429 - 4}{3} = 0{,}074; \; \text{C.R.} = \frac{\text{C.I.}}{\text{R.I.}} = \frac{0{,}075}{0{,}89} = 0{,}081 < 0{,}10$$

Table 18. Matrices of relevant importance of the alternative in relation to attribute K_7 (Mining performance)

	A_1	A_2	A_3	A_4	Weights
A_1	1,000	0,200	3,000	3,000	0,2211
A_2	5,000	1,000	4,000	3,000	0,5479
A_3	0,333	0,250	1,000	2,000	0,1308
A_4	0,333	0,333	0,500	1,000	0,1004
Σ	6,666	1,783	8,500	9,000	

$$\lambda = 4{,}165 \; ; \; \text{C.I.} = \frac{\lambda_{max} - n}{n-1} = \frac{4{,}165 - 4}{3} = 0{,}055; \; \text{C.R.} = \frac{\text{C.I.}}{\text{R.I.}} = \frac{0{,}055}{0{,}89} = 0{,}062 < 0{,}10$$

Table 19. Matrices of relevant importance of the alternative in relation to the attribute K_8 (Impact to surface)

	A_1	A_2	A_3	A_4	Weights
A_1	1,000	0,250	2,000	3,000	0,2292
A_2	4,000	1,000	4,000	3,000	0,5101
A_3	0,500	0,250	1,000	0,333	0,0919
A_4	0,333	0,333	3,000	1,000	0,6752
Σ	5,833	1,833	10,000	7,333	

$$\lambda = 4{,}225 \; ; \; \text{C.I.} = \frac{\lambda_{max} - n}{n-1} = \frac{4{,}225 - 4}{3} = 0{,}075; \; \text{C.R.} = \frac{\text{C.I.}}{\text{R.I.}} = \frac{0{,}075}{0{,}89} = 0{,}084 < 0{,}10$$

At the end of the procedure, a synthesis of the problem of choosing the excavation method is performed, so that all alternatives are multiplied by the weights of individual decision criteria, and the obtained results are added, as shown in Table 20.

Table 20. Choice of the optimal alternative of the excavation method

Criterion	Weight criteria	A_1	Weight x A_1	A_2	Weight x A_2	A_3	Weight x A_3	A_4	Weight x A_4
K_1	0,2792	0,5050	0,1409	0,0868	0,0242	0,2441	0,0682	0,1641	0,0458
K_2	0,0967	0,5769	0,0558	0,0716	0,0069	0,2399	0,0232	0,1125	0,0109
K_3	0,0799	0,4658	0,0372	0,0691	0,0055	0,1679	0,0134	0,2973	0,0237
K_4	0,1417	0,6256	0,0886	0,0614	0,0087	0,1659	0,0235	0,1988	0,0282
K_5	0,0359	0,0568	0,0200	0,5917	0,0212	0,1302	0,0047	0,2212	0,0079
K_6	0,3016	0,4583	0,1382	0,0691	0,0208	0,2372	0,0715	0,2247	0,0678
K_7	0,0454	0,2211	0,0100	0,5479	0,0249	0,1308	0,0059	0,1004	0,0046
K_8	0,0195	0,2292	0,0044	0,5101	0,0099	0,0919	0,0018	0,6752	0,0132
			0,4774		0,1223		0,2122		0,2021

The alternative with the highest value is the most acceptable or optimal method of excavation for a specific ore deposit, which means that alternatives A1 - Method of roof directional excavation with backfilling in horizontal levels will be selected for exploitation of this deposit.

CONCLUSION

The paper presents the procedure for choice of the optimal excavation method of ore deposit through two basic phase:

1. The choice of the excavation method according to the natural characteristics of the deposit.
2. The choice of the excavation method by the procedure of multicriteria analysis from the group of possible excavation methods selected on the basis of natural characteristics.

The choice of the excavation method by the procedure of multicriteria analysis was performed by applying the AHP method in specific conditions of the ore deposit. One of the leading problems in the application of this method is the definition of decision-making attributes at the second level (decision-making criteria) and the assessment of their relevant weights. The authors defined the criteria and estimated the values of their relative weight based on their own experiences in previous scientific research.

Received May 2023, accepted May 2023)

REFERENCES

[1] Portsevsky, A.K. (2000). Underground mining of mineral deposits. Moskow.
[2] Portsevsky, A.K. (2016). Technology of excavation of minerals by underground means. Moskow.
[3] Shekhostov, V.S. (2011). Design of systems for the development of ore deposits. Novokuznetsk.
[4] Imenitov, V.R. (1984). Processes of underground mining in the devepopment of ore deposits. Nedra.
[5] Majstorović, S., Miljanović, J., Tošić, D. (2020). Methods of Underground Exploitation, University of Banja Luka, Faculty of Mining Prijedor.
[6] Torbica, D. (2020). Choice of optimal excavation methods on L-29C deposit in Undergound Mine Bešpelj Bauxite Mines Jajce by Multicriteria makind decision, University of Banja Luka, Faculty of Mining Prijedor.
[7] Ataei, M., Jamshidi, M., Sereshki, F., & Jalali, S.M.E. (2008). Mining method selection by AHP approach. Journal of the Southern African Institute of Mining and Metallurgy,108(12), 741-749.
[8] Jamshidi, M., Ataei, M., Sereshki, F., Jalali, S.M.E. (2009). The Application of AHP approach to selection of optimum underground mining method, Case study: JAJARM Bauxite Mine (IRAN), Arch. Min. Sci., Vol. 54 (2009), No 1, p. 103–117.
[9] Bogdanović, D., Nikolić, D., & Ilić, I. (2012). Mining method selection by integrated AHP and PROMETHEE method. Anais da Academia Brasileira de Ciências, 84(1), 219-233. http://dx.doi.org/10.1590/S0001-37652012005000013.
[10] Saaty, T.L. (1980). Analytic hierarchy process, planning, priority setting, resource allocation, McGraw-Hill, New York.
[11] Čupić, M., Suknović, M. (1995). Multicriteria decision – methods and examples, University Brothers Karić, Belgrade.
[12] Nikolić, I., Borović S., (1996). Multicriteria optimisation, methods, examples in logistics, software, Belgrade.
[13] Popović G., Đorđević B., Milanović D., (2019). Multiple Criteria Approach in the Mining Method Selection, Industrija, Vol.47, No.4. pp 47-62.

CONSTRUCTION

Construction infrastructure

Editors

Prof. Ph.D. Dragan Lukić
Prof. Ph.D. Miroslav Bešević

Original scientific article
http://dx.doi.org/10.59456/afts.2023.1528.011Y

CORRUPTION AND INFRASTRUCTURE DEVELOPMENT BASED ON STOCHASTIC ANALYSIS

Yanan Fan[1], Mohammad Heydari[2], Mahdiye Saeidi[3], Kin Keung Lai[4], Jiahui Yang[2], Xinyu Cai[2], Ying Chen[2]

[1]Faculty of Earth Sciences and Environmental Management, University of Wrocław, Wrocław, Poland
[2]Business College, Southwest University, Chongqing 400715, China, e-mail: MohammadHeydari1992@yahoo.com
[3]Payame Noor University, Department of Tehran West, Iran
[4]International Business School, Shaanxi Normal University, Xi'an 710062, China

SUMMARY

The effects of corruption in urban development and urban affairs management in several south Asian countries are examined through a series of specific, distinctive, and provocative cases for which the data is more readily available. The stories and themes provide a starting point for analyzing corruption as a symptom and factor of underdevelopment, affecting efforts to use and allocate scarce resources for a higher quality of life in cities. It shows how corruption stifles imaginative and creative solutions to urban challenges while increasing future revenue sources. 3Ps has provided a chance for the public section to look at various funding expertise and options from the business sector to prepare the public infrastructure.

On the other hand, governments in the source of budget limitations and other competing demands for state sources can't supply each citizenry's infrastructure. Besides, the private sector has been considered a better resource manager, and the government should concentrate on policymaking. Where P3s are put to fair use, the advantages are immense. Unfortunately, vulnerable to bribery.

This is the case; whatever benefits 3P offers in reducing the urban infrastructure deficit may be eroded due to corruption, which could lead to an increase in construction or facility costs.' rehabilitation. Secondly, a PPP process marred by corruption could lead to inferior construction substances. One of the fund's big chunks will be diverted to the public officials' bribing via the project company. Thirdly, a corrupt process could compromise officials' integrity that has been charged with accountability for inspecting and approving construction works.

Keywords: *Urban Infrastructure, Optimization, Private sector, Public-Private Partnerships (PPP), Public sector.*

INTRODUCTION

The symptom of crime is an (unaddressed) problem for city administrators, who are either helplessly confronted by various aspects of crime or are so entrenched in it that they are unlikely to become significant players in enacting effective anti-corruption laws. There is a call for more accountability. It is proposed that current corruption activities be converted into regularized payment service fees to honour good teamwork and decrease corruption's counter-productive developmental consequences.

The partnership among the public and private sections, so-called P3s, has some historical genealogy supplementing or restoring the *"traditional"* governmental accountability to supply and introduce standard economic interest services. Nonetheless, as with every type of private section partnership, P3s are instruments that present difficulties to public management [1]. This is all truer because *"with sweeping privatisation of public sector and other significant government roles, the ability and capacity of governments in public administration are seriously reduced"* [1]. Starting very differently in shaping and form, these cooperation models have to balance the private partner's managerial autonomy and democratic responsibility of the public section. They are characterised via horizontal connections and shared accountabilities [2,3]. They also epitomise that the cutting lines among the private and public spheres blur and have to be re-analyzed.

Overall, P3s are shaped to upraise potentials for a – qualitative and quantitative – development of public services due to increased managerial, technical, or financial efficiency [4]. Having an *"iconic condition around the world"* [5], they are usually viewed as a professional and sophisticated option for current urban infrastructure administration. This promise, also optimizm from P3 many times, advocates are required, did not fully realise. The reasons can be endogenous to the shape of a single project or more general exogenous elements in PPPs' execution procedure (as an instance, e.g., [6]). Numerous weaknesses could be noted here, as deal complexity requires long-run equity or issues associated with computing public section expenses [2].

Even if the 3P execution and implementation procedure seem to be comparable to contracts on other shapes of standard accountabilities among the private and the public section, there are essential distinctions, specifically considering contract duration and shape and the composition of players involved. PPPs' characteristics might make them specifically vulnerable to bribery, even if a fair number of contexts address the general monitor-impact of private section inclusion [7].

The paper's contribution to the ongoing argument on the utilize of P3s in addition to that is twofold. First, a problem more or less ignored via the proper context is analysed theoretically. Second, tackling the origins of immoral behaviour and bribery in P3s is more related. These instruments are utilized in developing nations whose legal order might shield P3s sufficiently towards corruption and improve nations, and these legal tools are not available in emerging markets. Hence, carving out the vulnerable points in 3P contracts might raise awareness considering this issue and enable DMs to install suitable monitor mechanisms, if required, on the project level.

P3s address innovative techniques utilized via the public section for agreement via the private section, which brings its capital and capability to deliver projects on time to the budget. In contrast, the public section retains the accountability to provide these services to the public to benefit the crowd and offer economic improvement and life quality development [8]. PPP projects' worldwide popularity is justified because P3s can effectively eschew the often-negative impacts of either exclusive on the one hand, public ownership and distribution services, or outright privatization. Additionally, P3s mix both entities' best: the public section via its regulatory acts and protection of the public interest; and the private section with its sources, technology, and management skills.

IMMORAL BEHAVIOUR AND BRIBERY AS GOVERNANCE ISSUES IN P3S

Immoral behaviour and corruption as governance issues in P3s regarding an extensive range of acts and measures that can be categorized as *"immoral Behaviour"* such as nepotism, or *"corruption"* in the literature of P3s, socio-economic, political, or more philosophical point of view on this title are of interest [9]. as the component element in the author's perspective, the – most clandestine – Using delegated authority for personal benefit, whether by government officials or others, stands out [10]. This fact is even more related as – in the literature of current institutional economics's economic theory– some principal-agent-connection exists in all assigned power cases. A principal who delegated authority and an agent who wielded it but couldn't move on it be managed via the principal characterise such a solution. This is right; although not all obligations breaches are the same, principal-agent issues can be considered immoral or corrupt.

The underlying presumption is societal agreement on the acceptable range of actions and a clear awareness of where authority or assigned power abuse begins Caiden, & Caiden, [9]; Von Arnim, Heiny and Ittner [10]. This concept encompasses a wide range of behaviors, regardless of whether or not the individual conduct is subject to prosecution in specific texts. While corruption is banned in most countries worldwide, prosecution schemes and attitudes toward immoral behavior varies significantly. As a result, even if unique conduct is socially acceptable – such as distorting the tendering process in favour of a business with whom a public official may be associated – it leads to the negative impacts of corruption.

According to principal-agent and contract theory, P3s are vulnerable to immoral behavior because of three classifications: the very incomplete and somewhat discretionarily decided to contract via high transaction expenses, the multi-step classifications of implementation and execution, and the underlying ones multi-level or life-cycle concept. This susceptibility can take the form of a variety of specialized routes for immoral behavior, exposing them to it more than other contractual arrangements or public-private collaborations [11,12]. These characteristics provide both reasons and opportunities for such behavior.

Individuals' decisions will be based on the incentive in a particular solution and the predicted expenses – including transaction expenses – and benefits from their decision, given that they have no implicit perspective on more or less moral behavior. As a result, immoral behavior can be described as an income function for both the *"bribe payer"* and the *"bribe."* The core concept is that the private sector has an incentive to bribe government officials (not vice versa). While the decision to collaborate through the private sector is political (pre-tender), management is in charge of the tendering and implementation process (ex-ante and ex-post to the project execution). As a result, in the vast majority of circumstances, the bribe's recipient will be the general public: During the pre-tendering phase, corruption may occur at the political level, with businesses attempting to persuade politicians to open up portions for P3s or, more concretely, to turn a single project into a 3P. When a private section aspires to join a freshly formed P3, the goal will be to reach the management level. The government apportioned the genuine cost of serving the market (which is usually a monopoly). The same principle applies to bribery throughout the project's execution phase or after it has been completed (in the literature of re-negotiations or agreements renewal).

P3S SELECTION IN THE URBAN INFRASTRUCTURE INVESTMENT PLANNING PROCEDURE

As mentioned earlier, the P3 procedure might be regarded as one of the more expansive public investment administration procedure branches. A project is simultaneously chosen as one of the potential PPPs, and after that, it follows a P3-specific procedure. Nonetheless, such branching may occur at various points in the public investment procedure. As an instance, this can be:

The following budgeting as one of the public investment projects, like the case in the Netherlands and Australia, the procurement options (e.g., PPPs) have been evaluated following a project approval and budgeting as one of the public investment projects. In the case of the subsequent implementation of the project as a PPP, the budget allocations would be adjusted analogously [13].

Following the project approval and appraisal as one of Chile’s public investments, each project underwent a cost-advantage evaluation through the National Planning Commission and met a specific social return rate for public investment. Moreover, the P3 projects have been taken from the above list.

Following a strategic or prefeasibility options analysis that has been done in the Republic of Korea, a potent P3 has been specified since a comprehensive project appraisal like cost-benefit analysis and or technical feasibility investigations. Notably, they are part of the PPP appraisal procedure. The same strategy has been observed in South Africa. The PPP has been implemented as a part of the initial need’s analysis and option evaluation of a potential public investment project.

MATERIALS AND METHODS

The urban project selection problem

The decision analysis and SCM studies have considerably attracted the Urban project selection problem. It is becoming one of the beneficial research topics for operational research and administrative science disciplines. For example, Ho et al. [14] assessed integrated and individual DM strategies thoroughly during 2000-2008 for aiding the urban project selection issue. Additionally, Chai et al. [15] provided a systematic assessment of literature based on the DMs methods that assisted the urban project selection between 2008 and 2012. It classified the above methods into three classes: mathematical programming, artificial intelligence, and (Multiple Criteria Decision-Making = MCDM).

It should be noted that the current project management demands the DMs for maintaining the strategic partnerships with some but reliable projects that efficiently decline the project expenses and enhance the competitive advantage [16]. Hence, both the common price factor and the promising urban project selection policy must rely on broader quantitative and qualitative criteria like delivery, quality, lead-time, and flexibility [17]. Finally, Dickson [18] specified 23 criteria that should be considered when the project manager identifies the urban project selection.

The urban project selection problem addressed in the present paper is presented here. Firstly, a set of candidate projects would be assessed in terms of criteria by engaging a group of experts. Notably, all experts prefer to order the criteria' importance. Therefore, all experts know the upper and lower bounds regarding the evaluation outputs for all projects in each criterion's deterministic values. Hence, an individual expert possibly produces interval evaluation values for measuring each project function. An (Interval project selection matrix = ISSM) is established to cover the project assessment and choice.

Moreover, various experts can create distinct intervals for specific projects. The interval formulation is triggered from the observation that different weight elicitation techniques in MCDM can produce different weights, even for an analogous issue. Thus, it has been assumed hard to reach the exact weights [19]. Analyzing a set of projects using interval values is essential in decision analysis. The present paper has aimed to develop an advanced procedure for resolving the (Stochastic multi-objective acceptability analysis = ISSM) mentioned above and providing a detailed rank of the candidate project s. Though most of the investigations on the multi-criteria urban project selection help guide the project manager to choose suitable projects effectively, it would be essential to know the impacts of interval values on the project assessment and choice. There is not enough information about such an attractive and critical topic as far as we are aware. The present study fills the above gap by shaping an Interval Urban project selection Matrix and utilizing the SMAA-2 to supply the candidate projects' holistic rank. Finally, this kind of investigation addresses the powerful incentives and guidelines for the managerial, policy-associated, and academic implications.

(Stochastic multi-objective acceptability analysis = SMAA) algorithm introduced by Lahdelma et al. [20] has been proposed as one of the methods seeking for aiding (Multiple-criteria decision-making = MCDM) with numerous experts or professionals in situations wherein there is limited or no weight information. Notably, the criteria values are uncertain, and it does not require the experts to explain their input data implicitly or exactly. Moreover, it supplies multiple meaningful and beneficial indices like adaptability indices for all alternatives that measure diverse input data, which give all other options the best-ranking position, confidence factor demonstrating the analysis reliability, and the central-weight that illustrates the preferences of an expert who supports an option. Consequently, Lahdelma & Salminen [19] extended SMAA by examining each rank and providing the holistic SMAA-2 evaluation to recognize suitable compromise alternatives. However, for those issues that have ordinal criteria information, Lahdelma et al. [21] developed one of the novel SMAA-O methods, and Durbach [22] presented an SMAA by gaining the functions (SMAA-A) for a discrete choice decision, which examines what combination(s) of the aspirations would be essential for making each alternative the prioritized one. Also, Lahdelma & Salminen [23] developed the cross-confidence elements according to the calculation of confidence elements for other options using others' central weights.

Moreover, Lahdelma & Salminen [24] combined the SMAA-2 and DEA methods to assess the multicriteria options. They also devised the SMAA-P technique in 2009, which combined the prospect theory's piece-wise linear difference functions with the SMAA method. Furthermore, Lahdelma et al. [25, 26] presented and compared the simulation and multi-variate Gaussian distribution techniques for treating dependency information and uncertainty of the SMAA-2 (Multiple-criteria decision analysis = MCDA) method. Consequently, Tervonen and Lahdelma [27] presented effective techniques for conducting computations via Monte Carlo simulation, analyzing complexity, and evaluating the presented algorithms' accuracy. In this regard, Corrente et al. [28] integrated the stochastic multicriteria acceptability analysis and (Preference ranking organization algorithm for enrichment evaluation = PROMETHEE) for exploring the parameters consistent with the preference information presented by a DM and Angilella et al. [29] as well as Angilella et al. [30] combined Choquet integral-preference algorithm with the stochastic multi-objective acceptability analysis algorithm for obtaining appropriate recommendations and Robust Ordinal Regression (ROR). Finally, Durbach and Calder [31] investigated literature wherein the DMs could not or do not wish assessment of the tradeoff information in SMAA accurately.

Besides the method development on SMAA, a lot of applied papers are found in related publications such as forest planning [31], facility location [21]., descriptive multi-attribute choice algorithm [32], elevator planning [33], estimating a satisficing model of choice [32], mutual funds' performance analysis [34-46], the project portfolio optimisation [47] as well as data envelopment analysis (DEA) aggregation of cross-efficiency [48].

A major share of the present is presented briefly here. We express an ISSM for describing the urban project selection problem wherein all experts have particular but uncertain evaluation outcomes on a set of candidate projects. Hence, this urban project selection problem with interval values has been considered one of the stochastic optimization problems [34-46]. Secondly, the SMAA-2 algorithm, concepts of the rank acceptability index, confidence factor, and central weight vector have been proposed. Thirdly, the SMAA-2 method has been applied for the urban project selection issue with interval data and proposed one of the candidate projects' holistic ranks [49-52]. Though experts in the field mainly explored the classical urban project selection problem, the present paper has dealt with a novel aspect and functional and academic values and significance.

HOW TO EXPLAIN THE PROBLEM?

The urban project selection issue investigated in the present paper is shaped. Hence, a set of I candidate projects is evaluated based on J criteria by engaging a committee of K experts. Each measure is supposed to be beneficial. We may take the transformation of reciprocal or negativity about the cost-type criteria. Therefore, a decision matrix $G_{IJ} = \left[x_{ij} \right]_{IJ}$ depicts the fundamental framework of the multicriteria urban project selection issue:

(1)

$$G_{IJ} = \begin{bmatrix} x_{11} & x_{12} & \dots & x_{1J} \\ x_{21} & x_{22} & \dots & x_{2J} \\ \vdots & \vdots & \vdots & \vdots \\ x_{I1} & x_{I2} & \dots & x_{IJ} \end{bmatrix}$$

here $x_{ij}, x_{ij} \in [0,1], i = 1,2,...,I,\ j = 1,2,...,J$ refer to each expert's exact values and thus have been normalized to eliminate the data's magnitude [52]. Moreover, the analysis score of a project is calculated through the weighted sum of the criteria measures concerning the above project, namely:

(2)

$$S_i = \sum_{j=1}^{J} x_{ij} w_{ij}, i = 1,2,...,I$$

So that w_{ij} represents the weights of a factor j related to the project i, and $\sum_{j=1}^{J} w_{ij} = 1, w_{ij} \geq 0$?

Therefore, each expert $k, k = 1, 2, ..., K$ has been realised via a particular preference on the criteria sequence. Hence, without losing generality, we consider that the criteria would be arranged in descending order of importance for a specific expert $k, k = 1, 2, ..., K$, namely $w_{i1}^k \geq w_{i2}^k \geq \cdots \geq w_{iJ}^k$. Thus, the sequence would change among various experts. As a result, a particular expert $k, k = 1, 2, ..., K$ can express this mathematical algorithm for aggregating the most desirable function for each project i :

(3)

$$\begin{aligned} & US_i^k = \max \sum_{j=1}^{J} x_{ij} w_{ij}^k \\ & \text{s.t. } w_{i1}^k \geq w_{i2}^k \geq \cdots \geq w_{iJ}^k, i = 1, 2, ..., I \\ & \sum_{j=1}^{J} w_{ij}^k = 1, w_{ij}^k \geq 0, i = 1, 2, ..., I, k = 1, 2, ..., K \end{aligned} .$$

Theorem 1.

An optimal score of the projects i obtained from a mathematical algorithm (3) equalled $\max_{j=1,2,...,J} \left\{ \frac{1}{j} \sum_{t=1}^{j} x_{it} \right\}$.

Proof. After denoting $v_{ij}^k = w_{ij}^k - w_{i(j+1)}^k \geq 0, j = 1, 2, ..., J-1, v_{iJ}^k = w_{iJ}^k \geq 0$, we obtain

(4)

$$\begin{aligned} \sum_{j=1}^{J} w_{ij}^k &= \left(w_{i1}^k - w_{i2}^k \right) + 2\left(w_{i2}^k - w_{i3}^k \right) + \cdots + \left(J-1 \right)\left(w_{i(J-1)}^k - w_{iJ}^k \right) + J\left(w_{iJ}^k \right) \\ &= v_{i1}^k + 2v_{i2}^k + \cdots + Jv_{iJ}^k \\ &= \sum_{j=1}^{J} jv_{ij}^k \\ &= 1. \end{aligned}$$

We also incorporate $\varphi_{ij}^k = \sum_{t=1}^{j} x_{it}$ and then have

(5)

$$\begin{aligned} \sum_{j=1}^{J} x_{ij} w_{ij}^k &= x_{i1} w_{i1}^k + x_{i2} w_{i2}^k + \cdots + x_{iJ} w_{iJ}^k \\ &= \left[\left(w_{i1}^k - w_{i2}^k \right) x_{i1} \right] + \left[\left(w_{i2}^k - w_{i3}^k \right)\left(x_{i1} + x_{i2} \right) \right] + \cdots + \\ &\quad \left[\left(w_{i(J-1)}^k - w_{iJ}^k \right)\left(x_{i1} + x_{i2} + \cdots + x_{i(J-1)} \right) \right] + \left[w_{iJ}^k \left(x_{i1} + x_{i2} + \cdots + x_{iJ} \right) \right] \\ &= v_{i1}^k \varphi_{i1}^k + v_{i2}^k \varphi_{i2}^k + \cdots + v_{iJ}^k \varphi_{iJ}^k \\ &= \sum_{j=1}^{J} v_{ij}^k \varphi_{ij}^k . \end{aligned}$$

Hence, mathematical algorithm (3) is the same as the explanation below [35]:

(6)

$$\begin{aligned} & US_i^k = \max \sum_{j=1}^{J} v_{ij}^k \varphi_{ij}^k \\ & \text{s.t.} \sum_{j=1}^{J} j v_{ij}^k = 1 \\ & v_{ij}^k \geq 0,\ j = 1,2,...,J \end{aligned}.$$

The twofold of (6) is

(7)

$$\begin{aligned} & \min z_i^k \\ & \text{s.t.} \quad z_i^k \geq \frac{1}{j} \varphi_{ij}^k \end{aligned}.$$

Moreover, the optimal objective value of (7) would be obtained when $z_i^k = \max\limits_{j=1,2,...,J} \left\{ \frac{1}{j} \varphi_{ij}^k \right\}$ the optimal, accurate value of (3) is for $US_i^k = \max\limits_{j=1,2,...,J} \left\{ \frac{1}{j} \sum_{t=1}^{j} x_{it} \right\}$. Therefore, it is the most desirable assessed value specified via an expert k for the project i with a decision matrix (1). Based on the recognized sequence of criteria supplied via a typical expert, algorithm (3) is understandable and easily applied [49-52]. It may be effectively solved without eliciting the weights' exact values.

Accordingly, considering the least favourable assessment scores via the expert k for the project i is crucial, and thus an analogous mathematical algorithm is given below:

(8)

$$\begin{aligned} & LS_i^k = \min \sum_{j=1}^{J} x_{ij} w_{ij}^k \\ & \text{s.t.} \ w_{i1}^k \geq w_{i2}^k \geq \cdots \geq w_{iJ}^k, i = 1,2,...,I \\ & \sum_{j=1}^{J} w_{ij}^k = 1, w_{ij}^k \geq 0, i = 1,2,...,I, k = 1,2,...,K \end{aligned}.$$

Theorem 2.

The optimum score of the projects i carried out from a mathematical algorithm (8) is $\min\limits_{j=1,2,...,J} \left\{ \frac{1}{j} \sum_{t=1}^{j} x_{it} \right\}$.

Regarding the strength of the obtained least and most favourable assessment scores for the project i via the expert k, we express an ISSM $\Omega_{IK} = \left(\left[LS_i^k, US_i^k \right] \right)_{IK}$ that describes the uncertain judgment of each expert on each project. Proper assessment of the project i by an expert k must lie in $\left[LS_i^k, US_i^k \right]$:

(9)

$$\Omega_{IK} = \begin{bmatrix} \left[LS_1^1, US_1^1 \right] & \left[LS_1^2, US_1^2 \right] & \cdots & \left[LS_1^K, US_1^K \right] \\ \left[LS_2^1, US_2^1 \right] & \left[LS_2^2, US_2^2 \right] & \cdots & \left[LS_2^K, US_2^K \right] \\ \vdots & \vdots & \vdots & \vdots \\ \left[LS_I^1, US_I^1 \right] & \left[LS_I^2, US_I^2 \right] & \cdots & \left[LS_I^K, US_I^K \right] \end{bmatrix}.$$

Be consistent with [36]; it is possible to view the derived ISSM as one of the stochastic MCDM issues. Therefore, we initiate the SMAA-2 algorithm reported via Lahdelma and Salminen [19] to efficiently solve the stochastic MCDM issues by presenting each alternative's holistic rank.

SMAA ANALYSIS

It is widely accepted that stochastic multi-objective acceptability analysis represents one of the families of methods for helping multiple-criteria decision-making with uncertain, inexact, or relatively missing input data. Therefore, the reasoning behind stochastic multicriteria acceptability analysis is discovering the weight space for describing the preferences, making all alternatives the most preferred choice, or granting a specific ranking place for a particular option. In this regard, Lahdelma et al. [20] initiated this topic and proposed the rank acceptability indices, confidence factor, and central weight vector for other options. Then, Lahdelma & Salminen [19] extended the initial stochastic multicriteria acceptability analysis by addressing each rank in the evaluation and provided more holistic SMAA-2 studies to recognize acceptable compromise alternatives graphically.

ISSM Analysis

According to the interval project selection matrix introduced in Section 4.1, a committee of K - experts possesses a set of I projects to be assessed and chosen. On the other hand, any expert-particular assessment values and weights are unknown. Therefore, it is assumed that it is possible to represent each expert evaluation's decision maker's preferences through a real value utility function $g(i,w), i=\{1,2,...,I\}$. The weight vector w quantifies the decision makers' subjective preferences within the experts' judgments. Uncertain evaluation of values from the experts on the project s are also expressed by the stochastic variables ξ_{ik} with the density function $f(\xi)$ or approximated in the space $X \subseteq \Re^{I\times K}$. Also, the unknown weight vector is represented by a weight distribution with the density function $f(w)$ in a set of possible weights illustrated in Eq. (10):

$$W = \left\{ w \subseteq \Re^{K} : \sum_{k=1}^{K} w_k = 1, w_k \geq 0 \right\}. \tag{10}$$

The total lack of the weight vector information is represented in the *"Bayesian"* spirit through a weight distribution that is consistent in W, i.e., $f(w) = \frac{1}{Vol(\mathrm{W})} = \frac{(K-1)!}{\sqrt{K}}$.

Therefore, the utility function would then be used for mapping the stochastic experts' evaluation values and weight distribution into the utility distribution $g(\xi_i, w)$.

We denote a ranking function representing each project rank as an integer from the best position (=1) to the worst rank (=I) that is:

$$rank\ (\xi_i, w) = 1 + \sum_{l} \rho(g(\xi_l, w) > g(\xi_i, w)), \tag{11}$$

where $\rho(\mathrm{true}) = 1$ and $\rho(\mathrm{false}) = 0$.

Notably, SMAA-2 relies on the evaluation of the sets of desirable rank weights $W_i^r(\xi)$ defined as

(12)

$$W_i^r(\xi) = \{w \in W : rank(\xi_i, w) = r\},$$

So that the weight $w \in W_i^r(\xi)$ guarantees that the alternative ξ_i reaches rank r.

Indexes

This sub-section presents multiple helpful indexes introduced via SMAA-2. The first is the (Rank acceptability indices = RAI), b_i^r illustrated as the expected volume of a set of desirable rank weights. Moreover, b_i^r measures different valuations granting the alternative ξ_i rank r that is computed by

(13)

$$b_i^r = \int_X f(\xi) \int_{W_i^r(\xi)} f(w) dw d\xi .$$

According to the above relation, the rank acceptability indices b_i^r have been considered to belong to the interval $[0,1]$. At the same time, $b_i^r = 0$ it denotes that the alternative ξ_i reaches rank r and $b_i^r = 1$ report that the option ξ_i constantly obtains the position r, neglecting the weights' impacts. Furthermore, it is possible to directly employ the rank acceptability indices in the multicriteria assessment of other options. However, for large scale problems, one of the iterative processes has been presented where analysis of *n* best ranks *(nbr)* acceptability is done at each interaction *n*:

(14)

$$a_i^n = \sum_{r=1}^{n} b_i^r .$$

nbr-acceptability a_i^n has been proposed to be one of the various preferences granting alternative ξ_i any of the *n-best* ranks. Therefore, the evaluation proceeds till one or more choices reach a sufficient majority of the weights.

It is possible to depict the weight space concerning *n* best-rank related to an alternative via the concept "central *nbr* weight vector" w_i^n :

(15)

$$w_i^n = \int_X f(\xi) \sum_{r=1}^{n} \int_{W_i^r(\xi)} f(w) w dw d\xi / a_i^n .$$

Concerning the weight distribution, the central *nbr*-weight vector has been considered the most acceptable single-vector representation to prefer a DM who assigns an alternative any rank from one to *n*.

The 3rd indices are the *nbr*-confidence element p_i^n, which is defined as the probability that the alternative reaches any rank from one to *n* in case of determination and computation of the central *nbr* weight vector through

(16)

$$p_i^n = \int_{\xi: rank(\xi_i, w_i^n)} f(\xi) d\xi .$$

The study reported by Lahdelma and Salminen [19] contains further information on the indices, and Tervonen and Lahdelma [27] presented a manual on the practical stochastic multicriteria acceptability analysis implementation.

HOLISTIC ANALYSIS FOR THE RANK ACCEPTABILITY

About the rank described above the strength of acceptability, the step below is the development of a complementary method, which combines RAI into (Holistic acceptability indices = HAI) related to each alternative:

(17)

$$a_i^h = \sum_{r=1}^{I} \alpha^r b_i^r ,$$

Here α^r represent the meta weights for making the HAI and satisfying $1 = \alpha^1 \geq \alpha^2 \geq \cdots \geq \alpha^I \geq 0$?

Eliciting the so-called meta-weights has been considered crucial for a weight determination process of the lexicographic Model (of Brand Evaluation) decision problem that acceptably allocates the most massive value to α^1 and the last one to α^I. Like assignment of the weights to the ranks, Barron & Barrett [50] introduced three mechanisms called the reciprocal of the ranks strategy; that is $\alpha^r(RR) = \frac{1/r}{\sum_{r=1}^{I} 1/r}, r = 1,2,...,I$, (Rank-order centroid = ROC) algorithm; that is, $\alpha^r(ROC) = \frac{1}{I}\sum_{r=1}^{I}\frac{1}{r}, r = 1,2,...,I$ and rank-sum way; that is, $\alpha^r(RS) = \frac{2(I+1-r)}{I(I+1)}, r = 1,2,...,I$.

Therefore, it is possible to apply rank-order centroid for determining $\alpha^r, r = 1,2,...,I$ because of their higher effectiveness, accuracy, and understandability, indicating one of the suitable implementation tools [43].

As seen, holistic evaluation of the rank acceptability index would result in an overall measure of acceptability of each alternative that would help rank and arrange the options effectively.

NUMERICAL EXAMPLE

For applying the SMAA-2 algorithm for solving the ISSM, we draw the data from the numerous criteria urban project selection problems studied via Heydari, et al. [39]. Therefore, three criteria called quality, service, and price are rated using the 3-point scale, i.e., 1, 2, and 3, reflecting low, middle, and high for the price criterion, and good, middle, and inadequate for the requirements of service and quality. Hence, our problem is selecting five among 14 candidate projects that contain a committee of 6 experts.

All experts enjoy a particular preference on the criteria significance, i.e., price-quality $\succ$ service, price $\succ$ service $\succ$ quality, quality $\succ$ price $\succ$ service, quality $\succ$ service $\succ$ price, service $\succ$ price $\succ$ quality, and service $\succ$ quality $\succ$ price that are respectively represented via notations “1”, “2”, “3”, “4”, “5” and “6” (See table 1).

Table 1. Data on ISSM

Project	Price	Quality	Service	Price (Norm)	Quality (Norm)	Service (Norm)
1	2	1	1	0.0600	0.0370	0.0400
2	3	1	1	0.0400	0.0370	0.0400
3	1	2	2	0.1200	0.0741	0.0800
4	2	2	2	0.0600	0.0741	0.0800
5	3	2	1	0.0400	0.0741	0.0400
6	1	2	3	0.1200	0.0741	0.1200

7	1	3	1	0.1200	0.1111	0.0400
8	1	1	3	0.1200	0.0370	0.1200
9	2	2	1	0.0600	0.0741	0.0400
10	2	2	3	0.0600	0.0741	0.1200
11	3	3	1	0.0400	0.1111	0.0400
12	3	2	2	0.0400	0.0741	0.0800
13	2	3	1	0.0600	0.1111	0.0400
14	2	1	3	0.0600	0.0370	0.1200

Source: Zhang, et al. [31]

The ISSM $\Omega_{IK} = \left(\left[LS_i^k, US_i^k \right] \right)_{IK}$ has been gained utilizing Eqs. (3) and (8), where table 2 shows the results of each expert's interval analysis for each project.

Table 2. Interval urban project selection matrix.

Project	Expert					
	1	2	3	4	5	6
1	[0.0457,0.0600]	[0.0457,0.0600]	[0.0370,0.0485]	[0.0370,0.0457]	[0.0400,0.0500]	[0.0385,0.0457]
2	[0.0385,0.0400]	[0.0390,0.0400]	[0.0370,0.0390]	[0.0370,0.0390]	[0.0390,0.0400]	[0.0385,0.0400]
3	[0.0914,0.1200]	[0.0914,0.1200]	[0.0741,0.0970]	[0.0741,0.0914]	[0.0800,0.1000]	[0.0770,0.0914]
4	[0.0600,0.0714]	[0.0600,0.0714]	[0.0670,0.0741]	[0.0714,0.0770]	[0.0700,0.0800]	[0.0714,0.0800]
5	[0.0400,0.0570]	[0.0400,0.0514]	[0.0514,0.0741]	[0.0514,0.0741]	[0.0400,0.0514]	[0.0400,0.0570]
6	[0.0970,0.1200]	[0.1047,0.1200]	[0.0741,0.1047]	[0.0741,0.1047]	[0.1047,0.1200]	[0.0970,0.1200]
7	[0.0904,0.1200]	[0.0800,0.1200]	[0.0904,0.1156]	[0.0756,0.1111]	[0.0400,0.0904]	[0.0400,0.0904]
8	[0.0785,0.1200]	[0.0923,0.1200]	[0.0370,0.0923]	[0.0370,0.0923]	[0.0923,0.1200]	[0.0785,0.1200]
9	[0.0580,0.0670]	[0.0500,0.0600]	[0.0580,0.0741]	[0.0570,0.0741]	[0.0400,0.0580]	[0.0400,0.0580]
10	[0.0600,0.0847]	[0.0600,0.0900]	[0.0637,0.0847]	[0.0741,0.0970]	[0.0847,0.1200]	[0.0847,0.1200]
11	[0.0400,0.0756]	[0.0400,0.0637]	[0.0637,0.1111]	[0.0637,0.1111]	[0.0400,0.0637]	[0.0400,0.0756]
12	[0.0400,0.0647]	[0.0400,0.0647]	[0.0570,0.0741]	[0.0647,0.0770]	[0.0600,0.0800]	[0.0647,0.0800]
13	[0.0600,0.0856]	[0.0500,0.0704]	[0.0704,0.1111]	[0.0704,0.1111]	[0.0400,0.0704]	[0.0400,0.0756]
14	[0.0485,0.0723]	[0.0600,0.0900]	[0.0370,0.0723]	[0.0370,0.0785]	[0.0723,0.1200]	[0.0723,0.1200]

Source: Zhang, et al. [31]

Consequently, meta-weights for the formulation of the holistic acceptability indexes include:

$$\alpha^{12} = \left(1.00, 0.69, 0.54, 0.44, 0.36, 0.30, 0.25, 0.20, 0.16, 0.13, 0.10, 0.07, 0.05, 0.02\right). \quad (18)$$

As a result, using the open-source software described by Heydari, et al., [42], it is possible to solve the SMAA-2 model efficiently.

NORMAL DISTRIBUTION

It has been assumed that interval data $\left[LS_i^k, US_i^k \right]$ have a normal distribution. Their variance and mean are introduced $\mu_i^k = \frac{LS_i^k + US_i^k}{2}$ $\left(\sigma^2\right)_i^k = \frac{US_i^k - LS_i^k}{6}$

Table 3 and Figure 1 present outputs obtained for rank acceptability and holistic acceptability indexes extracted from the SMAA-2 method.

Table 3. Normal distribution of holistic acceptability index and rank acceptability indices

Project	b^1	b^2	b^3	b^4	b^5	b^6	b^7	b^8	b^9	b^{10}	b^{11}	b^{12}	b^{13}	b^{14}	a^h
1	0.00	0.00	0.00	0.00	0.00	0.00	0.00	0.00	0.00	0.00	0.00	0.01	0.15	0.64	0.0307
2	0.01	0.01	0.00	0.01	0.02	0.03	0.03	0.02	0.04	0.04	0.08	0.17	0.23	0.30	0.0960
3	0.00	0.25	0.46	0.23	0.05	0.00	0.00	0.00	0.00	0.00	0.00	0.00	0.00	0.00	0.5392
4	0.00	0.00	0.00	0.00	0.00	0.09	0.07	0.08	0.07	0.00	0.00	0.00	0.00	0.00	0.2311
5	0.00	0.00	0.00	0.00	0.00	0.00	0.00	0.00	0.00	0.00	0.04	0.05	0.07	0.03	0.0607
6	0.91	0.08	0.01	0.00	0.00	0.00	0.00	0.00	0.00	0.00	0.00	0.00	0.00	0.00	0.9708
7	0.00	0.02	0.01	0.01	0.02	0.01	0.00	0.00	0.00	0.00	0.00	0.00	0.00	0.00	0.5128
8	0.07	0.04	0.06	0.06	0.01	0.02	0.03	0.01	0.00	0.00	0.00	0.00	0.00	0.00	0.5038
9	0.03	0.04	0.08	0.06	0.07	0.06	0.05	0.02	0.01	0.00	0.00	0.00	0.00	0.00	0.0962
10	0.00	0.01	0.01	0.02	0.03	0.00	0.00	0.00	0.00	0.00	0.00	0.00	0.00	0.00	0.4833
11	0.02	0.07	0.07	0.06	0.01	0.09	0.01	0.00	0.00	0.00	0.00	0.00	0.00	0.00	0.1793
12	0.00	0.00	0.00	0.01	0.03	0.08	0.03	0.02	0.02	0.09	0.00	0.01	0.00	0.00	0.1468
13	0.00	0.00	0.00	0.00	0.00	0.00	0.01	0.03	0.01	0.09	0.04	0.03	0.00	0.00	0.2634
14	0.01	0.00	0.01	0.05	0.09	0.08	0.04	0.00	0.06	0.06	0.01	0.00	0.00	0.00	0.2420

Source: Zhang, et al. [31]

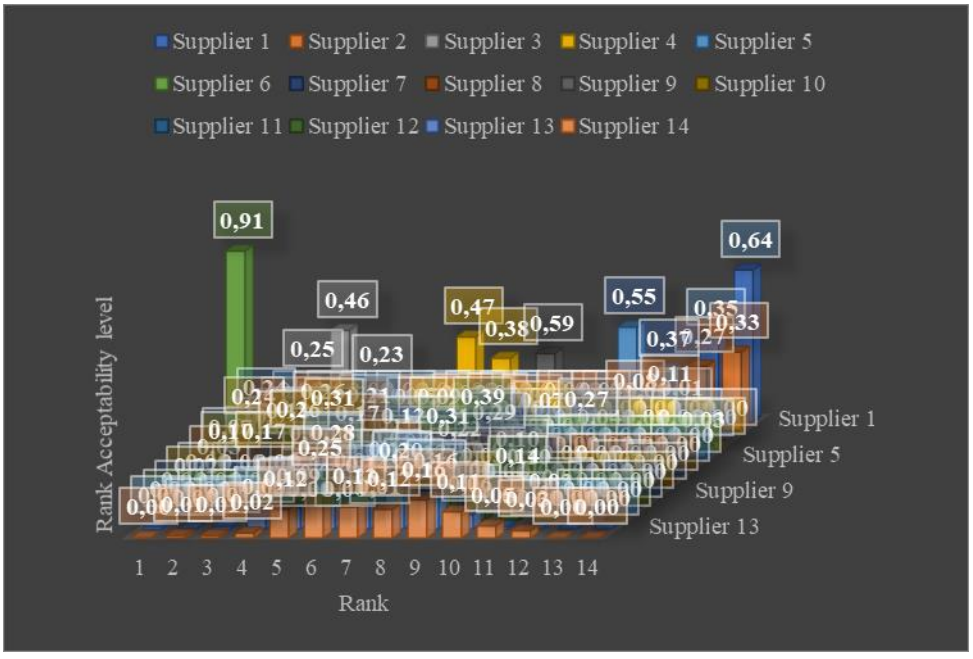

Figure 1. Normal distribution of rank acceptability index. Source: Zhang, et al. [31].

As shown by the HAI in Table 3, a detailed rank of each project s: $6 \succ 3 \succ 7 \succ 8 \succ 10 \succ 13 \succ 14 \succ 4 \succ 11 \succ 12 \succ 9 \succ 2 \succ 5 \succ 1$ has been obtained. Therefore, the chosen project is 6, 3, 7, 8, and 10; the most desirable project is project 6, with an HAI of 97.08% and the first rank support of 91% of possibility. In contrast, the minimum profitable project is 1, the holistic rank indices, and finally, the last-rank support is 3.07 and 64% of potential.

EQUITABLE DISTRIBUTION

Consider that interval data have a uniform distribution. Based on the mentioned assumption, HAI and RAI are presented in Figure 2 and Table 4.

Table 4. Equitable distribution of HAI, RAI

Project	b^1	b^2	b^3	b^4	b^5	b^6	b^7	b^8	b^9	b^{10}	b^{11}	b^{12}	b^{13}	b^{14}	a^h
1	0.00	0.00	0.00	0.00	0.00	0.00	0.00	0.00	0.00	0.00	0.00	0.03	0.55	0.41	0.0362
2	0.01	0.00	0.00	0.00	0.01	0.01	0.01	0.01	0.02	0.02	0.04	0.07	0.36	0.47	0.0587
3	0.02	0.03	0.06	0.06	0.01	0.02	0.00	0.00	0.00	0.00	0.00	0.00	0.00	0.00	0.5321
4	0.00	0.00	0.00	0.00	0.01	0.06	0.03	0.02	0.08	0.01	0.00	0.00	0.00	0.00	0.2365
5	0.00	0.00	0.00	0.00	0.00	0.00	0.00	0.00	0.00	0.03	0.04	0.01	0.00	0.02	0.0708
6	0.82	0.13	0.04	0.01	0.00	0.00	0.00	0.00	0.00	0.00	0.00	0.00	0.00	0.00	0.9359
7	0.01	0.01	0.01	0.01	0.01	0.01	0.00	0.00	0.00	0.00	0.00	0.00	0.00	0.00	0.5103
8	0.00	0.09	0.07	0.06	0.07	0.02	0.04	0.03	0.02	0.01	0.00	0.00	0.00	0.00	0.4813
9	0.03	0.03	0.09	0.00	0.05	0.08	0.05	0.03	0.02	0.01	0.01	0.01	0.00	0.00	0.1023
10	0.00	0.00	0.00	0.00	0.00	0.00	0.00	0.01	0.06	0.07	0.05	0.09	0.01	0.00	0.4715
11	0.02	0.07	0.08	0.04	0.08	0.09	0.02	0.00	0.00	0.00	0.00	0.00	0.00	0.00	0.1997
12	0.00	0.01	0.01	0.02	0.05	0.00	0.02	0.04	0.09	0.04	0.09	0.02	0.00	0.00	0.1595
13	0.00	0.00	0.00	0.00	0.00	0.01	0.05	0.08	0.04	0.01	0.00	0.02	0.00	0.00	0.2682
14	0.01	0.01	0.03	0.06	0.01	0.02	0.06	0.06	0.04	0.00	0.01	0.00	0.00	0.00	0.2497

Source: Zhang, et al. [31]

According to the figure, the sequence of the candidate projects using the SMAA-2 method based on the uniform distribution includes: $6 \succ 3 \succ 7 \succ 8 \succ 10 \succ 13 \succ 14 \succ 4 \succ 11 \succ 12 \succ 9 \succ 5 \succ 2 \succ 1$, and thus the chosen project s project s 6, 3, 7, 8, and 10, too. The above sequence has a minor difference from the one obtained from the normal distribution. Therefore, there is just one difference related to the rank solutions of projects 2, 5. However, the most profitable project 6's holistic rank indices have been 93.59% in detail. The first rank support equalled 82% of possibility, so that the two are lower than the average distribution. The last rank support and HAI the least favourable supplier 1 equalled 41% and 3.62%.

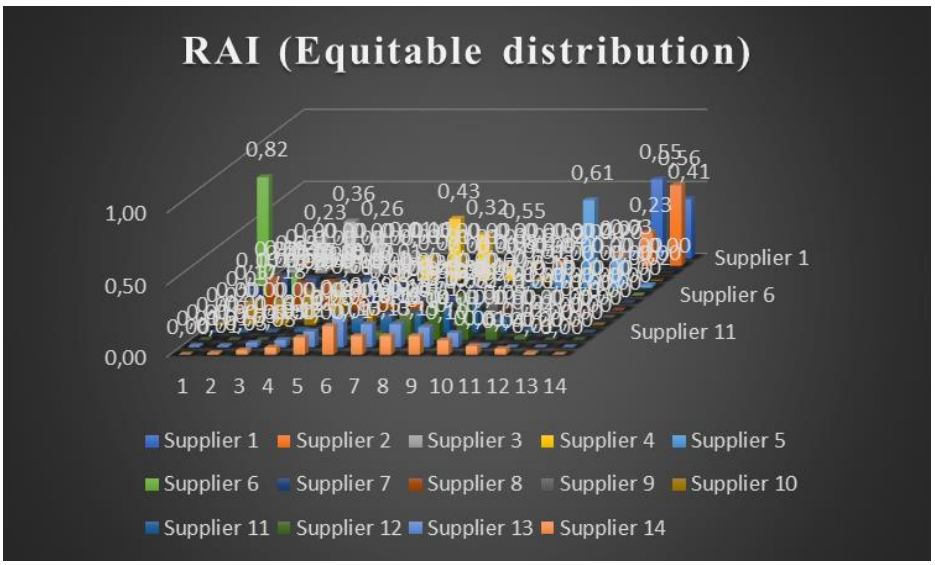

Figure 2. RAI (Equitable distribution). Source: Zhang, et al. [31]

It could be concluded that based on regular and uniform distribution assumptions, SMAA-2 possibly produces complete ranks with adequate discrimination power amongst each alternative. All experts have uncertain evaluations throughout the projects.

The multicriteria urban project selection problem in cooperating with a group of professionals is an issue that has been addressed mainly in the publications of supply chain management and decision science. Various professionals can present uncertain evaluation outputs for each project about the exact input data. Nonetheless, there is not enough information on this issue in the publications. Therefore, the present research dealt with this tremendous surge via initialising the interval values to optimise and innovative application of the SMAA-2 algorithm to catch the candidate project's overall rank.

Hence, it has been supposed that interval data are normally or smoothly distributed in the research. One of the meta-weight schemes for deriving the holistic rank indices has been elicitation from earlier studies. Finally, we re-examined one of the numerical examples from the current research to show our approach efficiency.

Therefore, this part of the research provided the DMs with more fantastic methodological choices and enriched the urban project selection problem's method and theory. Hence, additional investigations must determine unknown sets for DMs and investigate more function distributions over uncertainty.

CONCLUSION

Multicriteria urban project selection problem with A panel of experts has been broadly discovered in decision science and SCM context. Different experts might create uncertain assessment results for all projects given certain input data. However, the extant context has largely gone unnoticed on this subject.

This paper gets involved in this massive upsurge by first optimizing the interval values and then applying the SMAA-2 method in a novel way to catch an overall rank overall candidate project s. In this study, the interval data are assumed to be distributed normally or uniformly. A metal weight design to derive holistic rank indexes is obtained from the previous context.

A numerical instance for the current research was re-examined to denote the efficiency of the utilized algorithm. According to the gateways outlined above, PPPs' implementation might be impacted via governance issues, either forecasted ex-ante or ex-post. First, the project's overall effectiveness is on

the line, at least once bribery occurs: the likely increase in expense efficiency of P3s – which is debatable because it is nearly impossible to evaluate ex-ante – when compared to traditional public provision, must not be offset by the costs of corruption [47]. As previously stated, increased transaction costs or a worse value for the project's money may be the result and a far lower possibility of a project being managed more efficiently as a 3P than through public procurement. This would supply the expected advantages from P3s and cause enhanced expenses compared to the current situation.

Second, and related to the first point, competition may be distorted: if the private sector effectively suppresses the market system through unethical actions, it becomes a price maker rather than a price taker, akin to the classic monopoly solution, even if it cannot exist in a competitive environment [54]. As a result, bribery exists. This is a specific sort of adverse selection in which an inefficient bidder becomes the competitive, winning bidder. In the case of the 3P shape data, inefficiencies can lead to increased expenses for the government (where payments are fixed) or non-optimal rates for customers (e.g., in all concession algorithms) and insufficient service provision.

Finally, nepotism or corruption in the public sector has the disadvantage of *"weak interest"* in the public section [41]: as with P3s, current principal-agent issues can be reshaped in the sense that – due to asymmetric data and financial leeway – political or public interest becomes less important than the business interests of oligopolistic market actors. As a result, biased P3s projects monopolise semi-open market solutions [54].

This problem is exacerbated because the public section is only constrained by political considerations and public legislation, which do not apply to the private section. In certain circumstances, responsibility in the traditional sense is not given; yet, the public interest may suffer as a result. Nonetheless, P3s have become a critical tool for the public sector to finance and administer much-needed urban infrastructure and services over the last few decades.

Independent of the potential benefits of these collaborations, unique challenges may arise that risk their long-term success and make them less appealing – in terms of effectiveness and performance – than the current scenario. Immoral behavior and corruption may be among the most difficult aspects of the paper, but they are only tangentially mentioned. Several aspects may be identified to aid in controlling these governance challenges, the most important of which is the appropriate mix of controlling and penalties [52-54].

They focus on the external dimension, which increases the chances of exposure, rather than the project-specific measurement of direct expenses and incomes. In this literature, increased transparency is critical, regardless of whether it is imposed due to legal framework changes or public attention. This holds at both the administrative and political levels. Ex-ante and ex-post audits, particular whistle-blower programs or job rotations, and the general utility of the *"four-eyes principle"* could all help reduce corruption by reducing *"discretion of arrangements authorities by making greater use of centrally recognized rules on contracts"* [12].

If such a practice is uncovered, both in terms of fines and incarceration, increasing the costs of specific, undesirable behavior through harsher penalties (for both public and private participants) has a similar effect. Furthermore, payment strategies for public management are discussed in this literature: If in the general area, life-long career mechanisms are no longer in place or securing life-long employment for an individual in a particular position becomes unlikely, the risk of bribery will be far higher than it is now. Overall, the P3 method's unique sensitivity to corrupt activities might be considered inherent and so difficult to eliminate. Suggested strategies to limit the risk of immoral behavior in P3 implementation can never eliminate it, but they can increase the expenses and diminish the benefits; however, reduce it in the long run, starting with adjusting the parameters of individuals DM [27-32, 54-62]. This paper provides the decision-maker with more methodological options and adds to the theory and method of the urban project selection problem. In future research, the designation of uncertain sets for decision-making will be considered and more practical distributions across the uncertainty.

(Received August 2022, accepted September 2022)

REFERENCES

[1] Farazmand, A. (1999). Globalization and public administration. Public administration review, 509-522.
[2] Hodge, G. (2006, December). Public private partnerships and legitimacy. In University of New South Wales Law Journal Forum (Vol. 12, No. 2, pp. 43-48).
[3] Mörth, U. (2009). The market turn in EU governance—the emergence of public–private collaboration. Governance, 22(1), 99-120.
[4] Kwak, Y. H., Chih, Y., & Ibbs, C. W. (2009). Towards a comprehensive understanding of public private partnerships for infrastructure development. California management review, 51(2), 51-78.
[5] Hodge, G., & Greve, C. (2010). Public-private partnerships: governance scheme or language game? Australian journal of public administration, 69, S8-S22.
[6] Hodge, G. A., & Greve, C. (2007). Public–private partnerships: an international performance review. Public administration review, 67(3), 545-558.
[7] Sclar, E. (2001). You don't always get what you pay for: The economics of privatization. Cornell University Press.
[8] Baizakov, S. (2008). Guidebook on promoting good governance in public-private partnership.
[9] Caiden, G. E., & Caiden, N. J. (2018). Administrative corruption. In Classics of administrative ethics (pp. 177-190). Routledge.
[10] Von Arnim, H. H., Heiny, R., & Ittner, S. (2006). Korruption. Begriff, Bekämpfungs-und Forschungslücken.
[11] Anderson, M. B., Petrie, M., Alier, M. M., Cangiano, M. M., & Hemming, M. R. (2006). Public-private partnerships, government guarantees, and fiscal risk. International Monetary Fund.
[12] Iossa, E., & Martimort, D. (2014). Corruption in Public-Private Partnerships, Incentives and Contract Incompleteness. CESifo DICE Report, 12(3), 14-16.
[13] Alkan, R. M., Erol, S., Ozulu, I. M., & Ilci, V. (2020). Accuracy comparison of post-processed PPP and real-time absolute positioning techniques. Geomatics, Natural Hazards and Risk, 11(1), 178-190.
[14] Ho, W., Xu, X., & Dey, P. K. (2010). Multi-criteria decision making approaches for supplier evaluation and selection: A literature review. European Journal of operational research, 202(1), 16-24.
[15] Chai, J., Liu, J. N., & Ngai, E. W. (2013). Application of decision-making techniques in supplier selection: A systematic review of literature. Expert systems with applications, 40(10), 3872-3885.
[16] Ghodsypour, S. H., & O'brien, C. (2001). The total cost of logistics in supplier selection, under conditions of multiple sourcing, multiple criteria and capacity constraint. International journal of production economics, 73(1), 15-27.
[17] Chen, C. T., Lin, C. T., & Huang, S. F. (2006). A fuzzy approach for supplier evaluation and selection in supply chain management. International journal of production economics, 102(2), 289-301.
[18] Dickson, G. W. (1966). An analysis of vendor selection systems and decisions. Journal of purchasing, 2(1), 5-17.
[19] Lahdelma, R., & Salminen, P. (2001). SMAA-2: Stochastic multicriteria acceptability analysis for group decision making. Operations research, 49(3), 444-454.
[20] Lahdelma, R., Hokkanen, J., & Salminen, P. (1998). SMAA-stochastic multi-objective acceptability analysis. European Journal of Operational Research, 106(1), 137-143.
[21] Lahdelma, R., Salminen, P., & Hokkanen, J. (2002). Locating a waste treatment facility by using stochastic multicriteria acceptability analysis with ordinal criteria. European Journal of Operational Research, 142(2), 345-356.
[22] Durbach, I. (2006). A simulation-based test of stochastic multicriteria acceptability analysis using achievement functions. European Journal of Operational Research, 170(3), 923-934.
[23] Lahdelma, R., & Salminen, P. (2006a). Classifying efficient alternatives in SMAA using cross confidence factors. European Journal of Operational Research, 170(1), 228-240.
[24] Lahdelma, R., & Salminen, P. (2006b). Stochastic multicriteria acceptability analysis using the data envelopment model. European journal of operational research, 170(1), 241-252.
[25] Lahdelma, R., Makkonen, S., & Salminen, P. (2006). Multivariate Gaussian criteria in SMAA. European Journal of Operational Research, 170(3), 957-970.
[26] Lahdelma, R., Makkonen, S., & Salminen, P. (2009). Two ways to handle dependent uncertainties in multi-criteria decision problems. Omega, 37(1), 79-92.
[27] Tervonen, T., & Lahdelma, R. (2007). Implementing stochastic multicriteria acceptability analysis. European Journal of Operational Research, 178(2), 500-513.
[28] Corrente, S., Figueira, J. R., & Greco, S. (2014). The smaa-promethee method. European Journal of Operational Research, 239(2), 514-522.

[29] Angilella, S., Corrente, S., & Greco, S. (2015). Stochastic multi-objective acceptability analysis for the Choquet integral preference model and the scale construction problem. European Journal of Operational Research, 240(1), 172-182.
[30] Angilella, S., Corrente, S., Greco, S., & Słowiński, R. (2016). Robust Ordinal Regression and Stochastic Multi-objective Acceptability Analysis in multiple criteria hierarchy process for the Choquet integral preference model. Omega, 63, 154-169.
[31] Zhang, Q., Lai, K. K., & Yen, J. (2019). Multicriteria supplier selection using acceptability analysis. Advances in Mechanical Engineering, 11(10), 1687814019883716.
[32] Durbach, I. (2009). On the estimation of a satisficing model of choice using stochastic multicriteria acceptability analysis. Omega, 37(3), 497-509.
[33] Tervonen, T., & Figueira, J. R. (2008). A survey on stochastic multicriteria acceptability analysis methods. Journal of Multi-Criteria Decision Analysis, 15(1-2), 1-14.
[34] Babalos, V., Philippas, N., Doumpos, M., & Zopounidis, C. (2012). Mutual funds performance appraisal using stochastic multicriteria acceptability analysis. Applied Mathematics and Computation, 218(9), 5693-5703.
[35] Xiaohu, Z., Heydari, M., Lai, K. K., & Yuxi, Z. (2020). Analysis and modeling of corruption among entrepreneurs. REICE: Revista Electrónica de Investigación en Ciencias Económicas, 8(16), 262-311.
[36] Heydari, M. D., & Lai, K. K. (2019). The Effect Employee Commitment on Service Performance through a Mediating Function of Organizational Citizenship Behaviour Using Servqual and Collaborative Filtering Modeling: Evidence From China's Hospitality Industry. J. Tour. Hosp, 8, 2167-0269.
[37] Heydari, M., Lai, K. K., & Xiaohu, Z. (2020). Risk Management in Public-Private Partnerships. Routledge.
[38] Heydari, M., Lai, K. K., & Xiaohu, Z. (2021). Corruption, Infrastructure Management and Public–Private Partnership: Optimizing through Mathematical Models. Routledge.
[39] Heydari, M., Xiaohu, Z., Keung, L. K., & Shang, Y. (2020). Entrepreneurial intentions and behaviour as the creation of business: based on the theory of planned behaviour extension evidence from Polish universities and entrepreneurs. Propósitos y representaciones, 8(2), 46.
[40] Heydari, M., Xiaohu, Z., Lai, K. K., & Wang, S. B. (2019). Social-Psychology and Situational Elements Affecting Individual Social Behavior. J Hotel Bus Manage, 8(196), 2169-0286.
[41] Heydari, M., Xiaohu, Z., Lai, K. K., & Yuxi, Z. (2020). EVALUATION OF ORGANIZATIONAL PERFORMANCE STRATEGIES. Proceedings of National Aviation University, 82(1).
[42] Heydari, M., Xiaohu, Z., Lai, K. K., & Yuxi, Z. (2021). How Might Entrepreneurial Activities Affect Behaviour and Emotions?. Proceedings of the National Aviation University, 87(2), 65-77.
[43] Heydari, M., Xiaohu, Z., Saeidi, M., Lai, K. K., & Yuxi, Z. (2020). Entrepreneurship Process As The Creation Of Business By Engaging Family Members: Based On The Perceived Emotion. REICE: Revista Electrónica de Investigación en Ciencias Económicas, 8(15), 210-241.
[44] Heydari, M., Xiaohu, Z., Saeidi, M., Lai, K. K., & Yuxi, Z. (2020). Entrepreneurial Cognition and effect on Neuro entrepreneurship. Gelpat Caderno Suplementar, 3.
[45] Heydari, M., Xiaohu, Z., Saeidi, M., Lai, K. K., Shang, Y., & Yuxi, Z. (2020). Analysis of the role of social support-cognitive psychology and emotional process approach. European Journal of Translational Myology, 30(3).
[46] Heydari, Mohammad. (2021). "A Cognitive Basis Perceived Corruption and Attitudes Towards Entrepreneurial Intention." PhD diss. Nanjing University of Science and Technology, Nanjing, Jiangsu, China.
[47] Yang, F., Song, S., Huang, W., & Xia, Q. (2015). SMAA-PO: project portfolio optimization problems based on stochastic multicriteriasz acceptability analysis. Annals of Operations Research, 233(1), 535-547.
[48] Yang, F., Ang, S., Xia, Q., & Yang, C. (2012). Ranking DMUs by using interval DEA cross efficiency matrix with acceptability analysis. European Journal of Operational Research, 223(2), 483-488.
[49] Ng, W. L. (2008). An efficient and simple model for multiple criteria supplier selection problem. European journal of operational research, 186(3), 1059-1067.
[50] Barron, F. H., & Barrett, B. E. (1996). Decision quality using ranked attribute weights. Management science, 42(11), 1515-1523.
[51] Xia, W., & Wu, Z. (2007). Supplier selection with multiple criteria in volume discount environments. Omega, 35(5), 494-504.
[52] Tervonen, T. (2014). JSMAA: open source software for SMAA computations. International Journal of Systems Science, 45(1), 69-81.
[53] Durbach, I. N., & Calder, J. M. (2016). Modelling uncertainty in stochastic multicriteria acceptability analysis. Omega, 64, 13-23.
[54] Priddat, B. P. (2005). Schwarze Löcher der Verantwortung: Korruption—Die negative Variante von Public-Private Partnership. In Korruption (pp. 85-101). VS Verlag für Sozialwissenschaften.

[55] Becker, G. S., & Stigler, G. J. (1974). Law enforcement, malfeasance, and compensation of enforcers. The Journal of Legal Studies, 3(1), 1-18.
[56] Durbach, I. N. (2009). The use of the SMAA acceptability index in descriptive decision analysis. European Journal of Operational Research, 196(3), 1229-1237.
[57] Flyvbjerg, B., Holm, M. S., & Buhl, S. (2002). Underestimating costs in public works projects: Error or lie?. Journal of the American planning association, 68(3), 279-295.
[58] Kangas, A. S., Kangas, J., Lahdelma, R., & Salminen, P. (2006). Using SMAA-2 method with dependent uncertainties for strategic forest planning. Forest policy and economics, 9(2), 113-125.
[59] Peirson, G., & McBride, P. (1996). Public/private sector infrastructure arrangements. CPA communique, 73, 1-4.
[60] Sack, D. (2004). Public Private Partnership im „aktivierenden Staat ". In vhw Forum Wohneigentum. Zeitschrift für Wohneigentum in der Stadtentwicklung und Immobilienwirtschaft. Berlin (pp. 285-288).
[61] Schomaker, R. M. (2020). Conceptualizing corruption in public private partnerships. Public Organization Review, 20(4), 807-820.
[62] Sze, B. W. P., Lai, K. K., & Fu, Y. (2016). Project Selection via Stochastic Multi-criteria Acceptability Analysis, Asia Pacific Industrial Engineering and Management Systems Conference (APIEMS-2016).

Original scientific article
http://dx.doi.org/10.59456/afts.2023.1528.029B

CONVERGENCE PROBLEMS WITH ANSYS'S SOLID 65 FINITE ELEMENT IN CONCRETE-FILLED TUBULAR (CFT) COLUMNS AS A CASE STUDY

Barghlame Hadi[1]

[1]*Department of Civil engineering, Ilkhchi Branch, Islamic Azad University, Ilkhchi, Iran*
e.mail, hadi.barghlame@iauil.ac.ir

ABSTRACT

Using limited materials for numerical modeling of structural samples and comparing the behavior of samples with each other in order to reduce the number of straw test samples in order to reduce laboratory costs is one of the best methods today. ANSYS is one of the finite element software that is used for modeling reinforced concrete elements by Solid65 element. As a case study, a concrete-filled steel column under cyclic loading is examined and the best value for the Crushed Stiffness Factor (CSTIF) parameter that is one of Solid65 element parameters is suggested to confirm the modeling. By investigating the results, it can be concluded that this parameter is one of the most important factors that plays a significant role in convergence in ANSYS software for modeling CFT columns.
.

Keywords: *Convergence problem, ANSYS, SOLID65, Crushed Stiffness Factor, CDTIF, concrete-filled steel column, cyclic loading*

INTRODUCTION

In order to compare the modeling results of samples with different Crushed Stiffness Factors (CSTIF) and to choose a appropriate coefficient to match the results of laboratory test samples with numerical samples, this study should be done on a reinforced concrete member as a case study. Since concrete-filled steel columns have been used especially in tall buildings, bridges and special and important structures in recent years due to many advantages which includes suitable ductility and strength with less volume and weight compared to common reinforced concrete columns, , this case study has been done on CFT columns.

In order to numerical modeling of the CFT columns in ANSYS software, many studies have been done. Abedi et al. in 2008 presented a new section by using internal longitudinal symmetric stiffeners in the inner part of the steel wall of the circular and octagonal columns. This new section has led to an increase in the strength and ductility of the section under axial and seismic loading [1]. Hsiao et al. in 2015, Wang et al. in 2016 and Aghdamy et al. in 2017 by examining the cross-section of a tubular steel column with two layers of internal and external steel walls (with a circular cross-section) that were filled with concrete.

By loading these columns under the effect of constant axial load and seismic load, they concluded that by using the internal steel wall in addition to the external steel wall, it is possible to increase the resistance of the section against applied loads [2,3 and 4]. Zhou and Wenchao in 2016 by examining the double-skin steel wall section with a circular inner steel wall inside the section with a rectangular

outer steel wall under axial and seismic loading found that the use of this new section increased ductility and strength [5]. Hassaneina et al. in 2018 and Vernardos and Gantes in 2019 compared and investigated the types of double- skin steel walled sections with the combination of rectangular and circular steel walls, both in the form of external walls and in the form of internal walls, under lateral loading [6,7]. Zheng et al. in 2018 investigated the sections of two concrete-filled tubular steel columns.

They have investigated the effect of strength of core concrete and the influence of the slenderness factor on the ultimate strength of the column. In this research, the results have shown that double-skin concrete-filled steel columns with slenderness factor greater than 60 have had a lower lateral load capacity [8]. Chen et al. in 2019 have investigated the CFT columns with octagonal section of steel wall and concluded that this section has a high-energy absorption capability [9]. In 2019, Wang et al. studied the seismic behavior of a square concrete-filled steel tube (CFT) column when subjected to cyclic stress. Nine large-scale square CFT columns were studied, each with a distinct shear stud configuration and axial compressive load ratio constructed according to engineering practice requirements.

The damage mechanism, force-displacement relationship, deformation capacity, stiffness degradation, and energy dissipation capability of these specimens were all reviewed. The axial compressive load ratio has a considerable influence on the hysteresis loops of the square CFT columns, according to test data. In specimens with a low axial compressive load ratio, the shear stud significantly improves local buckling of the steel tube [10]. In a cyclic loading test of six full-sized square columns, including one traditional reinforced concrete (RC) column and five steel tube-reinforced concrete (STRC) composite columns, Zhang et al. in 2019 investigated the cyclic behavior of steel tube-reinforced, high-strength concrete columns with high-strength steel bars.

The test's main characteristics were the cross-sectional form of the inner steel tube, the strength matching of the outer concrete and the concrete core, and the presence of steel fiber in the outer concrete. The addition of steel fibers to concrete matrix can improve the tensile behavior and hinder cracking of concrete, thereby reducing the damage of concrete. Besides, it can slow down the slope of descending branch on the compressive stress-strain curves of concrete. In comparison to RC columns, steel fiber reinforced high-strength STRC composite columns showed improved seismic performance, according to the study. Steel fibers in exterior concrete successfully decreased the degree of damage and increased the specimens' ductility, robust ability, and energy dissipation capacity [11].

Wang et al. tested six stiffed CFDST beam-columns under continuous axial load and cyclic lateral load in the year 2020. The axial load level and the hollow section ratio were the main test parameters. All specimens' load, deformation, and strain were measured and studied. In terms of lateral resistance, ultimate displacement, ductility, and energy dissipation ability, the effect of parameters was addressed. They discovered that under cyclic stress, the stiffened specimens had a good energy dissipation capability. Additionally, the longitudinal stiffeners might significantly decrease local tube wall buckling. Stiffened CFDST members have stronger ductility and energy dissipation capability than unstiffened CFDST members [12].

In this study, a concrete-filled steel column is tested under seismic loading and compared with the results of numerical modeling with different Crushed Stiffness Factor (CSTIF) under the same loading conditions. The purpose of this research is to find the best value for the Crushed Stiffness Factor (CSTIF) factor to match the numerical modeling results with the experimental results.

SECTION FOR CONCRETE-FILLED STEEL COLUMN AS A CASE STUDY

The cross section of the column that we want to examine is shown in Figure 1. The steel wall have an inner diameter of 0.254 m and a thickness of 0.008 m, while the columns have a length of 2 meters. As a result, the diameter of outer steel wall is 0.27 m.

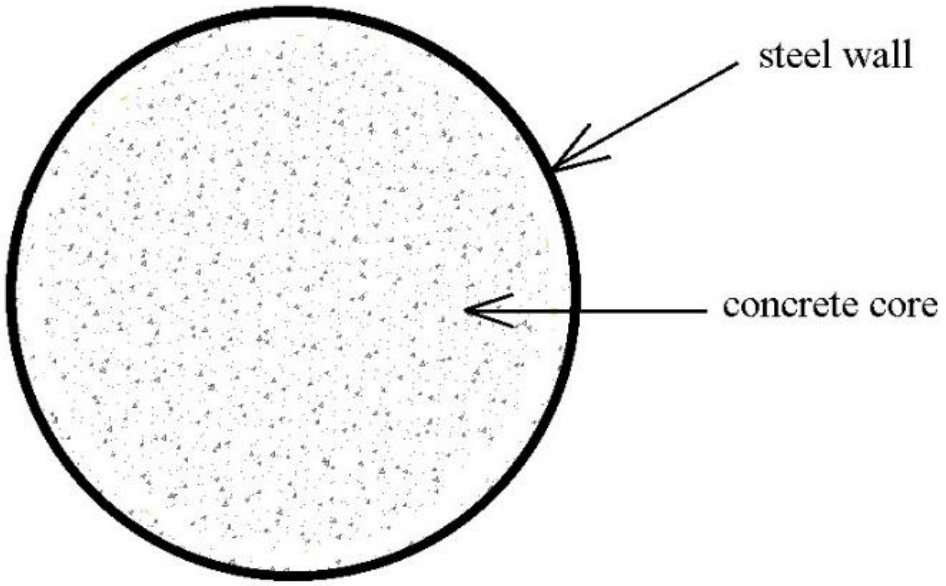

Figure 1. Proposed section of CFT with internal steel mesh located in nearby steel wall

FINITE ELEMENT MODELING OF CFT COLUMN

ANSYS finite element software has been used to model concrete-filled steel column. Furthermore, SOLID65 three-dimensional element has been used to model core concrete. This element is defined by a hexagon, eight nodes with three translational degrees of freedom in each node.

This solid element may fracture under tension and crush in compression, as well as deform plastically and creep. Moreover, SOLID 45 element has been used to model the steel wall. This element is compatible with the steel wall's shell element and the concrete core's isoperimetric solid element.

Plasticity, stress stiffening, large deflection, and huge strain capacities are all features of this element. The shape and coordinates of the nodes in the element coordinate system are shown in Figure 2 [13]. With the assumption of the cleanness of the steel and sufficient adhesion of the core concrete to the steel (perfect bond with no slip assumption), the coincident nodes of the steel and the core concrete can be connected to each other by merging [15]. In this research, no contact element was used and assumed a perfect bond by merging the coincide nodes of steel and core concrete.

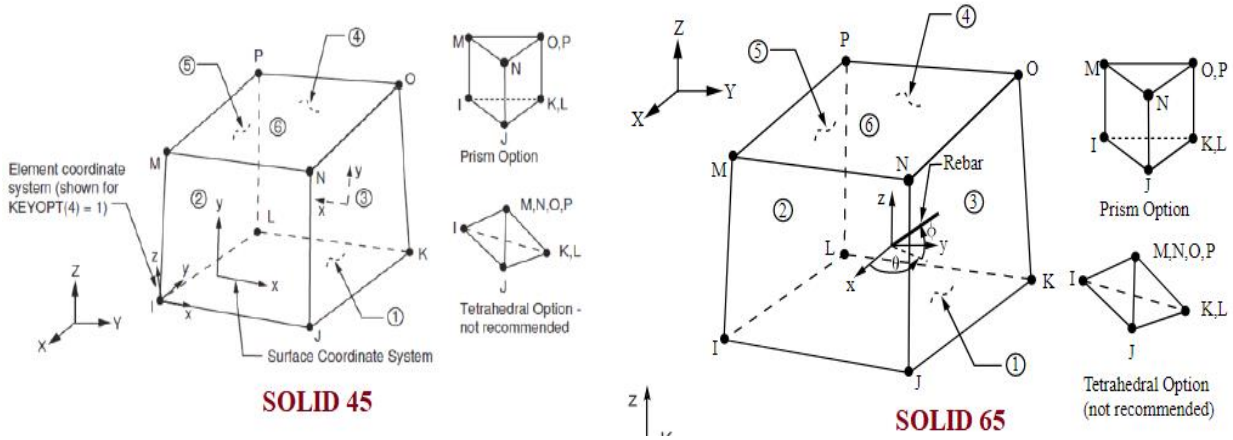

Figure 2. Geometry and node coordinate of elements used in modeling

The behavior of materials used in the modeling of the samples of columns is indicated in Figure 3 [1].

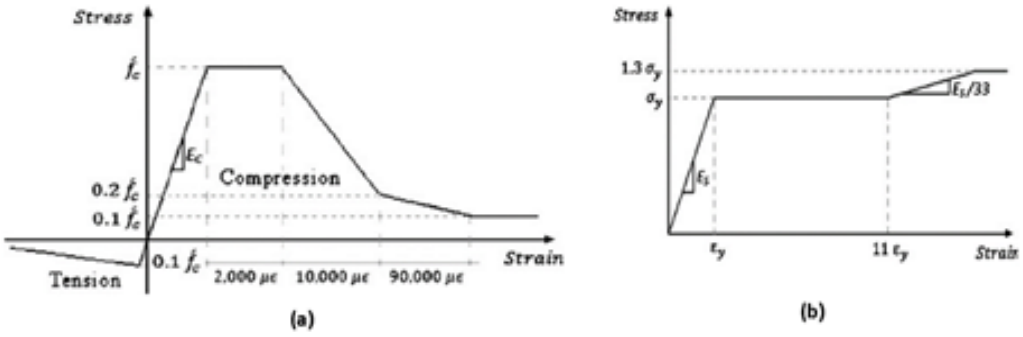

Figure 3. Stress-strain relationship curves for the a) core concrete and b) steel in steel wall and steel mesh

VALIDATION OF FINITE ELEMENT MODELING OF LABORATORY SAMPLES

Numerical results obtained from the nonlinear analysis and the experimental results of CFT columns have been compared with each other. Furthermore, after applying 30 percent of the column's nominal load bearing capacity as an axial load, lateral cyclic displacement has been applied to the top of the column in this cyclic loading. In the first and second stages, when the column is under axial stress, the columns are subjected to axial loading; they are then exposed to cyclic loading until the column is damaged, as illustrated in Figure 4.

The cross-section axial capacity (Nc) were adopted. The EN 1998-1 limits the design axial load to no more than 30% of the design column resistance for all composite columns in moment-resisting frames [9]. In this paper, the axial bearing capacity of the circular CFST columns can be calculated according to the ACI design code as expressed by Eq.1, where As and Ac are cross-sectional areas of the steel tube and the concrete core, respectively, *fy* and *fc′* are the yield strength of the steel tube and the concrete compressive cylinder strength, respectively [16].

$$N_{c,ACI} = A_s f_y + 0.85 A_c f_c' \quad (1)$$

Seamless pipes were employed in the steel walls of the columns. The steel walls have an inner diameter of 0.254 m and a thickness of 0.008 m, while the columns have a length of 2 meters. As a result, the diameter of outer steel wall is 0.27 m. Table 1 lists the other features of the tested columns, such as the steel mesh and concrete core properties. The interior steel mesh of the examined samples is also 0.227 m in diameter and near to the steel wall.

Figure 4: Experimental samples under axial and cyclic loading

Table 1: The Specifications of experimental samples

Sample name	Length (m)	Steel Wall Young's modulus (MPa)	f_y (MPa) Steel Wall	f_c' (MPa)
CFT	2.00	25614	337	32.4

Compressive strain, and Young's modulus about concrete for both CFT and UGCFT samples is respectively 0.00126 and 25614 MPa. According to the EN ISO 6892-1 standard, the yield strength of the steel wall and steel mesh is 337 and 326 MPa, respectively, and its elastic modulus is about 200000 MPa.

The ATC-24 code is used to apply cyclic loading to experimental samples and finite element models, as illustrated in Figure 5 [14].

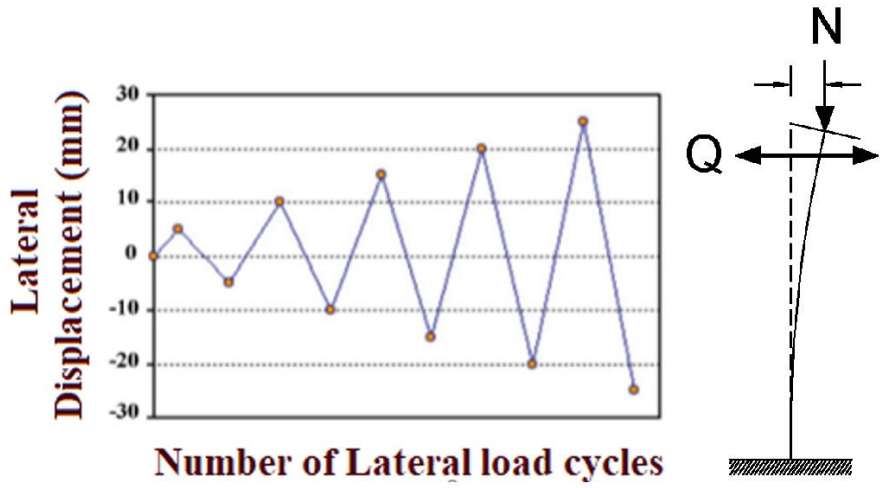

Figure 5. The cyclic loading history based on ATC-24 code

To model the numerical samples, first the inner concrete core is modeled by Solid65 element. In the next step, the external steel wall is modeled by Solid45 element. The essential thing is that the meshing of these parts is done in such a way that the nodes are coincided. Finally, all the nodes are merged.

The cross section of column modeled by Ansys software is shown in Figure 6. Figure 7 shows the modeled samples of experimental columns. All the nodes of the external steel wall located at 0.20 m from the base plate column have been fixed.

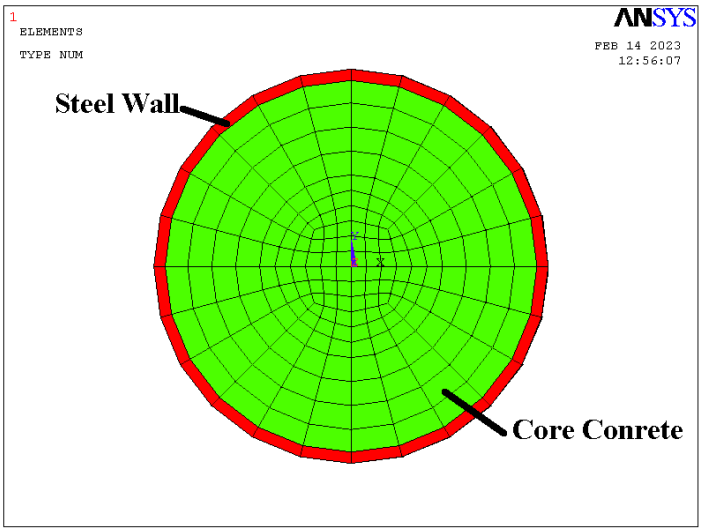

Figure 6. The modeling scheme of column samples in ANSYS

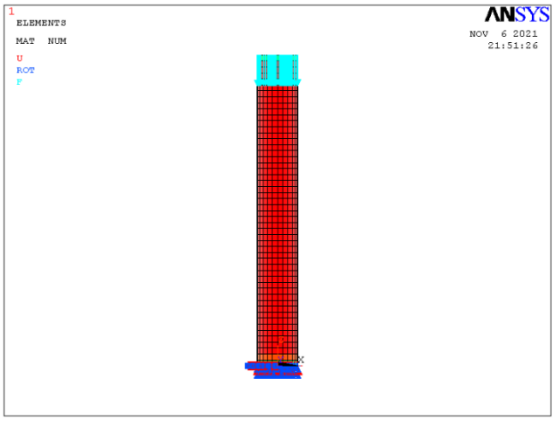

Figure 7. Modeling of experimental samples in ANSYS

The characteristics of the comparative samples modeled with different crushed stiffness factor are presented in the Table 2.

Table 2: The characteristics of concrete-filled steel column samples under investigating.

Row	Sample name	f'_c (MPa) for core concrete	f_y (MPa) Steel Wall	Crushed Stiffness Factor (CSTIF)
1	CSTIF=E-5	32.4	337	0.00001
2	CSTIF=E-4	32.4	337	0.0001
3	CSTIF=E-3	32.4	337	0.001
4	CSTIF=E-2	32.4	337	0.01
5	CSTIF=0.1	32.4	337	0.1
6	CSTIF=0.5	32.4	337	0.5
7	EXP	32.4	337	experimental

The hysteretic loops for experimental and numerical samples listed in Table 2 modeled in ANSYS under the same situation are compared in Figures 8 and 13. A gauge that it set up on the top level of the column measured the lateral displacement in the test. It seems that the steel mesh has maintained its performance until the end of loading in the laboratory. Loading continues until the column undergoes large deformations and collapses.

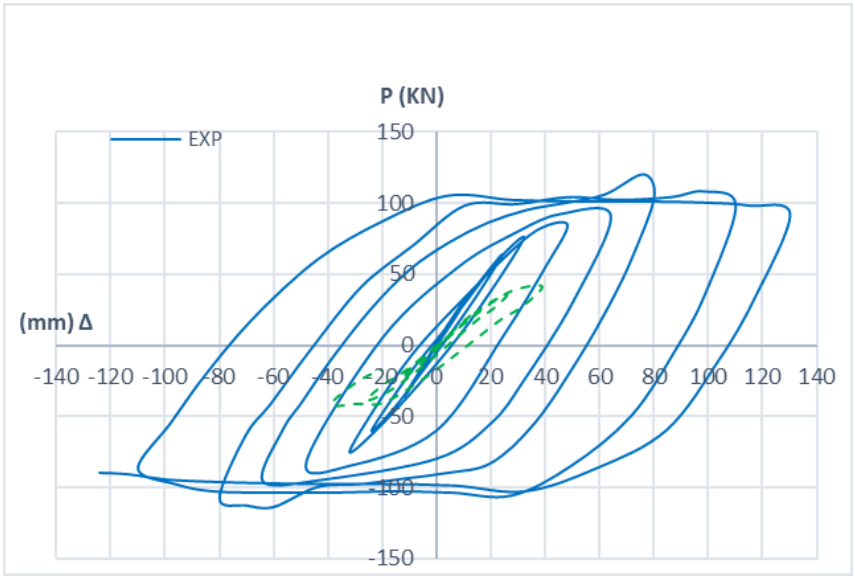

Figure 8. The lateral load- lateral displacement responses of CSTIF=E-5 and experimental sample

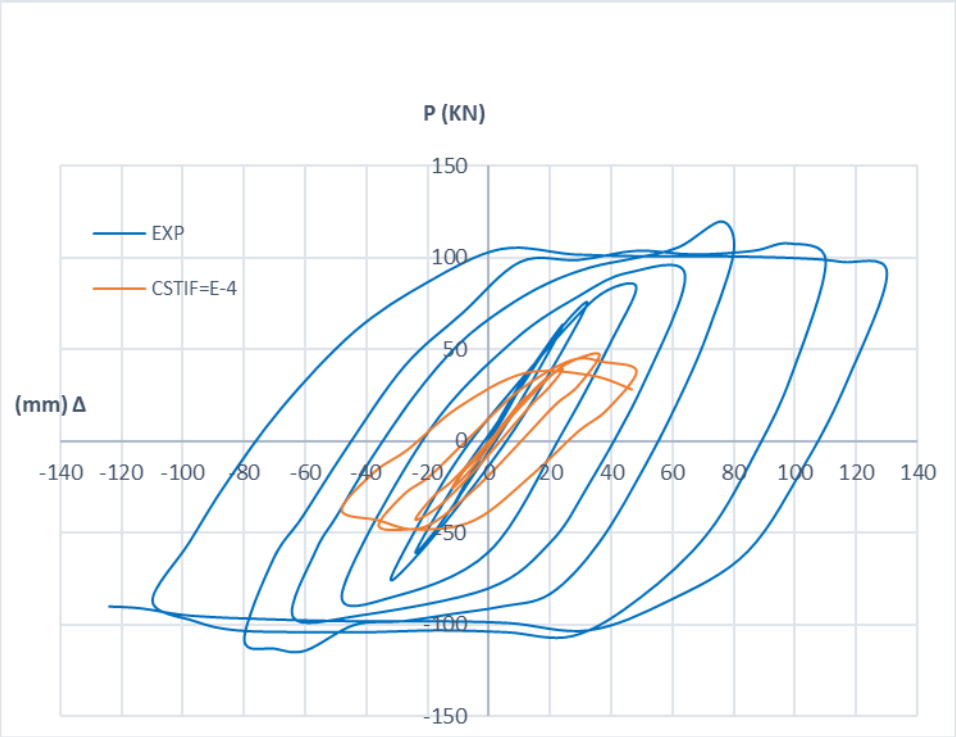

Figure 9. The lateral load- lateral displacement responses of CSTIF=E-4 and experimental sample

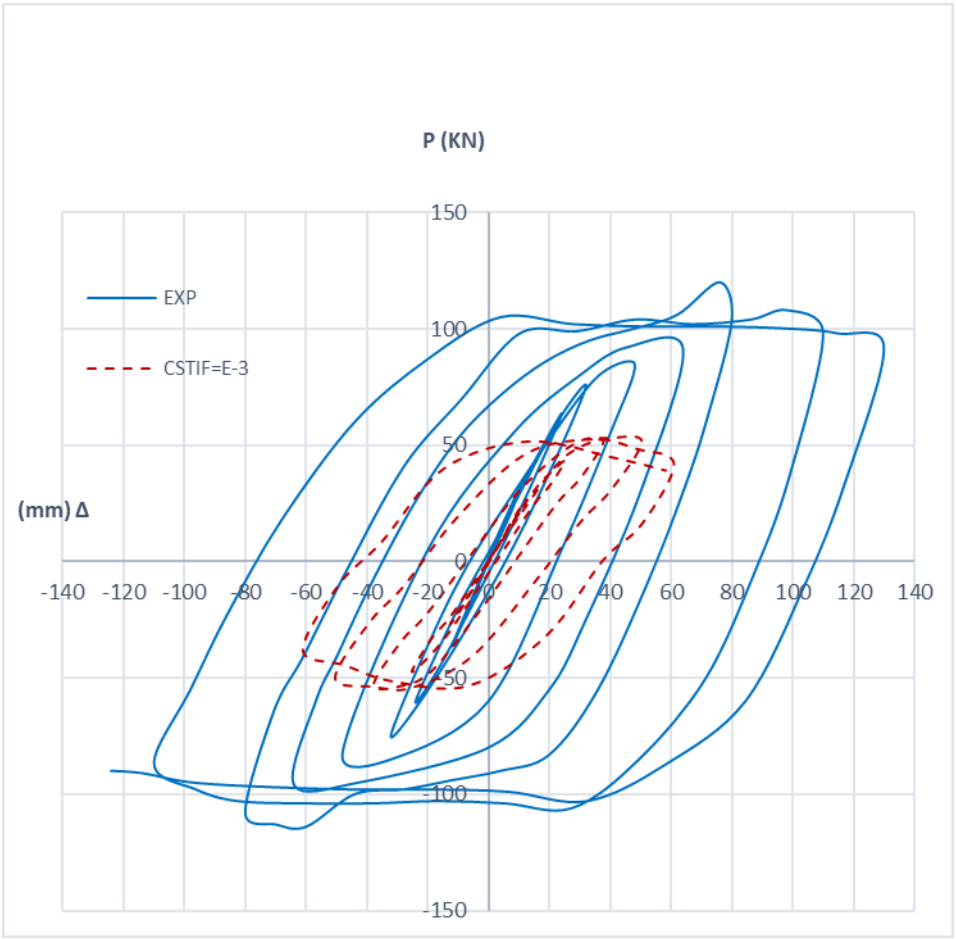

Figure 10. The lateral load- lateral displacement responses of CSTIF=E-3 and experimental sample

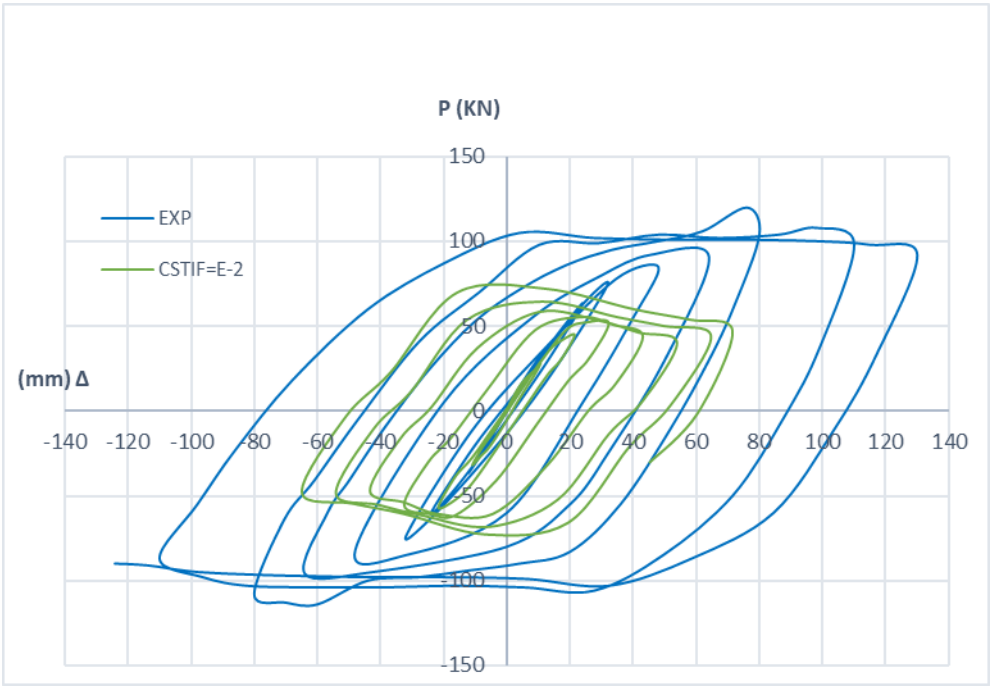

Figure 11. The lateral load- lateral displacement responses of CSTIF=E-2 and experimental sample

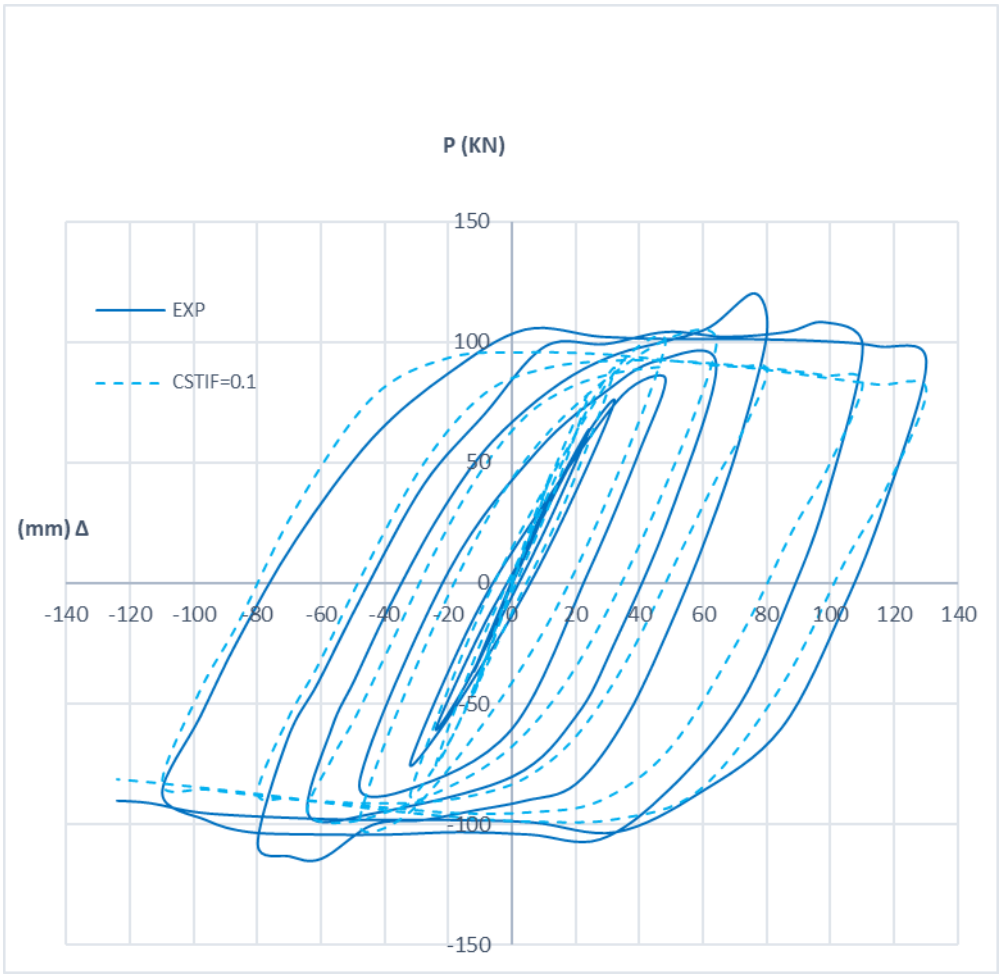

Figure 12. The lateral load- lateral displacement responses of CSTIF=E-2 and experimental sample

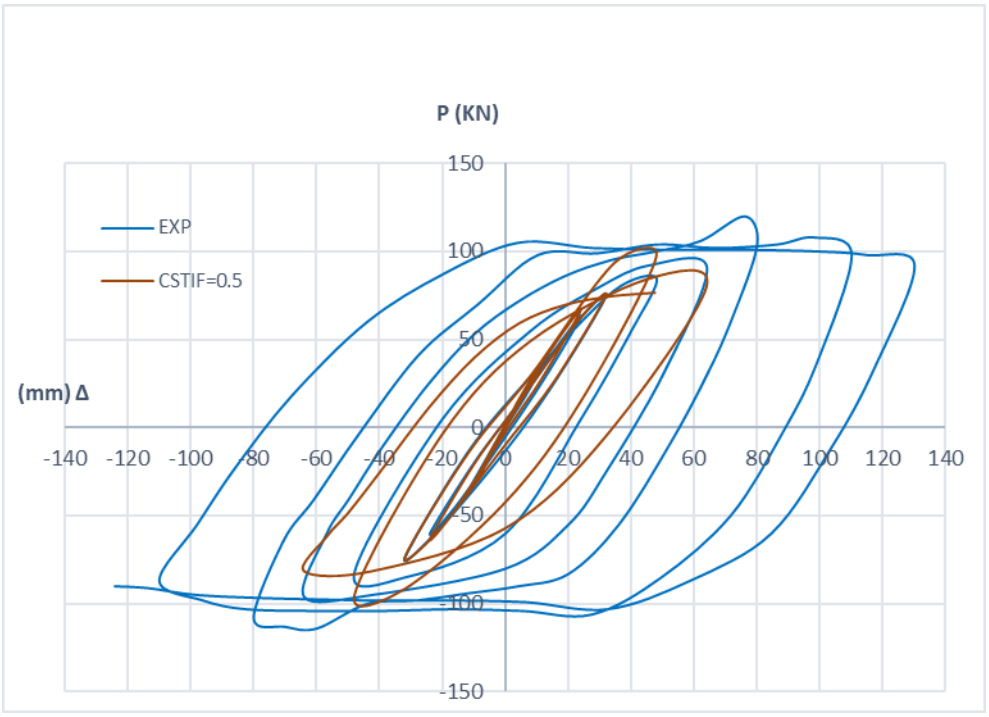

Figure 13. The lateral load- lateral displacement responses of CSTIF=E-2 and experimental sample

The envelope curves for experimental and numerical samples listed in Table 2 modeled in ANSYS under the same situation are compared in Figures 14.

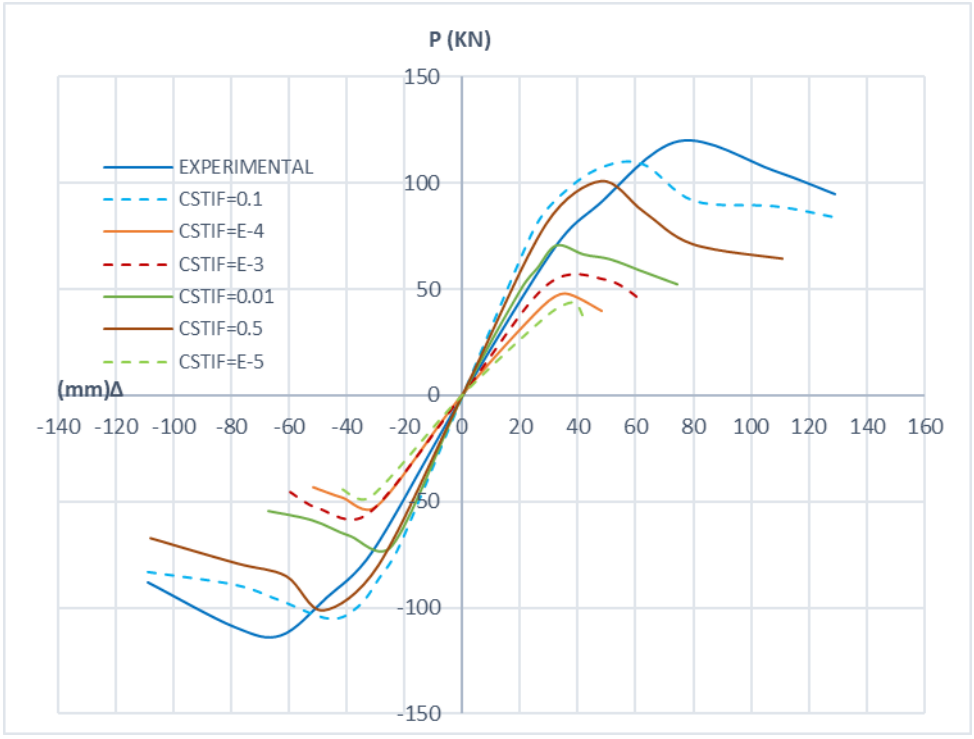

Figure 14. The envelope curves experimental samples and numerical models under axial and cyclic loading

According to the graphs shown and the obtained results, it can be concluded that in the concrete-filled steel column as a case study, with selecting Crushed Stiffness Factor (CSTIF) is equal to 0.1 the modeling results are close to each other.

CONCLUSIONS

It can be concluded that in the investigated column as a case study, the Crushed Stiffness Factor plays a significant role in matching the laboratory results with the numerical modeling results. Due to the confinement of the concrete by the external steel wall, the value of Crushed Stiffness Factor is equal to 0.1 for the concrete-filled steel columns, and it is expected that the value of this Factor may differ according to the conditions of the problem.

(Received February 2023, accepted February 2023)

REFERENCES

[1] Abedi, K., Ferdousi, A. and Afshin, H. (2008). A novel steel section for concrete-filled tubular columns. Thin-Walled Structures, 46: 310-319.
[2] [2] Hsiao, P., Hayashi, K., Nishi, P., Lin, X. and Nakashima, M. (2015). Investigation of Concrete-Filled Double-Skin Steel Tubular Columns with Ultrahigh-Strength Steel. Journal of Structural Engineering, 141: 1-8.
[3] Wang, R., Han, L., Zhao, X. and Rasmussen, K. (2016). Analytical behavior of concrete filled double steel tubular (CFDST) members under lateral impact. Thin-Walled Structures J, 101: 129-140.
[4] Aghdamy, S., Thambiratnam, D., Dhanasekar, M. and Saiedi, S. (2017). Effects of load-related parameters on the response of concrete-filled double-skin steel tube columns subjected to lateral impact. Journal of Constructional Steel Research, 138: 642-662.
[5] Zhou, F. and Xu, W. (2016). Cyclic loading tests on concrete-filled double-skin (SHS outer and CHS inner) stainless steel tubular beam-columns. Engineering Structures J, 127: 304-318.
[6] Hassaneina , F., Elchalakanib, M., Karrechb, A., Patelc, V. and Daher, E. (2018). Finite element modelling of concrete-filled double-skin short compression members with CHS outer and SHS inner tubes. Marine Structures J, 61: 85-99.
[7] Vernardos, S. and Gantes, Ch. (2019). Experimental behavior of concrete-filled double-skin steel tubular (CFDST) stub members under axial compression: A comparative review. Structures J, 22: 383-404.
[8] Zheng, Y., He, Ch. and Zheng, L. (2018). Experimental and numerical investigation of circular double-tube concrete-filled stainless steel tubular columns under cyclic loading. Thin-Walled Structures J, 132: 151-166.
[9] Chen, J., Chan, T.M., Kai Leung Su, R. and Miguel Castro, J. (2019). Experimental assessment of the cyclic behaviour of concrete-filled steel tubular beam-columns with octagonal sections. Engineering Structures J, 180: 544-560.
[10] Wang, B., Liang, J. and Lu, Zh. (2019). Experimental investigation on seismic behavior of square CFT columns with different shear stud layout. Journal of Constructional Steel Research, 153: 130-138.
[11] Zhang, J., Li, X., Cao, W. and Yu, Ch. (2019). Cyclic behavior of steel tube-reinforced high-strength concrete composite columns with high-strength steel bars. Engineering Structures J, 189: 565-579.
[12] Wang, Z., Zhang, J., Li, W. and Wu, H. (2020). Seismic performance of stiffened concrete-filled double skin steel tubes. Journal of Constructional Steel Research, 169: 1-19.
[13] ANSYS, ANSYS User's Manual Revision 12.0, ANSYS, Inc.
[14] ATC-24, Guideline for Cyclic Seismic Testing of Components of Steel Structures.
[15] Abdalla, Kh., Al-Rousan, R., Alhassan, M., Lagaros, N. (2019). Finite-element modelling of concrete-filled steel tube columns wrapped with CFRP. Proceedings of the Institution of Civil Engineers – Structures and Buildings, 1-14.
[16] Guler, S., Copur, A. and Aydogan, M. (2013). Axial capacity and ductility of circular UHPC-filled steel tube columns. Magazine of Concrete Research, 65: 898-905.

Original scientific article
http://dx.doi.org/10.59456/afts.2023.1528.039J

STEP TOWARDS INTELLIGENT TRANSPORTATION SYSTEM WITH VEHICLE CLASSIFICATION AND RECOGNITION USING SPEEDED-UP ROBUST FEATURES

Janak Trivedi[1], Mandalapu Sarada Devi[2], Brijesh Solanki[3]

[1]*Faculty of Electronics & Communication Engineering Department, Government Engineering College Bhavnagar, Affiliated to Gujarat Technological University, A.I.C.T.E., India,*
e-mail; trivedi_janak2611@yahoo.com
[2]*Faculty of Electronics & Communication Engineering Department, Ahmedabad Institute of Technology, Affiliated to Gujarat Technological University, A.I.C.T.E., India.*
[3]*Faculty of Electrical Engineering Department, Government Engineering College Bhavnagar, Affiliated to Gujarat Technological University, A.I.C.T.E., India.*

SUMMARY

Vehicle classification is a crucial task owing to vehicles' diverse and intricate features, such as edges, colors, shadows, corners, and textures. The accurate classification of vehicles enables their detection and identification on roads and facilitates the development of an electronic toll-collection system for smart cities. Furthermore, vehicle classification is useful for traffic signal control strategy. However, achieving accurate vehicle classification poses significant challenges due to the limited processing time for real-time applications, image resolution, illumination variations in the video, and other interferences. This study proposes a method for automated automobile detection, recognition, and classification using statistics derived from approximately 11,000 images. We employ SURF-based detection and different classifiers to categorize vehicles into three groups.

The Traffic Management System (TMS) is crucial for studying mobility and smart cities. Our study achieves a high automobile classification rate of 91% with the medium Gaussian Support Vector Machine (SVM) classifier. The paper's main objective is to analyze five object classifiers for vehicle recognition: Decision Tree, Discriminant Analysis, SVM, K-Nearest Neighbor Classifier (KNN), and Ensemble Classifier. In the discussion section, we present the limitations of our work and provide insights into future research directions.

Keywords: *Classifier, feature extraction, Support Vector Machine (SVM), Speeded Up Robust Features (SURF), k-mean.*

INTRODUCTION

With the development of hardware and the reduction in manufacturing costs, there has been a significant increase in surveillance devices, and high-resolution video cameras have been increasingly employed in such systems. Consequently, many video sources generate large volumes of information that require analysis and interpretation, but this amount of information needs to be reduced for human operators to handle. Thus, researchers utilize technology such as the Intelligent Transportation System (ITS). Automatic extraction of vehicles from surveillance videos using artificial intelligence is a

prominent research topic. Vehicle classification using traditional methods poses two main problems: the need for human supervision to classify vehicles and the availability of variations in different vehicle models. Computer vision-based traffic management is more intelligent, faster, and more efficient than human operators. Artificial Intelligence (AI) plays a significant role in ITS using computer vision. One of the most exciting aspects of AI is its potential to revolutionize the computer industry and any industry that affects our lives. Deep learning and machine learning are part of AI, and they offer a new direction with high accuracy for an automatic vehicle recognition system in computer-vision techniques. Deep learning works similarly to the human brain in the proposed system, and its layer-by-layer structure extracts useful information for the given dataset.

Recent progress in artificial intelligence (AI) has significantly impacted the research related to vehicle detection, identification, and classification. Vehicle classification has applications in multiple domains, including recognizing emergency vehicles in automated toll-collection systems. Janak et al. have presented a comprehensive review of the utilization of computer vision-based Intelligent Traffic Control systems in Smart Cities [1]. Vehicle classification can be implemented through online, offline, and real-time applications. Automated vehicle classification can be specifically advantageous in toll plazas, where it can rapidly identify the vehicle type and automatically collect the toll charge. Furthermore, vehicle classification and recognition can assist in developing an adaptive traffic control system and identifying emergency vehicles. These advancements in vehicle classification and recognition using AI have the potential to pave the way for the development of more efficient and intelligent transportation systems, thus making our cities smarter and safer.

The deep learning algorithm represents a recent trend in object detection and recognition in artificial intelligence systems utilizing computer vision. In deep learning, tiny feature extraction plays a crucial role in identifying the type or class of a vehicle from selected images. Feature extraction is crucial in acquiring helpful information about the detected features. Feature matching is essential in applications such as motion tracking, image retrieval, object recognition, object classification, and human activity recognition. The limitation of the changing pixel values due to light intensity can be overcome by selecting the most appropriate features. These features include edges, corners, blobs, gradient values, magnitude, and phase.

Various classifiers are used to analyze images selected from various web search tools. Feature extraction, a general term for creating combinations of variables to solve classification problems while adequately representing the information, is a critical step. Many machine learning practitioners believe that properly optimized feature extraction is key to successful model construction. Features are pieces of information obtained from an image. Feature extraction is achieved through various image characteristics, such as color, shape, corners, position, and dominant edges. These features are critical for recognition, matching, and detection. The number and size of features play an important role in different real-time applications. Feature detectors such as SHIFT and SURF are popularly used. In our research, we classified vehicles into bikes, cars, and trucks, using k-means clustering algorithms and SURF on a generated dataset of around 11k images.

Various methods and approaches for vehicle detection, recognition, and classification contribute to versatile traffic light control systems at intersections. Vehicle recognition helps determine the number and type of vehicles on specific roads. This system is also useful in identifying emergency vehicles, such as ambulances and traffic management systems (TMS), which can handle difficult situations in real time. The application of deep learning and artificial intelligence (AI) is essential in developing Intelligent Transportation Systems (ITS) in smart cities. These techniques are valuable and trending in the field of ITS research.

Vehicle classification helps in traffic signal control strategy. For example, high-emissions vehicles stopped less frequently, so recognizing these vehicles and clearing the traffic jams beneficial in terms of air quality. Vehicle classification helps optimize infrastructures and increase the return on toll gates by traffic flows. Vehicle classification can classify *(A) According to purpose*: (1) Passenger vehicles: like car, bus, taxi, etc. (2) Goods vehicles: like truck, tempo, container, etc. (3) Special purpose vehicles: like ambulance, fire brigade, etc. *(B) According to load carrying capacity:* (1)

Light Motor Vehicles (LMV): like cars, jeep, etc. (2) Medium Motor Vehicles (MMV): like tempos, pick up vans, etc. (3) Heavy-duty Motor Vehicles (HMV): tractor, truck, container, etc. *(C) According to number of wheels:* (1) Two wheelers: like motor-cycle, scooters, etc. (2) Three wheelers: like auto rickshaw (3) Four wheelers: like cars, jeep, mini vans, etc. (4) Six wheelers: like truck, bus, etc. *(D) According to fuel used:* (1) Petrol vehicles: like motor-cycle, cars, etc. (2) Diesel vehicles: like cars, trucks, buses, etc. (3) Gasoline vehicles: like LPG vehicles, CNG vehicles, etc. (4) Electric vehicles: like Yo bikes, cars, etc. (5) Hybrid vehicles: like vans, cars, etc. *(E) According to drive of vehicles:* (1) Front wheel drive vehicles: like cars (2) Rear wheel drive vehicles: like truck, buses, etc. (3) Four-wheel drive vehicles: like military vehicles. This article has classified bike, car, and truck-vehicle accordingly to their purpose category using computer vision technique.

This study investigates using an alternative classifier for a dataset of approximately 11,000 images randomly collected from various web search tools. A comprehensive literature review of various methods is presented in Section 2, followed by a detailed explanation of different feature detection techniques in Section 3, including Scale Invariant Feature Transform (SIFT) and Speeded-Up Robust Feature (SURF) detection. Section 4 provides the details of five primary classifiers and 22 sub-classifiers. The vehicle recognition process's workflow is presented in Section 5, utilizing SURF and k-means algorithms, as depicted in Figure (1). Section 6 presents the results regarding feature selection, performance analysis, and verification and testing on random images, as shown in Figures (4-6). The study concludes with a discussion of limitations, a summary of the findings, and future research directions.

LITERATURE SURVEY

Recently, computer vision techniques using deep learning and artificial intelligence have been extensively employed for developing Intelligent Transportation Systems (ITS). These systems require automatic detection, recognition, and classification of vehicles to enhance the Traffic Management System (TMS) efficiency in a smart city. Francesco et al. [2] have presented the European Process of smart city development using three interconnected processes, which include smart city planning theories, smart city development, and smart city rules and policy. For effective smart city planning, smart TMS is necessary.

The TMS comprises real-time vehicle information, accident detection, vehicle speed measurements, parking information, bus-train route information for users and commuters, and an automatic toll collection system. Antonello et al. [3] have discussed the integration of conventional vehicle reviews (which provide little information) with extensive knowledge from Information and Communication Technology (ICT) in constructing Transport System Models (TSMs).

The effective implementation of Intelligent Transportation Systems (ITS) in a smart city requires automated vehicle detection, recognition, and classification. The classification of vehicles is crucial for a wide range of applications, including vehicle speed detection, autonomous driving, intelligent parking systems, and toll collection. In the literature, various classification approaches have been proposed, such as the nearest neighbor classification approach for multispectral images as demonstrated in Hardin et al. [4], and the use of KNN classification by Ghosh Anil [5]. The creation of feature-based vector trees and the AdaBoost method-based classification with random forest and linear estimation of regression trees are discussed in Breiman [6] and Loh [7]. The decision tree-based application of classification from tree graphs is also explained by Paensuwan et al. [8]. These approaches have been shown to classify different types of vehicles effectively and can be applied to real-time ITS systems in smart cities.

Various vehicle classification methodologies have been proposed in the literature, including length-based or shape-based, information-based, vision-based, movement-based, and distinctive feature extraction-based approaches, as explained by Wen et al. [9]. Kim et al. [10] demonstrated on-street vehicle detection using the Pi-Histogram of Oriented Gradients (HOG) strategy with support vector

machines (SVMs). Stocker et al. [11] utilized a supervised learning approach with multilayer perceptron (MLP) feed-forward artificial neural networks (ANNs) for vehicle classification and identification. Arinaldi et al. [12] proposed SVM and Faster Region Convolutional Neural Networks (RCNN) based on vehicle identification and classification using MIT traffic data. Atiya [13] discussed simple pattern recognition-based algorithms, support vector classifiers, and support vector regression with different kernel principles.

In Intelligent Transportation Systems (ITS), automatic vehicle detection, recognition, and classification are essential for developing smart cities. The classification of vehicles is necessary for various purposes, such as vehicle speed detection, autonomous driving vehicles, intelligent parking systems, and toll collection.

Sarikan et al. [14] implemented K-Nearest Neighbors (KNN) and decision tree-based vehicle classification. Gorges et al. [15] clarified the utilization of street profile estimation calculation for grouping two-wheeled vehicles. Machine learning classifiers such as KNN, decision trees, and support vector machines (SVMs) have been employed to develop automatic vehicle classification systems. However, the accuracy rate of SVM and Artificial Neural Network (ANN)-based classification approaches is low, as discussed by Bautista et al. [16]. Convolutional Neural Network (CNN) has shown a higher accuracy rate for vehicle recognition than SVM and ANN.

In recent years, Bag of Features (BOF) has been used to classify Magnetic resonance images. Deepika et al. [17] utilized SVM for BOF-based classification and achieved 93% accuracy. Similarly, Pranata et al. [18] used BOF-based classification with SURF for detecting fractures in medical images. Sykora et al. [19] utilized SIFT and SURF for gesture recognition and SVM for classification. Anca and Ioan [20] discussed palm print characterization and recognition using SURF. Anzid et al. [21] employed SURF and different types of SVM (linear, non-linear, and multiclass) for multimodal image classification. These works demonstrate the potential of machine learning methods and feature extraction techniques for image classification and recognition.

FEATURE DETECTION

Feature detection is a crucial step in many computer vision applications, which involves extracting relevant features from an image for subsequent processing. One common method for feature detection is corner detection, which identifies points of interest in an image by detecting changes in the X and Y gradient values. Corners are useful features because they are invariant to changes in illumination or viewpoint. The Harris corner detector is a widely used corner detection algorithm that identifies corners based on changes in gradient in all directions. It operates in three cases: flat regions where there is no change in gradient, edges where there is a change of gradient value in one direction and corners where there is a change in gradient value in all directions. SIFT and SURF are popular feature detection methods that utilize the Hessian matrix to calculate and identify features.

SIFT Feature calculation

The SIFT (Scale-Invariant Feature Transform) feature calculation process involves selecting a 16 x 16-pixel neighborhood and dividing it into 4 x 4 block neighborhoods. Each neighborhood is rotated and aligned with the previously calculated orientation, and eight orientations are calculated at a 4 x 4 bin array which results in 128-dimensional features which are used for object detection and recognition applications. The unit magnitude can be used to normalize the illumination problem. The SIFT features have several properties, including finding feature points, repeatability of key points, scale-rotation invariance, and robustness to viewpoint changes, as explained by David in [22].

SURF feature calculation

In feature extraction, three important properties are repeatability, matching speed, and descriptiveness. The number and size of features are also critical factors. Feature extraction consists of two steps: feature detection and feature extraction. The SIFT method has been widely used due to its high

descriptiveness but comes at a high computational cost. In contrast, the SURF method improves upon the scale-invariant feature detector by using the Hessian matrix to detect the gradient magnitude and orientation to select points of interest. The Hessian matrix is calculated in Equation (1), and the sum of the Haar wavelet can also be used to improve orientation performance. Bay et al. [23] discussed the use of SURF and its advantages over the Difference of Gaussian (DoG) method.

(1)

For multivariate function, the Hessian matrix contains all the second partial derivate of function D. Dxx represents twice the partial derivative for x, Dyy represents twice the partial derivative for y, Dxy represents the partial derivative first with x, then for y Dyx represents the partial derivative first for y than with x.

The machine learning approach enables the automatic classification of objects without requiring manual labeling or feature extraction. Matlab is a powerful tool for classifying different objects in a given dataset. The accuracy, prediction, and output results are then validated. In machine learning, data can be divided into numerical and categorical classes. Numerical data are represented by numbers (floating point or integer), while discrete label groups represent categorical data. Using Matlab, five classifiers are tested, further subdivided into twenty-two classifiers.

DIFFERENT CLASSIFIERS

Decision Tree

A *decision tree* is a hierarchical structure that resembles a flowchart used for classification and prediction. Each node in the tree represents a test for a specific attribute, and each branch represents the result of that test. The terminal nodes of the tree, also known as leaf nodes, contain the class labels. Decision trees are one of the most widely used and powerful tools for classification and prediction. They can handle both categorical and numerical data, and different decision trees can be used based on the number of splits made during the classification process.

(1) Fine Trees: Many leaves for acceptable discrimination.
(2) Medium Trees: Moderate number of leaves for finer discrimination between classes.
(3) Coarse Trees: some leaves to roughly distinguish between classes [24].

Discriminant analysis

Discriminant analysis is a statistical method used to classify objects into two or more groups based on their measured characteristics or features. When the predicted variable is binary, discriminant analysis can be viewed as a regression analysis. Suppose we have a set of objects that belong to two categories, and we measure several quantities that help determine the category of the object, which we assign the values 0 and 1. The discriminant analysis classifier is used to classify numerical data only. Different types of discriminant analysis can be used to create linear or nonlinear boundaries between classes.

(1) Linear Discriminant: This creates linear boundaries between classes.
(2) Quadratic Discriminant: This creates nonlinear class boundaries [24].

SVM

The SVM algorithm seeks to find the one that maximizes the margin between the two classes, i.e., the distance between the hyperplane and the nearest data points from each class. The data points closest to the hyperplane are called support vectors, which play a critical role in determining the hyperplane's location. The SVM algorithm can also handle nonlinearly separable data by transforming the data into a higher-dimensional space using kernel functions. SVMs are popular machine learning classifiers due to their ability to handle high-dimensional data and generalize well to new, unseen data.

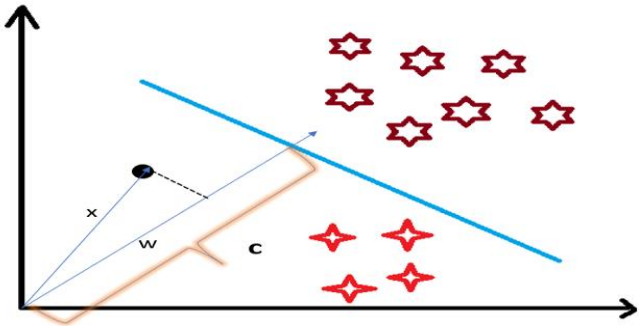

Figure 1 projection of vector x, vector w perpendicular to the hyperplane, and decision boundary c [25]

$$\vec{\mathbf{x}} \bullet \vec{\mathbf{w}} = c$$
$$\vec{\mathbf{x}} \bullet \vec{\mathbf{w}} > c$$
$$\vec{\mathbf{x}} \bullet \vec{\mathbf{w}} < c \qquad (2)$$

The inner product, which is the projection of one vector onto another, is utilized in the support vector machine (SVM) algorithm. The dot product of the x vector and the w vector is taken, and if the resulting value is greater than a threshold 'c', the point is classified as belonging to the positive samples category. Conversely, if the dot product is less than 'c', the point is classified as belonging to the negative samples category. If the dot product is equal to 'c', the point is on the decision boundary between the two categories. The SVM classifier is commonly used for both categorical and numerical classification tasks.

Different types of SVM depend on their kernel selections. A *kernel function* is a method used to take data as input and transform it into the required format for processing data.
(1) Linear SVM: This makes a linear separation between two classes. Data is classified with the help of hyperplane and straight-line.
(2) Quadratic SVM: This makes a non-linear separation between classes. It cannot be easily separated from a linear line. The quadratic kernel is used to perform this task.
(3) Cubic SVM: This makes a non-linear separation between classes. Use cubic kernels to make non-separable data into separable data.
(4) Fine Gaussian SVM: Gaussian kernels can separate nonlinearly separable data by mapping the input vectors into Hilbert space. Makes finely detailed distinctions between classes, with kernel scale set to sqrt(P)/4.
(5) Medium Gaussian SVM: Medium distinctions, with kernel scale set to sqrt(P).
(6) Coarse Gaussian SVM: Makes coarse distinctions between classes, with kernel scale set to sqrt(P)*4, where P is the number of predictors [24].

Nearest Neighbor Classifier (KNN)

The k-nearest neighbor (KNN) algorithm, also known as ANN or k-NN, is a nonparametric supervised learning classifier that leverages the concept of proximity to make predictions or classifications about the clustering of single data points. KNN classifiers can be used to classify both categorical and numerical data types and typically utilize either Hamming distance calculation for categorical data or Euclidean distance calculation for numerical data. The specific type of KNN algorithm employed depends on factors such as the distinctions between classes and the number of nearest neighbors set.

(1) Fine KNN: Finely detailed distinctions between classes. The number of neighbours is set to 1.
(2) Medium KNN: Medium distinctions between classes. The number of neighbours is set to 10.
(3) Coarse KNN: Coarse distinctions between classes. The number of neighbours is set to 100.
(4) Cosine KNN: Medium distinctions between classes, using a Cosine distance metric. The number of neighbours is set to 10.

(5) Cubic KNN: Medium distinctions between classes, using a cubic distance metric. The number of neighbours is set to 10.
(6) Weighted KNN: Medium distinctions between classes, using a distance weight. The number of neighbours is set to 10 [24].

Ensemble Classifier

Ensemble learning is a technique used to generate a diverse set of base classifiers, from which new classifiers are derived that outperform any individual classifier. The base classifiers may differ in algorithms, hyperparameters, representations, or training sets. Ensemble methods aim to reduce bias and variance in the classification process. The Ensemble Classifier is mainly used to classify categorical data, except for Subspace Discriminant, which is used for numerical data. Depending on their specific characteristics, there are different types of ensemble methods in KNN.

(1) Boosted Trees: The ensemble method is AdaBoost, with Decision Tree learners.
(2) Bagged Trees: The ensemble method is a Random Forest Bag with Decision Tree learners.
(3) Subspace Discriminant: The ensemble method is Subspace, with Discriminant learners.
(4) Subspace KNN: The **e**nsemble method is Subspace, with Nearest Neighbor learners. This kind of operation is suitable for many predictors.
(5) RUSBoosted Trees: The ensemble method is RUSBoost, with Decision Tree learners. This is good for skewed data (with many more observations of 1 class) [24].

WORKFLOW

5.1.1 Detailed discussion of the dataset creation

The first step is to collect images of bikes, cars, and trucks from various sources, resulting in a dataset of approximately 11,000 images, with 3.5 thousand bike images, 5.8 thousand car images, and 1.8 thousand truck images. These images were resized to a fixed resolution of 640 (width) x 480 (height) to ensure consistency, although this may impact the accuracy of the results. The dataset was split into training and testing sets, with 70% of images used for training and 30% used for testing from each vehicle category.

Operation on input images

We use the bag of visual words approach with k-means clustering for feature extraction, which involves iteratively clustering the feature descriptors extracted from representative images of each vehicle category into k mutually exclusive clusters. The resulting clusters are compact and separated by similar properties, and the center of each cluster represents a visual word or function. Feature descriptors can be extracted based on a feature detector or defined raster.The Speeded Up Robust Features (SURF) detector is widely used to extract features invariant to scale and rotation. These features are extracted from the representative images of each category using keypoint extraction, creating feature vectors, and clustering of features through the bag of visual words approach using k-means clustering. Based on these feature descriptors, a histogram of the frequency of visual words is then created for each image. These histograms are then used to train an image category classifier.

After the classifiers are trained, they must evaluate their performance using appropriate metrics. The confusion matrix is a commonly used tool to evaluate the performance of classification models. The confusion matrix summarizes the number of true positive (TP), false positive (FP), true negative (TN), and false negative (FN) predictions made by the model. From this, we can calculate various parameters such as True Positive Rates (TPR), False Negative Rates (FNR), Positive Predictive Values (PPV), and False Discovery Rates (FDR). These metrics can help assess the classifier's accuracy, precision, and recall. The workflow for evaluating the classifiers is typically shown in a figure, such as a Figure (2), which provides an overview of the entire process from training to evaluation.

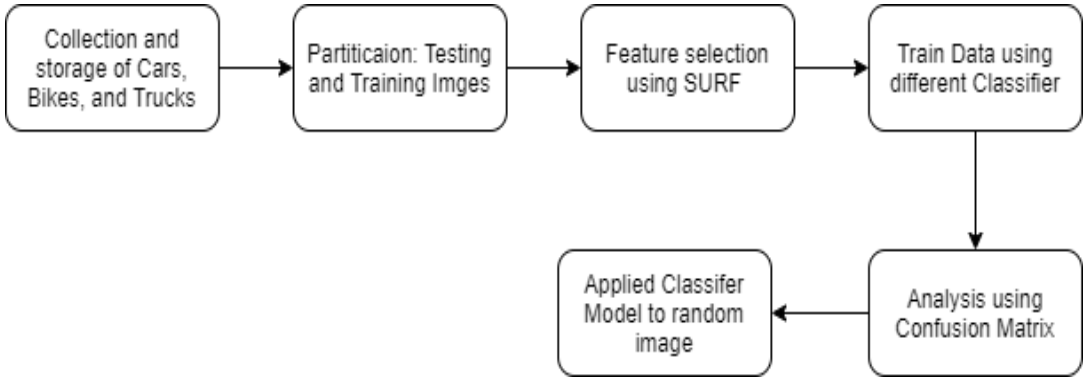

Figure 2 Workflow

RESULTS

In this study, the training dataset was used to validate various classifiers for categorizing vehicles into one of three categories: bike, car, and truck. A dataset of size 4800 x 451 was used for this purpose. A total of 22 different classifiers were evaluated using metrics such as True Positive Rates (TPR), False Negative Rates (FNR), Positive Predictive Values (PPV), and False Discovery Rates (FDR) with the help of a confusion matrix. The results for all the decision tree classifiers are shown in Figure 3(a).

To elaborate, Figure 3(a) demonstrates the accuracy of decision tree classifiers, where the fine tree classifier outperforms the medium and coarse trees. Additionally, Figure 3(b) shows support vector machine classifiers' accuracy and prediction speed, where a maximum accuracy of approximately 91% is achieved. The accuracy of a classifier is determined by its ability to accurately classify true positives (Tp), true negatives (Tn), false positives (Fp), and false negatives, which are taken into account during the calculation of classification accuracy.

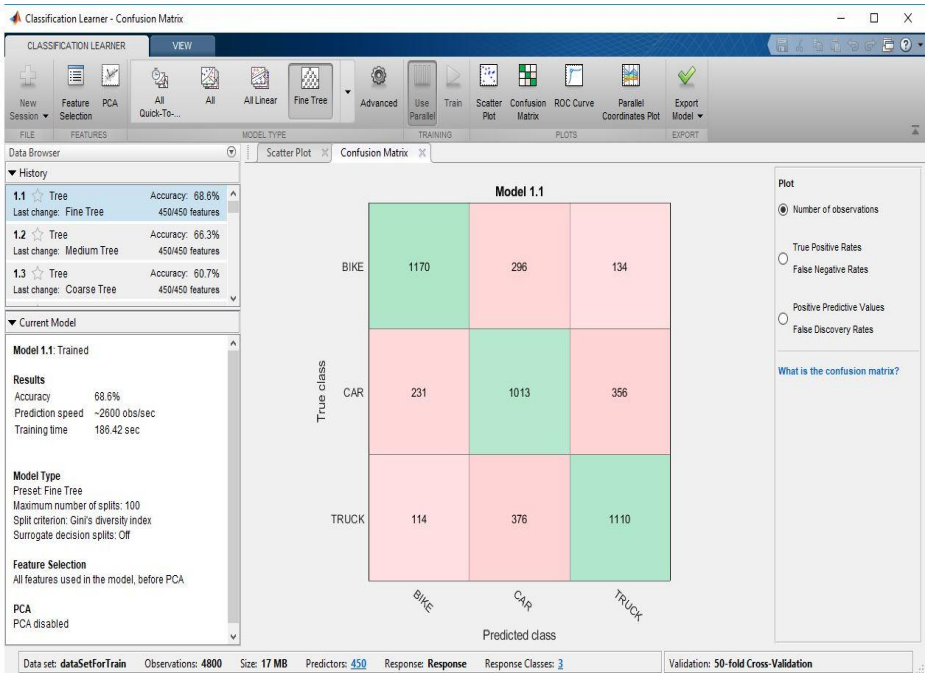

Figure 3 (a) Confusion matrix for decision tree classifiers

The number of accurate guesses divided by the number of predictions is the categorization accuracy as per equation (2) [17].

$$\text{Accuracy} = (Tp + Tn) / ((Tp + Tn + Fp + Fn) \quad (2)$$

In this study, we present our findings, categorized into three distinct areas: feature selection, performance analysis and comparison, and verification and testing on random images. Feature selection was conducted to identify the most relevant and informative features contributing significantly to the classification task.

Performance analysis and comparison were performed to evaluate the effectiveness of the proposed method against state-of-the-art approaches. Lastly, we conducted verification and testing on a set of random images to validate the generalizability and robustness of the proposed method. Our results provide valuable insights into the efficacy of the proposed approach and demonstrate its potential for real-world applications.

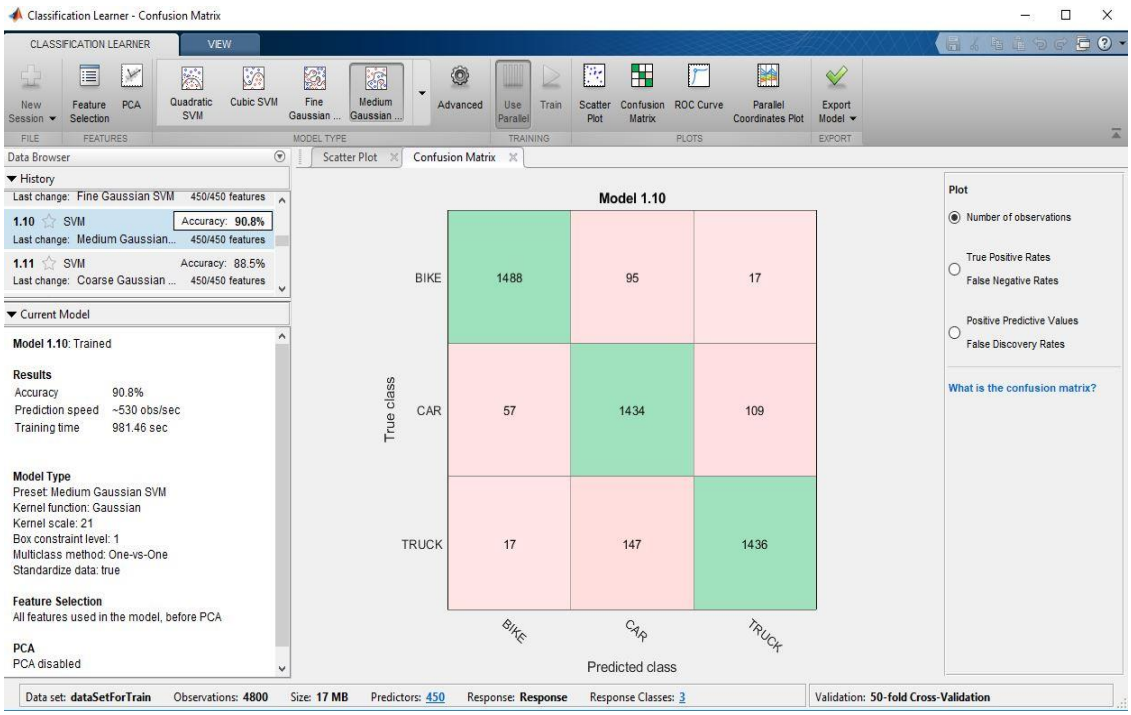

Figure 3 (b) Confusion matrix for SVM classifiers

Feature selection

This study investigates the effect of different feature selection methods on vehicle classification. We selected different images from each class of vehicles and extracted the number of features for each category. Specifically, we tested the k-means clustering method using around 250 words to classify bikes, cars, and trucks. We used the Speeded-Up Robust Features (SURF) algorithm to extract features, which were represented using the bag of visual words approach. Key points and descriptors were extracted from the images to identify features invariant to changes in image size, orientation, and compression. The number of features extracted from each vehicle category is presented in Annexure-I.

We compared the performance of the k-means clustering method using 250, 350, and 450 visual words for the same dataset of bikes, cars, and trucks. The results of our experiments, including the number of iterations and required time for each method, are summarized in Table 1.

Performance analysis and comparison

Multiple classifiers, including Support Vector Machine (SVM), K-Nearest Neighbors (K-NN), Decision Trees, Discriminant Analysis, and Ensemble classifiers using MATLAB, were evaluated for their performance in vehicle classification. We used the features extracted from the images of bikes, cars, and trucks, which were classified into different categories. The accuracy of each classifier was measured using cross-validation on the dataset.

The results of our experiments are summarized in Table 2, which shows that the medium Gaussian SVM classifier achieved the highest accuracy of nearly 91% for vehicle identification. These findings demonstrate the effectiveness of the proposed approach for vehicle classification and suggest that a medium Gaussian SVM classifier may be a suitable choice for similar applications.

Table 1. Number of iterations and the computational time for different images

Sr .No.	Number of Test Images	Bag of Visual words	Number of Iterations	Time Required (S)
1	100	250	25	84.755746
		350	17	76.971196
		450	20	80.409061
2	200	250	26	178.666412
		350	17	157.776405
		450	28	196.360222
3	300	250	22	256.148293
		350	18	237.015765
		450	30	341.758059
4	400	250	18	365.215308
		350	25	359.875082
		450	30	393.088333
5	500	250	28	523.370598
		350	29	497.012188
		450	18	442.437712
6	600	250	27	573.092221
		350	24	621.244559
		450	37	697.177003
7	700	250	75	1164.067380
		350	50	908.966623
		450	35	855.142737
8	800	250	22	859.710340
		350	20	843.597179
		450	19	826.786462
9	900	250	38	1083.519846
		350	22	943.515072
		450	19	1016.507187
10	1000	250	18	1024.145876
		350	27	1075.037355
		450	23	1130.071606

Annexure II presents the results of vehicle classification for bikes (B), cars (C), and trucks (T) in terms of true positive rate (TPR), false positive rate (FPR), positive predictive value (PPV), and false discovery rate (FDR) as percentages. We used different decision tree classifiers to identify the three types of vehicles, and the confusion matrix in the first row was used to assess the classification performance.

The diagonal elements in the confusion matrix indicate the correct identification of the selected vehicles. These results provide valuable insights into the effectiveness of the proposed approach for vehicle classification and can be used to optimize the system's performance in real-world applications

Table 2. Accuracy of different classifiers.

Sr. No.	Classifier Name		accuracy (%)	prediction speed (Obs/Sec)
1		Fine Trees	68.6	2600
2		Medium Trees	66.3	2500
3	Decision Trees	Coarse Tress	60.7	3100
4		Linear Discriminant	88.1	2400
5	Discriminant Analysis	Quadratic Discriminant	80.4	2000
6		Linear SVM	89	2100
7		Quadratic SVM	90	790
8		Cubic SVM	90.3	660
9		Fine Gaussian SVM	43.7	250
10	Support Vector Machines	Medium Gaussian SVM	90.8	530
11	(SVM)	Coarse Gaussian SVM	88.5	550
12		Fine KNN	77.7	220
13		Medium KNN	80.9	260
14	K-Nearest	Coarse KNN	81.1	260
15	Neighbor	Cosine KNN	81.7	240
16	Classifier	Cubic KNN	79.8	10
17	(KNN)	Weighted KNN	82.3	270
18		Boosted Trees	78.1	1300
19		Bagged Trees	83.3	1100
20		Subspace Discriminant	88.4	630
21	Ensemble	Subspace KNN	82.6	20
22	Classifier	RUSBoosted Trees	65.6	1500

Testing on random images

We assessed the performance of different classifiers for predicting the type of vehicle in a randomly selected image. Specifically, we used the medium Gaussian SVM classifier to test the system on a set of random images, and the results are presented in Figures (4) and Figure (5). These figures demonstrate the effectiveness of the proposed approach for vehicle classification and illustrate the classification results for a range of images. The results suggest that the medium Gaussian SVM classifier may be a suitable choice for similar applications, and provide important insights into the system's performance under realistic conditions.

Figure 4. True detection of bike and car

Figure 5. True & false detection of the truck

DISCUSSION

The images of bikes, cars, and trucks were classified and trained using Speeded Up Robust Features (SURF) and k-means clustering algorithms, with different visual feature word sizes of 250, 350, and 450 in MATLAB (as shown in Annexure-I). The most significant features were selected from each vehicle class, and the total number of features was calculated using MATLAB. While some features remained unchanged regardless of the visual feature word size selection, others varied with the change in visual feature word size. This study compared five object classifiers for the three vehicle categories: bike, car, and truck, using the identified features. The results demonstrate the effectiveness of the proposed approach for vehicle classification and provide valuable insights into the system's performance. These findings can be used to optimize the system for real-world applications, and the approach can be extended to other types of objects beyond vehicles.

After identifying the features of the objects, we applied twenty-two classifiers to classify different types of vehicles. These classifiers comprised sub-classifiers from five leading classification algorithms: Decision Tree (three sub-classifiers), Discriminant Analysis (two sub-classifiers), Support Vector Machines (six sub-classifiers), K-Nearest Neighbors (six sub-classifiers), and Ensemble Classifiers (five sub-classifiers). The vehicle dataset was used for training and classification into three categories: bikes, cars, and trucks. The medium Gaussian SVM classifier method of SVM demonstrated superior accuracy compared to the other twenty-one classifiers. Therefore, we recommend using the medium Gaussian SVM classifier for accurate vehicle recognition.

Variations in image resolution can impact the accuracy of inbuilt architecture and network results. To mitigate this issue, we created a custom dataset and evaluated it using a Convolutional Neural Network (CNN), as described by Trivedi et al. [26]. However, our current machine learning approach provided better accuracy for vehicle classification of bikes, cars, and trucks than the CNN approach, particularly for smaller datasets. Our machine learning approach yielded high accuracy, with the bike classification achieving a 99% prediction accuracy and the highest confidence values. In contrast, the truck classification demonstrated a lower highest confidence value than bikes and cars, with a confidence value of 85%.

Next, we applied various classifiers with our machine-learning approach to the same vehicle dataset used in this study. Prior work by Janak et al. [27] has discussed vehicle counting using morphology in different real-time traffic videos. However, the method was less accurate for congested traffic, resulting in a false count of on-road vehicles. To overcome this limitation, we focused on classifying three passenger vehicles using a machine-learning approach for static images only.

The present study has certain limitations. First, the results may vary for different iterations of trained datasets with varying environmental conditions. Additionally, all the images were resized to achieve better evaluation, which may require additional computation to implement these classifiers in real time directly. It may be necessary to increase the number of iterations and the size of the image dataset to increase the vehicle recognition process. It is worth noting that the Math Works website classifies the speed measurements as fast, medium, and slow for 0.01 s, 1 s, and 100 s, respectively, while *memory usage* is defined as small, medium, and large for data sizes of 1 MB, 4 MB, and 100 MB, respectively.

The classifiers' memory usage and prediction speed differ based on the selected algorithm. For the ensemble classifier, the speed and memory usage can range from medium to fast for SVM, high to low, or vice versa. For tree classifiers, memory usage is small, and speed is fast. The discriminant analysis classifier can have small or large memory usage, and the speed can be fast or slow depending on the selected method. KNN has medium memory usage and speed. It is worth noting that the prepared dataset differs from deep convolutional architecture networks, such as AlexNet, VGGNet, and ResNet. This study relies on hand-crafted features like SIFT and SURF, whereas CNN can learn features from data (images) and derive scores from the output that may impact the generalizability of the study's findings.

CONCLUSION AND FUTURE SCOPE

In this study, the accuracy and prediction speed of twenty-two different classifiers were evaluated using a machine learning approach for vehicle recognition of three categories - bikes, cars, and trucks. The medium Gaussian SVM classifier was more accurate than the other twenty-one classifiers. The study also compared the performance of different classifiers on image datasets of varying sizes and iteration times, as presented in Table 1 and 2. Additionally, the study compared the machine-learning approach with the deep-learning approach, as discussed in earlier work using CNN [26], for the same image dataset. The accuracy of the deep-learning approach was measured using a confidence value, while the machine-learning approach measured accuracy using TPR, FPR, PPV, and FDR values. The twenty-two classifiers were used to identify bikes, cars, and trucks.

The study found that SVM and KNN classifiers have True Positive Rates of almost 90%, while the Positive Predictive Values in SVM classifiers are above 93%. The False Positive Rates are almost below 10% in SVM classifiers, and False Discovery Rates are below 8% in SVM classifiers. Among the classifiers, the medium Gaussian SVM classifier provides the best accuracy of around 91%. Furthermore, the medium Gaussian SVM classifier was verified and tested on random images, as shown in Figures (4) - (5), which present the predicted and actual objects.

In summary, this study shows that the machine learning approach is effective for vehicle classification, especially when working with smaller amounts of data. The results of this approach outperform those of a deep learning approach, specifically a CNN, for the same dataset. However, the machine learning approach requires structured data and label information, whereas CNN can work with unstructured data and learn from it. In addition, the machine learning approach requires more computational time when working with larger amounts of data, while CNN requires more data to achieve accurate results. Therefore, the approach choice should be based on the specific data and the problem at hand.

The present study demonstrates the potential of machine learning approaches for accurately classifying different types of vehicles from static images. The future scope of this work is to extend the proposed classifier module for real-time applications that classify various objects. In real-time scenarios, classifying different objects requires the simultaneous extraction of feature information and image localization. The proposed work can be further extended to enable the classification of different objects with real-time scenarios using available surveillance systems. For this purpose, a more extensive dataset of various environmental conditions and sizes can be prepared to train the proposed models for accurate and robust object recognition in real time, which can lead to the development of intelligent surveillance systems capable of real-time object recognition with applications in various fields, including security, transportation, and healthcare.

In addition to the limitations mentioned, it should also be noted that the proposed work uses hand-crafted features like SIFT and SURF, which may not be as robust as the features learned by deep convolutional neural networks. Future work could investigate the use of deep learning methods to extract features directly from the image data.

The offered procedure in the study is a machine learning-based vehicle recognition and classification approach, which has several advantages and limitations. One of the significant advantages is that it can achieve high accuracy in vehicle recognition with smaller amounts of data compared to deep learning methods like CNN. Additionally, it provides a more structured approach to data processing, requiring labeled information to classify objects accurately. However, it also has limitations, including a longer computational time when working with larger amounts of data and using hand-crafted features that may not be as robust as deep learning-based features.

The suggested approach has practical applicability in various traffic flow situations, including continuous traffic flow, parking lots, toll facilities, interchanges and intersections, and identifying congestion on urban roads. In a continuous traffic flow situation, the proposed method can monitor traffic and recognize different types of vehicles, such as cars, trucks, and bikes, for better traffic management. In parking lots, the proposed method can help identify different vehicles and prevent unauthorized parking while in toll facilities, it can be integrated into the automatic toll collection system for better efficiency and accuracy.

The presented solution can be used for traffic control and monitoring at interchanges and intersections to prevent accidents and traffic jams. Additionally, it can identify urban road congestion and adjust traffic signals and routes accordingly for better traffic management. Overall, the proposed method can contribute significantly to developing intelligent surveillance systems capable of real-time object recognition, with practical applications in various fields, including transportation and security.

Furthermore, while the proposed work focuses on vehicle classification, it may generalize poorly to other object categories. Thus, future work could explore the applicability of this approach to other object recognition tasks. Additionally, the proposed work assumes that images are captured from a stationary camera, which may not be the case in real-world scenarios. Future work could investigate this approach's use in moving camera scenarios.

Finally, the proposed work has potential practical applications in the field of transportation, particularly in developing more efficient and accurate toll-collection systems. Further research could explore integrating this approach into such systems to improve their functionality and reduce traffic congestion.

(Received February 2023, accepted February 2023)

REFERENCES

[1] Trivedi, J., Devi, M.S. and Dave, D. (2017), ” Review Paper on Intelligent Traffic Control system using Computer Vision for Smart City”, Int. Jour. of Sci. & Engi. Res., Volume 8, Issue 6, pp.14-17.

[2] Russo, F., Rindone, C., Panuccio Panuccio P. (2016)," European plans for the smart city: from theories and rules to logistics test case, European Planning Studies," 24:9, 1709-1726, DOI:10.1080/09654313.2016.1182120

[3] Croce, A., Musolino, G., Rindone, C., and Vitetta A. (2019), “Transport System Models and Big Data: Zoning and Graph Building with Traditional Surveys, FCD and GIS”, Int. J. Geo-Inf., 8(4), 187, DOI:10.3390/IJGI8040187

[4] Hardin, P. and N. Thomson, C. (1992), "Fast Nearest neighbor Classification Methods for Multispectral Imagery", Professional Geographer 44 (2): 191–202, DOI:10.1111/J.0033-0124.1992.00191.X

[5] Ghosh, A. K. (2007), "On Nearest Neighbor Classification Using Adaptive Choice of K" Journal of Computational and Graphical Statistics 16 (2): 482–502, DOI:10.1198/106186007X208380

[6] Breiman, L. (2001), “Random Forests”, Machine Learning 45, 5–32,

[7] DOI: https://doi.org/10.1023/A:1010933404324

[8] Loh, W. (2002), "Regression Trees with Unbiased Variable Selection and Interaction Detection", Statistica Sinica 12, 361-386.

[9] Paensuwan, N., Yokoyama, A., C. Verma, S., and Nakachi Y. (2012) "Application of Decision Tree Classification to the Probabilistic TTC Evaluation" Journal of International Council on Electrical Engineering 1(3):323–30, DOI:10.5370/JICEE.2011.1.3.323

[10] Wen, X., Shao, L., Xue, Y., Fang, W. (2015), "A Rapid Learning Algorithm for Vehicle Classification" Information Sciences 295: 395–406, DOI:10.1016/j.ins.2014.10.040

[11] Kim, J. Jeonghyun Baek, J. and Kim, E. (2015), "A Novel On-Road Vehicle Detection Method Using ΠHOG" IEEE Transactions on Intelligent Transportation Systems 16 (6): 3414–29, DOI:10.1109/TITS.2015.2465296

[12] Stocker, M., Silvonen, P., Rönkkö, M., and Kolehmainen, M. (2016), "Detection and Classification of Vehicles by Measurement of Road-Pavement Vibration and by Means of Supervised Machine Learning" Journal of Intelligent Transportation Systems: Technology, Planning, and Operations 20 (2): 125–37, DOI:10.1080/15472450.2015.1004063

[13] Arinaldi, A., Arya Pradana, J., and Arventa Gurusinga, A. (2018), "Detection and classification of vehicles for traffic video analytics", Procedia Computer Science 144:259-68, DOI:10.1016/j.procs.2018.10.527

[14] Atiya, A. (2005), "Learning with Kernels: Support Vector Machines, Regularization, Optimization, and Beyond", IEEE Transactions on Neural Networks, 16 (3), DOI:10.1109/tnn.2005.848998

[15] Sarikan, S., Ozbayoglu, A., and Zilci, O. (2017), "Automated Vehicle Classification with Image Processing and Computational Intelligence" Procedia Computer Science 114:515–22, DOI:10.1016/J.PROCS.2017.09.022

[16] Gorges, C., Öztürk, K., Liebich R. (2018), "Road Classification for Two-Wheeled Vehicles" Vehicle System Dynamics 56 (8): 1289–1314, DOI:10.1080/00423114.2017.1413197

[17] Bautista, M. C., Dy, A. C., Manalac, I. M., Orbe, A. R. and Cordel, M. (2016), "Convolutional neural network for vehicle detection in low-resolution traffic videos," IEEE Region 10 Symposium, pp. 277-281, DOI:10.1109/TENCONSPRING.2016.7519418

[18] Bansal, D., Khanna, K., Chhikara, R., Kumar Dua, R. and Malhotra, R. (2020), "Classification of Magnetic Resonance Images using Bag of Features for Detecting Dementia", Procedia Computer Science 167, pp. 131–137, DOI:10.1016/j.procs.2020.03.190

[19] Pranata, Y. D., Wang, K.C., Wang, J.C., Idram, I., Lai, J.Y., Liu, J.W., and Hsieh, I.H. (2019), "Deep learning and SURF for automated classification and detection of calcaneus fractures in CT images," Computer Methods and Programs in Biomedicine 171, pp.27–37, DOI: https://doi.org/10.1016/j.cmpb.2019.02.006

[20] Sykora, P., Kamencay, P., and Hudec, R. (2014), "Comparison of SIFT and SURF Methods for Use on Hand Gesture Recognition Based on Depth Map", AASRI Conference on Circuits and Signal Processing (CSP 2014), pp- 19 – 24, DOI:10.1016/j.aasri.2014.09.005

[21] Ignat, A. and Pavaloi, I. (2021), "Keypoint Selection Algorithm for Palmprint Recognition with SURF", 25th Inter. Conf. on Knowledge-Based and Intelligent Information & Engineering Systems, Procedia Computer Science 192, 270–280, DOI: 10.1016/j.procs.2021.08.028

[22] Anzid, H., Le Goic, G., Mammass, D., Bekkari, A. and Mansouri, A. (2019), "Multimodal Images Classification using Dense SURF, Spectral Information and Support Vector Machine", Second International Conference on Intelligent Computing in Data Sciences, Procedia Computer Science 148, pp-107–115, DOI:10.1016/j.procs.2019.01.014

[23] LoweDavid, G. (2004), "Distinctive Image Features from Scale-Invariant Keypoints", International Journal of Computer Vision 60 (2): 91–110.

[24] Bay, H., Tuytelaars, T., and Gool L. (2006), "SURF: Speeded Up Robust Features." Computer Vision, ECCV 404–17, DOI:10.1007/11744023_32

[25] https://in.mathworks.com/help/stats/choose-a-classifier.html.

[26] https://www.analyticsvidhya.com/blog/2021/10/support-vector-machinessvm-a-complete-guide-for-beginners/

[27] Trivedi, J., Devi, M.S. and Dave, D. (2021), "Vehicle classification using the convolution neural network approach," Scientific Journal of Silesian University of Technology. Series Transport, 112, 201-209. ISSN: 0209-3324. DOI: https://doi.org/10.20858/sjsutst.2021.112.7.16

[28] Trivedi, J., Devi, M.S. and Dave, D. (2018), "Vehicle Counting Module Design in Small Scale for Traffic Management in Smart City", IEEE, 3rd Int. Conf. for Convergence in Tech. (I2CT), DOI: 10.1109/I2CT.2018.8529506

ATTACHMENTS

Annexure-I Number of features for different vehicles.

Sr . No.	Number of test images	Image class /Extracted Number features			
		Bikes A	Cars B	Trucks C	Total Number of Features
1	100	95783	67389	77560	161733
2	200	201081	140479	157553	337149
3	300	294684	204318	232975	490362
4	400	399111	273086	305896	655407
5	500	506155	344331	388061	826395
6	600	603543	420279	465669	1008669
7	700	696414	489869	549068	1175685
8	800	789421	552722	637420	1326534
9	900	886088	622349	724289	1493637
10	1000	986129	688459	826715	1652301

Annexure-II Vehicle classification using different classifiers.

	Decision Trees														
	Fine Trees					**Medium Trees**					**Coarse Trees**				
	B	C	T	TPR (%)	FPR (%)	B	C	T	TPR (%)	FPR (%)	B	C	T	TPR (%)	FPR (%)
B	1170	296	134	73	27	1153	336	111	72	28	966	520	114	60	40
C	231	1013	356	63	37	241	1023	336	64	36	222	940	438	59	41
T	114	376	1110	69	31	98	498	1004	63	37	114	479	1007	63	37
PPV (%)	77	60	69			77	55	69			74	48	65		
FDR (%)	23	40	31			23	45	31			26	52	35		

	Discriminant Analysis									
	Linear Discriminant					**Quadratic Discriminant**				
	B	C	T	TPR (%)	FPR (%)	B	C	T	TPR (%)	FPR (%)
B	1466	109	25	92	8	1340	242	18	84	16
C	78	1353	169	85	15	95	1450	55	91	9
T	20	168	1412	88	12	65	466	1069	67	33
PPV (%)	94	83	88			89	67	94		
FDR (%)	6	17	12			11	33	6		

	Support Vector Machines (SVM)														
	Linear SVM					**Quadratic SVM**					**Cubic SVM**				
	B	C	T	TPR (%)	FPR (%)	B	C	T	TPR (%)	FPR (%)	B	C	T	TPR (%)	FPR (%)
B	1471	109	20	92	8	1489	96	15	93	7	1496	85	19	94	6
C	77	1376	147	86	14	75	1382	143	86	14	75	1386	139	87	13
T	22	151	1427	89	11	15	135	1450	91	9	14	136	1450	91	9
PPV (%)	94	84	90			94	86	90			94	86	90		
FDR (%)	6	16	10			6	14	10			6	14	10		
	Fine Gaussian SVM					**Medium Gaussian SVM**					**Coarse Gaussian SVM**				
	B	C	T	TPR (%)	FPR (%)	B	C	T	TPR (%)	FPR (%)	B	C	T	TPR (%)	FPR (%)
B	209	1391	0	13	87	1488	95	17	93	7	1467	114	19	92	8
C	0	1600	0	100	0	57	1434	109	90	10	79	1376	145	86	14
T	0	1313	287	18	82	17	147	1436	90	10	33	163	1404	88	12
PPV (%)	100	37	100			95	86	92			93	83	90		
FDR (%)	0	63	0			5	14	8			7	17	10		

	Nearest Neighbor Classifier (NN)														
	Fine KNN					**Medium KNN**					**Coarse KNN**				
	B	C	T	TPR (%)	FPR (%)	B	C	T	TPR (%)	FPR (%)	B	C	T	TPR (%)	FPR (%)
B	1431	105	64	89	11	1480	80	40	93	7	1457	106	37	91	9
C	212	986	402	62	38	200	1123	277	70	30	182	1218	200	76	24
T	76	210	1314	82	18	87	232	1281	80	20	37	285	1218	76	24
PPV (%)	83	76	74			84	78	80			84	76	84		
FDR(%)	17	24	26			16	22	20			16	24	16		
	Cosine KNN					**Cubic KNN**					**Weighted KNN**				
	B	C	T	TPR (%)	FPR (%)	B	C	T	TPR (%)	FPR (%)	B	C	T	TPR (%)	FPR (%)
B	1517	47	36	95	5	1501	56	43	94	6	1483	75	42	93	7
C	252	1054	294	66	34	282	1001	317	63	37	179	1108	313	69	31
T	111	137	1352	85	15	118	156	1326	83	17	70	173	1357	85	15

PPV (%)	81	85	80			79	83	79			86	82	79		
FDR (%)	19	15	20			21	17	21			14	18	21		

	Ensemble Classifier														
	Boosted Trees					**Bagged Trees**					**Subspace Discriminant**				
	B	C	T	TPR (%)	FPR (%)	B	C	T	TPR (%)	FPR (%)	B	C	T	TPR (%)	FPR (%)
B	1340	203	57	84	16	1456	125	19	91	9	1478	100	22	92	8
C	178	1176	246	74	26	176	1232	192	77	23	81	1364	155	85	15
T	74	291	1235	77	23	74	217	1309	82	18	22	179	1399	87	13
PPV (%)	84	70	80			85	78	86			93	83	89		
FDR (%)	16	30	20			15	22	14			7	17	11		

	Subspace KNN					**RUSBoosted Trees**				
	B	C	T	TPR (%)	FPR (%)	B	C	T	TPR (%)	FPR (%)
B	1516	49	35	95	5	1147	351	102	72	28
C	221	1052	327	66	34	277	967	336	62	38
T	75	130	1395	87	13	102	484	1014	63	37
PPV (%)	84	85	79			75	54	70		
FDR (%)	16	15	21			25	46	30		

ENVIRONMENT

GIS Analysis, Eco tourism

Editors

Prof. Ph.D. Jovan Đuković,
Prof. Ph.D. Svjetlana Radmanović (Cupać)

Original scientific article
http://dx.doi.org/10.59456/afts.2023.1528.057L

GIS ANALYSIS OF THE VULNERABILITY OF FLASH FLOODS IN THE POREČKA RIVER BASIN (SERBIA)

Lukić Ana[1]

[1]*PhD student, University of Belgrade, Faculty of Geography and Public enterprise Roads of Serbia, Belgrade, Serbia, E-mail: analukic48@gmail.com*

ABSTRACT

The aim of this study is to identify and map the zones of different vulnerability to flash floods based on the geospatial analysis of natural conditions in the Porečka River basin (Republic of Serbia). The analysis covers the catchment area of the Porečka River (493.82 km^2). Geospatial analysis was conducted using GIS software (QGIS 3.18). The Flash Flood Potential Index (FFPI) was used to determine the terrain's predisposition to flash floods, where the input data for determining the value of the index were the values of the following coefficients: the terrain slope, the type of geological substrate, the way of land use, and the bareness of the terrain.

The analysis determined that 50.43% of the total territory of the basin belongs to the class of high and very high susceptibility to flash floods, and when looking at the length of watercourses in the basin, that percentage is 81.94%. The results of this study clearly indicate the advantages of using modern GIS technologies in the land use and risk management. Geospatial analysis is of particular importance in the field of managing regions that stand out as particularly vulnerable to some natural disasters.

Key words: *Flash floods, natural disasters, Porečka river, FFPI, GIS*

INTRODUCTION

Natural disasters are variations and extreme events which cause damage and destruction to human life safety, economic development, the living environment and resources [1]. Natural disasters are phenomena that disrupt the stability of natural systems by the action of natural processes, which have recently been significantly modified by anthropogenic influence [2]. Floods are natural hydrological disasters that cover with water areas that are not normally covered by water, whereby the consequences vary and can be catastrophic for the economic development of society, the environment, human lives, and health, as well as cultural heritage [3].

As a special type of flooding on watercourses, torrential floods are distinguished. Their occurrence is related to torrential watercourses, whose basic characteristic is a small amount of water during most of the year, but large flows after intense rainfall [2]. After intense rainfall, in addition to a large amount of water, a large amount of alluvial and other material (sand, gravel, mud, stones, leaves, branches, and even waste that previously reached the riverbeds) is carried by the riverbeds. A torrential mass formed in this way can negatively affect the environment.

The research area covers the Porečka River basin, which due to its natural features, which favor the occurrence of flash floods, is susceptible to the occurrence of such disasters. The Porečka River, like other rivers that belong to the Black Sea Basin in the territory of the Republic of Serbia, is

characterized by upper flows that have the characteristics of mountain rivers, large falls, and significant water speed, while the lower part has a wide bed, smaller falls with frequent meanders. In river basins with these characteristics, water management problems are common, such as floods, and sometimes strong soil erosion with the occurrence of flash floods [2].

The main goal of this research is the data collection and creation of a database on the natural characteristics of the Porečka River basin area, the application of various methodological procedures and GIS, on the basis of which the geospatial analysis of the collected data was performed, then the identification and mapping of zones at different risk of flash floods.

STUDY AREA

The Porečka River basin is located in the eastern part of the Republic of Serbia (Map 1 and 2). Administratively, it belongs to the Bor district. The largest part of the basin is located in the territory of the municipality of Majdanpek (71.55 %), while a smaller part includes the areas of the municipalities of Bor (26.52%) and Negotin (1.93%). The river catchment area extends from the West 21° 56′ 36″ to na East 22° 15′ 04″ longitude, and from South 44° 09′ 52″ to North 44° 27′ 31″ latitute, Figure 1. The study area covers 493.82 km^2 in total.

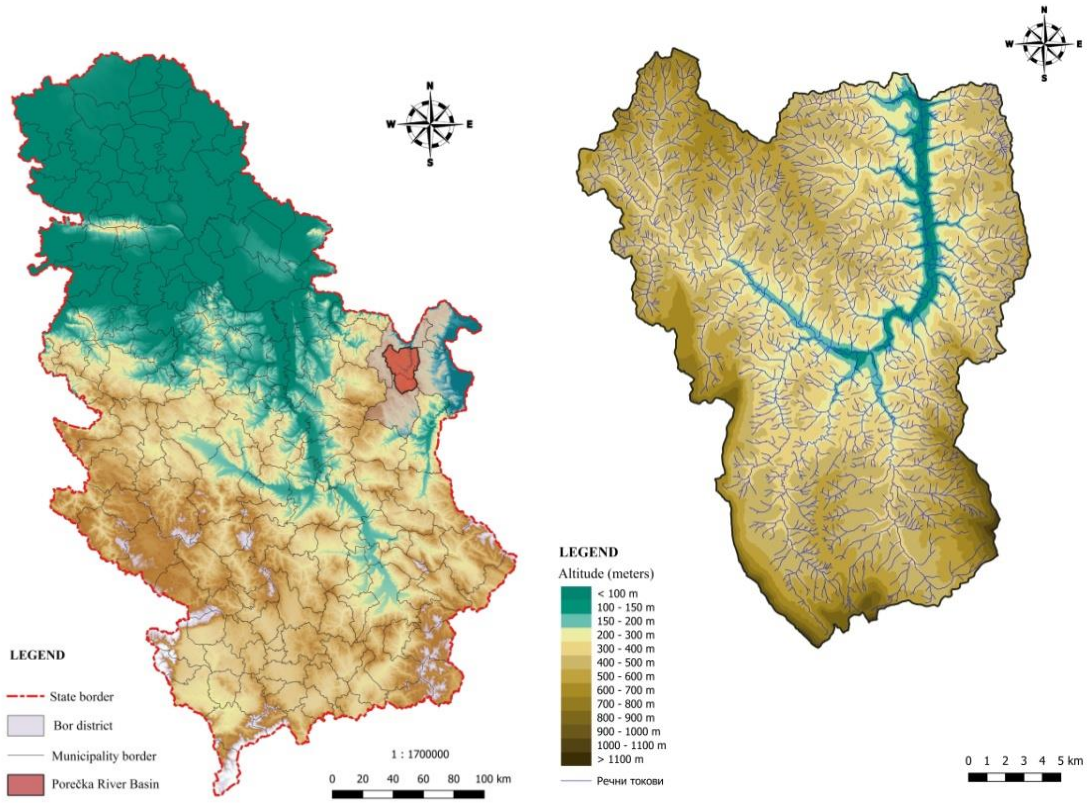

Figure 1. Map 1 and 2: Geographical location of the Porečka River Basin (Serbia)

The Porečka River, 21 km long, belongs to the Black Sea Basin and is a tributary of the Đerdap Lake (Danube River). It is formed by the joining of two rivers - Šaška (25.5 km) and Crnajka (18 km). The Crnajka River rises at the foot of the Deli Jovan mountain, and the Šaška River rises on the Liškovac mountain. The Porečka River flows through a wide valley plain where it meanders and receives 24 tributaries [5].

With the construction of HPP Đerdap I, its mouth was submerged and the Poreč Bay (4 km long) was formed, which is the largest bay of the Danube in the lower part of the course. The length of the watershed border is 122.60 km. The density of the river network is 2.34 km/km². The topography of the watershed is mainly hilly and mountainous and consists of mountains: Mali Krš, Veliki Krš, Deli Jovan, Stol i Liškovac.

The watershed area is characterized by a continental climate, but two characteristic microclimate areas are distinguished: the coastal belt of the Đerdap Lake with the Poreč Bay, with a moderate climate, and the hill-mountain belt with a colder climate and more snowfall [6]. The area of the watershed is largely covered by forest vegetation (68.04 % of the total area). The northeastern part of the Porečka River basin (7.63% of the total area) is located on the territory of the "Đerdap" National Park, which is considered to be very important from the point of preserving biodiversity and natural values.

MATERIAL AND METHODS

For the purpose of analyzing the risk of flash floods in the Poreč River basin, a method was used to determine the predisposition of the territory to the occurrence of flash floods - Flash Flood Potential Index (FFPI). The goal of the FFPI is a quantitative description of the risk of flash floods for a certain area, based on the characteristics of that area such as slope, type of soil (geological base), land use, and vegetation cover characteristics [7]. FFPI is calculated according to the formula [8]:

$$FFPI = \frac{M + S + L + V}{4}$$

Where: M – terrain slope coefficient, S – coefficient of the type of geological substratum, L – land use coefficient, V – terrain bareness coefficient. The values of the coefficients range from 1 to 10 (from the least susceptible to flooding to the most susceptible).

The terrain slope coefficient (M) was calculated on the basis of a DEM - Digital Elevation Model, with a resolution of 25 m. The DEM was taken from the database of the European Environment Agency (EEA) [9]. First, the slope is determined, which is expressed as a percentage, and then the following formula is applied:

$$M = 10^{n/3}$$

Where: n – slope (%) . If n ≥ 30%, then always M = 10.

To determine the coefficient of the type of geological substrate, data on the type of geological substrate obtained from basic geological maps were used, sheets: Donji Milanovac L34-129 [10], Bor L34-141 [11], Žagubica L34-140 [12] and Kučevo L34-128 [13]. Different types of rocks were assigned different coefficient values depending on their characteristics, and in connection with the susceptibility of such terrain to the occurrence and development of flash floods (Table 1).

Table 1: Coefficient values of the type of geological substrate

Type of rock	The value of the coefficient
Alluvial sediments	2
River terrace sediments	4
Deluvium-proluvium	8
Rock creep	8
Travertine	9
Tertiary clastic sediments	9
Volcanoclastic rocks	9
Igneous rocks	4
Mesozoic clastic sediments	8
Mesozoic carbonate and clastic sediments	7
Mesozoic carbonate sediments	5
Ultramafites	8
Paleozoic carbonate and clastic sediments	7
Paleozoic clastic sediments	8
Metamorphic rocks	7

The land use coefficient was obtained based on data from the digital database of the EEA - CORINE Land Cover (CLC, 2018) [14]. Each class is assigned values from 1 to 10, depending on the characteristics important for the occurrence and development of flash floods (Table 2).

Table 2: Land use coefficient values

CLC code	CORINE Land Cover class	The value of the coefficient
112	Discontinuous urban fabric	3
131	Mineral extraction sites	9
231	Meadows	6
242	Complex cultivation patterns	8
243	Land principally occuped by agriculture	7
311	Broad-leaved forests	4
313	Mixed forests	3
321	Natural grassland	5
324	Transitional woodland shrub	5
333	Sparsely vegetated areas	9
511	Water courses	1

The terrain bareness coefficient was obtained by analyzing multispectral images from the Sentinel-2 and Landsat 8 satellites taken from the Geological Topographic Institute in the USA [15]. BSI (Bare Soil Index) index was calculated for the researched area, according to the formula:

$$BSI = \frac{(SWIR+R)-(NIR+B)}{(SWIR+R)+(NIR+B)}+1$$

Where: SWIR - is the value of the short-wave infrared part of the spectrum, R - is the value of the red part of the spectrum, NIR - is the value of the near-infrared part of the spectrum, B - is the value of the blue part of the spectrum of electromagnetic radiation.
BSI is mainly used to distinguish between agricultural and non-agricultural land. The values of the BSI index range from 0 to 2 [16]. Given that the values of the bare terrain coefficient range from 1 to 10, in order to obtain such values, the dependence between the values was determined and a formula was obtained that was used for the final calculation of the coefficient:

$$V = 7.63 * \ln(BSI) + 8$$

After determining the value of each individual coefficient, the FFPI was calculated. Then, based on the analysis of the obtained FFPI values, the results were classified into four classes, according to the degree of susceptibility to floods. By analyzing the spatial distribution of FFPI values within the researched area, all watercourses were classified into 4 classes, which represent the possibility of flash floods occurring on them under appropriate conditions.

Geospatial analysis was conducted using GIS software (QGIS 3.18). The GIS method enables the wide application of quantitative methods and sophisticated technology. The availability of a large amount of data enables a deeper analysis of the landscape and more detailed land use planning. Computer technology, the application of GIS and various research methods have found wide application in the analysis of the natural conditions of the area, its susceptibility to natural disasters and finding solutions for the protection of the area and the repair of the resulting damage.

RESEARCH RESULTS

In order to identify the potential for the occurrence of flash floods, the determination of the FFPI was carried out, and as a prerequisite, the determination of the slope coefficients of the terrain, the type of geological substrate, the method of land use, and the bareness of the terrain was carried out. The values of the coefficients range from 1 to 10 (from the least susceptible to flash floods to the most susceptible).

Pronounced slopes in the hydrographic network and on the slopes of the watershed contribute to the intensification of rapid surface runoff, which shortens the time of water concentration in torrential flow [17], thus the slope of the terrain significantly affects the emergence and development of torrential flows and then torrential floods. Terrains with a slope coefficient of 10 occupy 33.37% of the total basin area. These are terrains with a slope of more than 16°, which are classified as very sloping and steep [18]. Terrains with a slope coefficient between 7 and 10 occur on 13.25% of the total area.

The spatial distribution of slope coefficient values and the distribution of slopes expressed in degrees (°) can be seen on Figure 2, and their percentage share in the total area of the basin is shown in Table 3.

The lithological composition of the terrain is considered an important modifier of natural processes in the watershed [19]. The geological structure is one of the factors that significantly influence the density of the hydrographic system and the size of the runoff. Very important characteristics of the geological substratum, on which the formation of conditions for the formation of torrential flows depend, are resistance and granulometric composition.

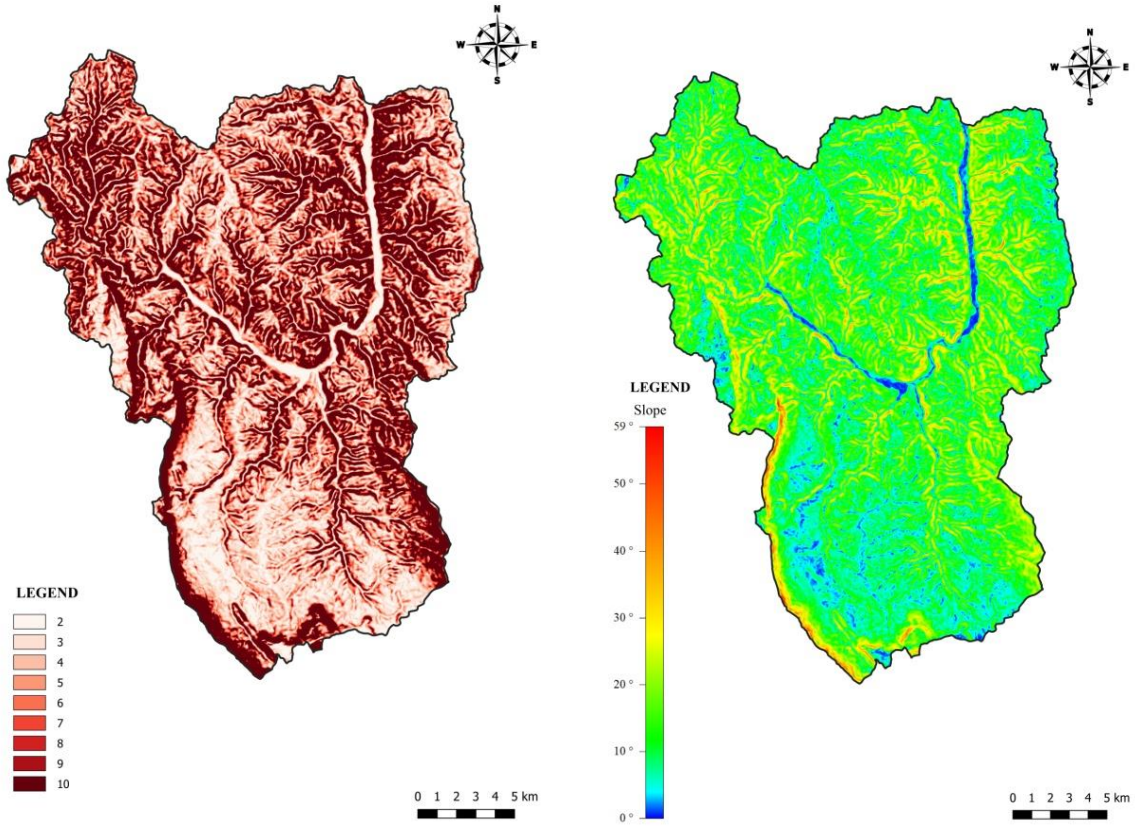

Figure 2. Map 3 and 4: Spatial distribution of slope coefficient values (3);
Terrain slope of the Porečka river basin (4)

Terrains assigned a value coefficient between 7 and 10 were evaluated as exceptionally susceptible types of geological substrate for the occurrence and development of torrential flows, and then floods. The coefficients were assigned according to the characteristics of the rocks, i.e. according to their susceptibility to torrential flows. Among them, the most common are metamorphic rocks, which occur at 36.44%. Other rock types rated as extremely vulnerable occupy 21.53% of the total area.

Therefore, highly susceptible terrains for the development of torrential flows occupy 57.97% of the total area of the basin. The spatial distribution of the types of geological substrate can be seen on Figure 3, while the percentage share in the total area of the basin is shown in Table 4.

Table 3: The value of the terrain slope coefficient and the terrain slope class of the Porečka River Basin

Coefficient value	Area (km^2)	Share in the total area (%)	Slope (°)	Area (km^2)	Share in the total area (%)
2	53.5	10.83	< 5	50.39	10.2
3	73.48	14.88	5 - 10	128.88	26.1
4	58.96	11.94	10 - 15	128.47	26.02
5	44.33	8.98	15 - 20	94.14	19.06
6	33.36	6.75	20 - 25	54.46	11.03
7	26.21	5.31	25 - 30	24.77	5.02
8	21.47	4.35	30 - 35	9.11	1.85
9	17.72	3.59	35 - 40	2.6	0.53
10	164.78	33.37	> 40	0.998	0.2

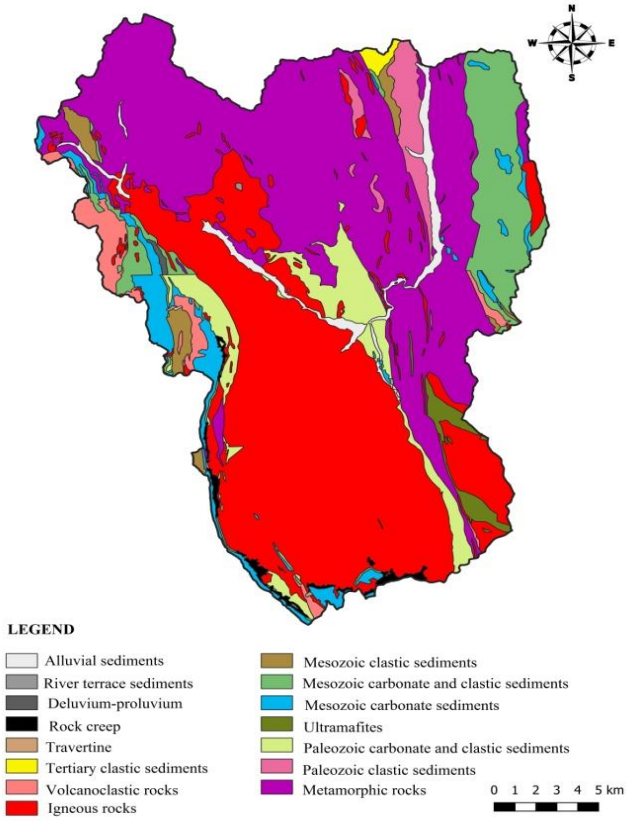

Figure 3. Map 5: Geological map of the Porečka River basin

Table 4: Geological structure of the Porečka River basin and coefficient values of the geological substratum

Type of rock	Area (km^2)	Share in the total area (%)	Coefficient values
Alluvial sediments	10.71	2.17	2
River terrace sediments	0.10	0.02	4
Deluvium-proluvium	0.52	0.11	8
Rock creep	3.51	0.71	8
Travertine	0.12	0.02	9
Tertiary clastic sediments	1.59	0.32	9
Volcanoclastic rocks	11.30	2.29	9
Igneous rocks	179.00	36.25	4
Mesozoic clastic sediments	7.42	1.50	8
Mesozoic carbonate and clastic sediments	38.33	7.76	7

Mesozoic carbonate sediments	17.73	3.59	5
Ultramafites	5.44	1.10	8
Paleozoic carbonate and clastic sediments	26.53	5.37	7
Paleozoic clastic sediments	11.61	2.35	8
Metamorphic rocks	179.94	36.44	7

Vegetation cover affects the process of emergence and formation of torrential water in different ways, considering that its presence improves the water regime of the soil and reduces surface runoff. In the case of the existence of forest cover, it is important to analyze its quality and composition, considering that degraded forests have less positive influence on the runoff regime compared to forests of good structure [19,20].

Vegetation increases unevenness on the land, which slows down the surface runoff of precipitation and increases the possibility of water infiltration into the soil [21]. Areas without or with very little vegetation, especially when they are under steep slopes, create the most favorable conditions for rapid surface runoff and the formation of torrential flood waves. However, areas under the forest cause weaker ascending currents, which increase the amount of precipitation by as much as 10% compared to the surrounding terrain [22]. On the contrary, barren areas and areas with scanty vegetation, especially when they are on steep slopes, create the most favorable conditions for rapid surface runoff and the formation of torrential flood waves. Proper forest management represents a significant contribution to a balanced runoff regime in the basin without the occurrence of frequent and catastrophic flash floods [20].

According to obtained results, mineral extraction sites and sparsely vegetated areas occupy 0.51% of the territory, followed by different types of agricultural land such as complex cultivation patterns (13.24%) and land principally occuped by agriculture (12.54%), which are represented 25.78% of the total area of the basin.

The spatial distribution of land use classes is shown on Figure 4, and the percentage share of different classes in the total area of the basin is given in Table 5.

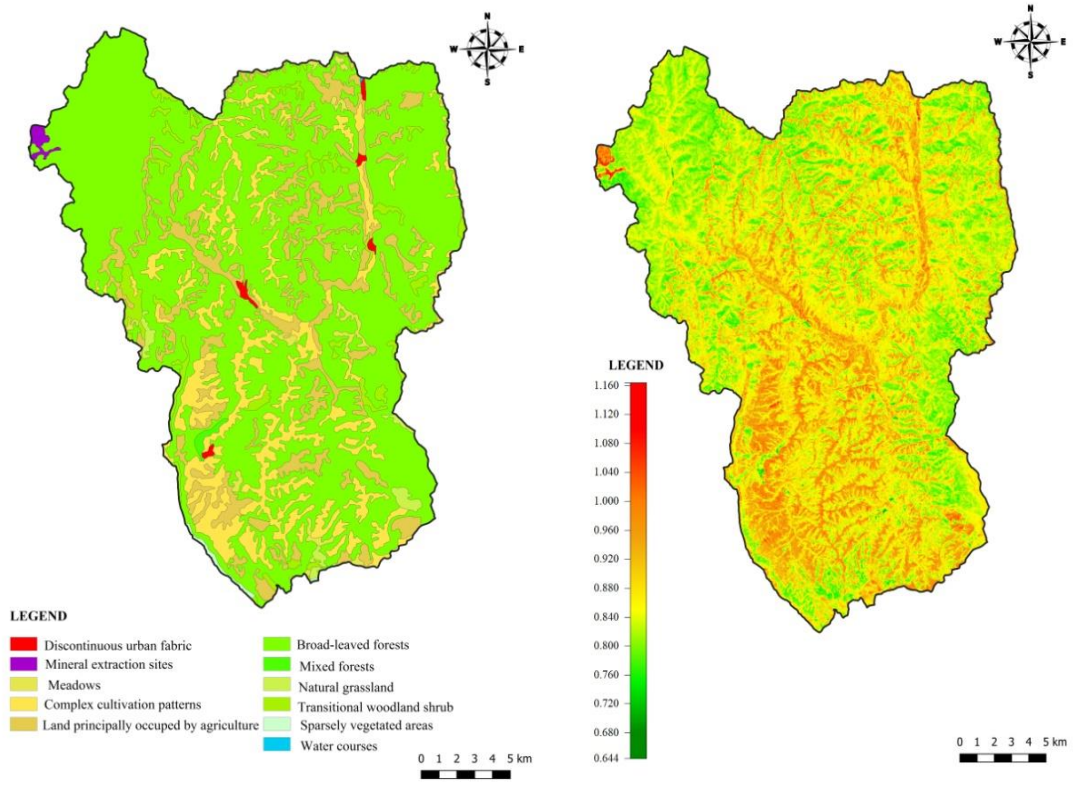

Figure 4. Map 6 and Map 7: Land use in the Porečka River basin (CORINE land cover) (6); Spatial distribution of the soil bareness coefficient (7)

Table 5: Land use classes and land use coefficient values

CLC code	CORINE Land Cover class	Area (km^2)	Share in the total area (%)	Coeff. values
112	Discontinuous urban fabric	1.65	0.33	3
131	Mineral extraction sites	1.39	0.28	9
231	Meadows	7.153	1.45	6
242	Complex cultivation patterns	65.38	13.24	8
243	Land principally occuped by agriculture	61.91	12.54	7
311	Broad-leaved forests	334.96	67.83	4
313	Mixed forests	1.03	0.21	3
321	Natural grassland	4.28	0.87	5
324	Transitional woodland shrub	14.90	3.02	5
333	Sparsely vegetated areas	1.12	0.23	9
511	Water courses	0.05	0.01	1

The soil bareness coefficient indicates the difference between agricultural and non-agricultural land, that is, the magnitude of the change in bare soil. Agricultural areas, sparsely vegetated areas, mineral extraction sites, urban fabric areas, and in some places areas of meadows, lawns, and pastures have a higher value, while areas under forests and woody shrubby vegetation (Transitional woodland shrub) have lower values. The spatial distribution of the values of the soil bareness coefficient is shown on Figure 4, Map 7.

The values of all the mentioned coefficients were imported into the FFPI calculation formula [8] using GIS software (QGIS 3.18), and the spatial distribution of the obtained index is shown on Figure 5, Map 8. After the classification of the obtained FFPI values, it was determined that the class of very

high susceptibility is represented at 7.54%, and high susceptibility at 42.90% of the total area of the basin. The class of medium susceptibility occupies 36.62 %, and the low 12.94 % of the total area of the basin.

The spatial distribution of susceptibility classes for the occurrence of flash floods is given on Figure 5, Map 9, while the percentage share of classes in the total area is shown in Table 6.

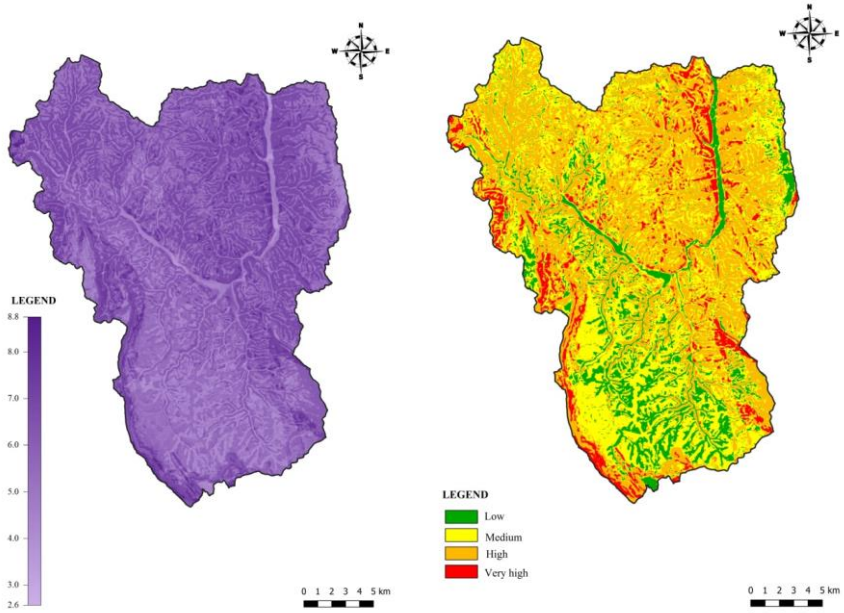

Figure 5, Map 8 and 9: Spatial distribution of FFPI in the territory of the Porečka River basin; Classes of susceptibility to flash floods in the Porečka River basin

Table 6: Share (%) of susceptibility classes to flash floods in the Porečka River basin

Susceptibility to flash floods	Area (km^2)	Share in the total area (%)
Low	63.91	12.94
Medium	180.86	36.62
High	211.83	42.90
Very high	37.22	7.54

When it comes to the Šaška River basin, 7.23% of the total area of the basin belongs to the class of very high susceptibility, and 39.31% of the total area belongs to the class of high susceptibility. The class of medium susceptibility includes 38.92 %, and low 13.94 % of the total area of the basin. In the Crnajka River basin, 5.68% of the total area of the basin belongs to the class of very high risk, and 31.56% to the high class.

The class of medium susceptibility occupies 41.33 %, and low 21.43 % of the total area of the basin. In the part of the Porečka River basin downstream from the confluence of the Šaška River and the Crnajka River, the very high vulnerability class extends to 9.08% of the total area of that part of the basin, and the high susceptibility class to 53.97%.

By analyzing the obtained results, it can be concluded that the Šaška River basin is more susceptible to flash floods than the Crnajka basin, and data on the representation of susceptibility classes for these

two rivers can be seen in Table 7. When observing the entire basin of the Poreč River, the most susceptible to flash floods is the part downstream from the composition of the Šaška River and the Crnajka River. More detailed results can are shown in Table 8.

Given that the predisposition of the terrain for the occurrence and development of flash floods was determined through the calculation of the FFPI, in order to determine the susceptibility of the watercourses themselves for the transport of stormwater, the hydrographic network was overlapped with the previously obtained susceptibility classes.

Table 7: Share (%) of susceptibility classes to flash floods in the Saška River and Crnajka River basins

Susceptibility to flash floods	Area in the Šaška basin (km^2)	Share in the total area of the Šaška basin (%)	Area in the Crnajka basin (km^2)	Share in the total area of the Crnajke basin (%)
Low	32.88	13.94	20.55	21.43
Medium	91.78	38.92	39.64	41.33
High	94.11	39.91	30.26	31.56
Very high	17.06	7.23	5.44	5.68
Total	235.83	100.00	95.89	100.00

Table 8: The share (%) of flash flood susceptibility classes in the part of the Porečka river basin downstream of the Šaška and Crnajka River basins

Susceptibility to flash floods	The area of the part of the Porečka River basin downstream from the composition of the Šaška and Crnajka rivers (km^2)	Share in the total area of the basin (%)
Low	10.46	6.46
Medium	49.38	30.49
High	87.41	53.97
Very high	14.71	9.08
Total	161.95	100.00

In addition, it was determined that 30.54% of the total length of streams in the territory of the basin belongs to the class of very high susceptibility to flash floods. On 51.4% of the total length of the streams, high susceptibility was determined. 14.45% of the total length belongs to the category of the medium, and 3.61% of the total length belongs to the category of low susceptibility to flash floods.

The spatial distribution of watercourses according to classes of susceptibility to flash floods is shown on Figure 6, and the percentage share of each class in the total length of the river network is shown in Table 9.

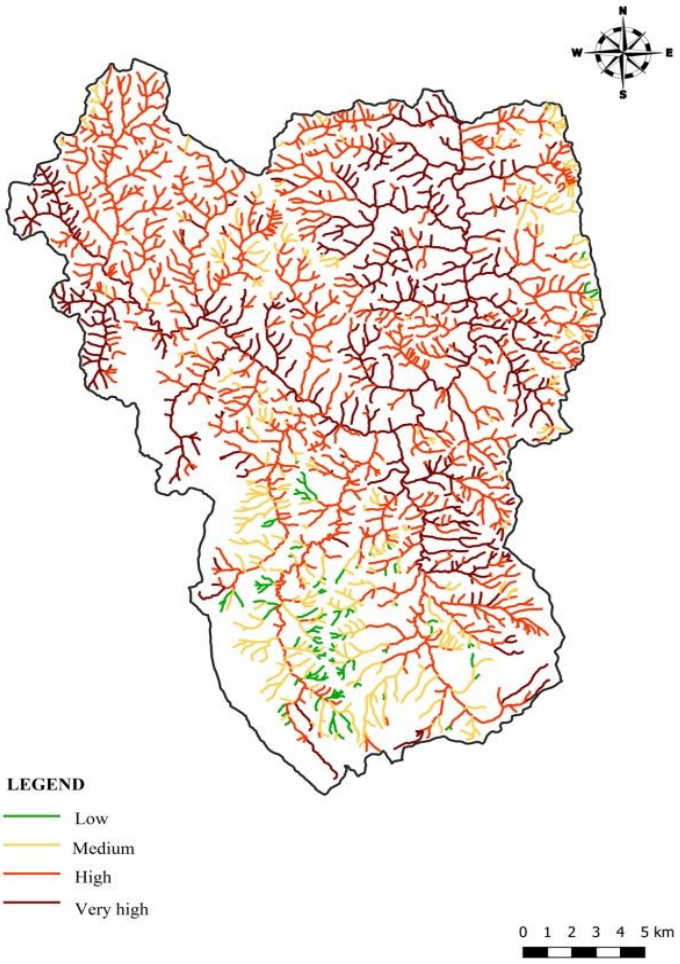

Figure 6. Map 10. Classes of susceptibility to flash floods in watercourses of the Porečka River basin

Table 9: Share (%) of susceptibility classes to flash floods in watercourses of the Porečka River basin

Susceptibility to flash floods	Length (km)	Share in the total length (%)
Low	41.81	3.61
Medium	167.29	14.45
High	594.89	51.4
Very high	353.42	30.54

CONCLUSION

The main goal of this paper was the geospatial analysis of the natural conditions in the Porečka River basin, and the identification and mapping of zones of different vulnerability to flash floods. In order to realize the aforementioned, it was necessary to collect numerous data, create a database on the natural

characteristics of the researched area and apply different methodological procedures through the use of GIS software.

The results show the following: 7.54% of the total area belongs to the class of very high susceptibility to flash floods, and 42.90% of the basin belongs to high susceptibility class - that is, the two classes of highest susceptibility are represented on 50.43% of the total area. In addition, it was determined that 30.54% of the total length of streams belongs to the very high-risk class, and 51.4% of the total length belongs to the high-risk class.

This means that 81.94% of the total length of streams is extremely susceptible to the generation of torrential waters. As a result of the analysis of the susceptibility of the researched area to the occurrence of flash floods, maps were obtained on which the spatial distribution of susceptibility classes was presented. The data obtained from this analysis can represent a starting point in risk

management. Such analyzes can be used in the identification and assessment of risks. Furthermore, the results can be used to define and establish preventive protective measures, protection measures in the event of an accident, and measures to mitigate and eliminate the consequences of the accident.

Received March 2023, accepted March 2023)

LITERATURE

[1] Wei, Y.M., J.L. Jin and Q. Wang (2012). Impact of Natural Disasters and Disasters Risk Management in China: Case of China's Expirience in Wenchuan Eartquaqe. Sawada, Y. and S. Oum (eds.), Economic and Welfare Impacts of Disasters in East Asia and Policy Responses. ERIA Research Project Report 2011-8, Jakarta: ERIA. pp.641-675.
[2] Dragićević, S., Filipović, D. (2009). Natural conditions and disasters in planning and protecting space. Belgrade: University of Belgrade - Faculty of Geography.
[3] European Parliament & Council. (2007). Directive 2007/60/EC on the assessment and management of flood risks. Official Journal of the European Union.
[4] Disaster Risk Assessment in the Republic of Serbia (2015). Ministry of the Interior of the Republic of Serbia.
[5] Pavlović, M. (2018). Geography of Serbia 1. Belgrade: University of Belgrade - Faculty of Geography.
[6] Spatial plan of the municipality of Majdanpek (Official Gazette of the Municipality of Majdanpek no. 15/12).
[7] Tincu, R., Lazar, G. & Lazar, I. (2018). Modified Flash Flood Potential Index in order to estimate areas with predisposition to water accumulation. De Gruyter, 10, 593–606.
[8] Smith, G. (2003): Flash Flood Potential: Determining the Hydrologic Response of FFMP Basins to Heavy Rain by Analyzing Their Physiographic Characteristics. NWS Colorado Basin River Forecast Center, Salt Lake City.
[9] European Environment Agency. (2018). EU-DEM, downloaded from: https://www.eea.europa.eu/data-and-maps/data/eudem
[10] Basic geological map of SFRY, scale: 1 : 100,000, Sheet: Donji Milanovac L34-129. Federal Geological Institute, Belgrade, 1978.
[11] Basic geological map of SFRY, scale: 1 : 100,000, Sheet: Bor L34-141. Federal Geological Institute, Belgrade, 1974.
[12] Basic geological map of SFRY, scale: 1 : 100,000, Sheet: Žagubica L34-140. Federal Geological Institute, Belgrade, 1968.
[13] Basic geological map of SFRY, scale: 1 : 100,000, Sheet: Kučevo L34-128. Federal Geological Institute, Belgrade, 1978.
[14] European Environment Agency. (2018). Corine Land Cover 2018, downloaded from: https://land.copernicus.eu/paneuropean/corine-land-cover/clc2018
[15] https://earthexplorer.usgs.gov/
[16] Polykretis, C., G.Grillakis, M., D. Alexakis, D. (2020). Exploring the Impact of Various Spectral Indices on Land Cover Change Detection Using Change Vector Analysis. A Case Study of Crete Island, Greece.
[17] Ristić, R., Stefanović, M. (2005). Extreme discharges on torrential catchments in Serbia. International Conference on Forest Impact on Hydrological Processes and Soil Erosion, Proceedings, Yundola (280-286).
[18] Zivanović, S. (2015). The influence of morphometric relief parameters on the risk of forest fires. Journal of Forestry, 4, p. 127-138.

[19] Petrović, A. (2014). Factors causing flash floods in Republic of Serbia. Doctoral dissertation. Belgrade: University of Belgrade - Faculty of Forestry.
[20] Kostadinov S., Petrović A. (2013). Forests in Serbia as the Factor of Global Climate Changes Mitigation, Proceeding of the International Conference on Climate and Global Change Impacts on Water Resources. pp. 81-86. WSDAC, UNESCO, Institute "Jaroslav Černi": Belgrade. ISBN 978–86–82565–41–3.
[21] Dukić, D., Gavrilović, Lj. (2008). Hydrology. Belgrade: Textbook Institute.
[22] Živković, N. (1995). The influence of physical-geographical factors on the height of runoff in Serbia. Belgrade: University of Belgrade - Faculty of Geography.

Review paper
http://dx.doi.org/10.59456/afts.2023.1528.069Dj

ECO TOURISM DEVELOPMENT BASED ON NATURAL AND ARTIFICIAL SURROUNDINGS IN SEMBERIJA AND MAJEVICA AREA

Đurić Dijana[1], Topalić Marković Jovana[2]

[1]*Faculty of Civil Engineering Subotica, University of Novi Sad, Serbia*
email: dijana.djuric.gf@gmail.com
[2]*Department of Civil Engineering and Geodesy, Faculty of Technical Sciences, University of Novi Sad, Serbia*

ABSTRACT

Tourism is one of the most developed industries in the world that is continuously growing. It has many different shapes and types with many different factors that affect its success. Over the years, tourism has changed. The new era of tourism is trying to put focus on present environmental problems such as the amount of waste, the use of natural resources and the pollution that it produces as a result of different activities.

In this paper, the effect of natural and artificial resources on the development of three types of eco-tourism is observed on the area of Semberija and Majevica in Bosnia and Herzegovina. Types of tourism that were research are: cultural and heritage tourism, spa (healing) tourism and recreational tourism. All these types have a great presence on the observed area.

The distribution and attendance of the three types of tourism mentioned above is largely dependent on natural elements, such as water and forest areas, which can have both a positive and a negative effect on its development. On the area of Semberija and Majevica, types of tourism largely depend from the location and its surrounding.

Keyword: *eco-tourism, protected areas, cultural and heritage tourism, spa tourism, recreational tourism*

INTRODUCTION

When we talk about the progress of certain parts of the world, some countries or regions, we often come across data that indicates that tourism, as the main industry of that area, has led to the improvement of the living conditions of the population. Today, in the world of migration, internet and developed air traffic, most places are a click away from reality. Nevertheless, it is still a special experience to visit a new place in person. As trips are no longer limited to the rich strata of society, the offer has become more diverse. In order for a location to attract tourists with its content, a lot of investment, marketing and data monitoring is required [1].

Various factors such as natural potentials, history, social status, infrastructure, competitiveness, etc. influence the development of tourism in an area. Tourism itself can have an impact on the economy of the area, through other sectors: construction, transport, agriculture, hospitality, marketing, etc., which affects the growth of employment and increases the standard of living. The combination of historical

and natural factors, as well as the good geographical position of Semberija and Majevica in the entity of Republic of Srpska, give a great opportunity for the development of tourism in this area [1].

The area of Semberija and Majevica in the Republic of Srpska entity is viewed from the aspect of tourism that has minimal environmental consequences and also provides tourists with rest, recreation and entertainment. It should be emphasized that a lot of locations that were intended for this type of tourism have become commercialized and urban, which has lost their original purpose, and that is an escape from urban life. It is crucial not to allow tourism to become an instrument for environmental degradation [2]. Precisely because of this, it is necessary to create a plan with goals that go to the limit of sustainability, and not beyond.

The term ecotourism was formulated by Hector Caballos - Lascuren, a Mexican architect, according to whom ecotourism is an ecologically responsible trip and visit to relatively preserved areas, in order to enjoy nature (and accompanying cultural features - both from the past and present) while improving nature protection, small negative impact of visitors and beneficial active impact on the local population. His definition of ecotourism was officially adopted by the IUCN at the 1st World Congress held in Montreal in 1966 [1,3].

Tourism in the Republic of Srpska entity is regulated through several laws. Those are: Law on Spas [4], Law on Tourism [5], Law on Hospitality [6] and Law on Tourist Tax [7]. There is a single cadastre of tourist sites of the Republic of Srpska on the website www.turizamrs.com [8] under the jurisdiction of the Tourist Organization of the Republic of Srpska. The lower level consists of tourist organizations of cities and municipalities [1].

Despite the existence of laws and a unified online network, tourism in the Republic of Srpska is not aligned in terms of functioning, due to the inadequate involvement of all municipalities. In this way, it is very difficult to determine the percentage of tourists and their ecological footprint, because their movement paths, as well as their stays and visits to localities, are not fully known. Research on that side is scarce and requires a more specific and detailed approach. Thus, the explored area for most foreign tourists is only a passing point to other, inner parts of Bosnia and Herzegovina such as Mostar or Višegrad, which are the most visited cities in the country [9].

On the researched area, tourism has recorded a growth in the number of visitors, overnight stays, accommodation capacity and tourist catering facilities with various activities since 2010 [1, 10,11,12,13,14].

LOCATION AND NATURAL CHARACTERISTICS OF THE AREA

The researched area is located in the northeast of Bosnia and Herzegovina, in Republic of Srpka entity, at the crossroads between Serbia, Croatia and internal Bosnia and Herzegovina. Due to good traffic connections, the first type of tourism that began to develop in this area was transit tourism. This type of tourism was dominant until the early 2000s [8] , when other types of tourism started to develop.

The researched area constists of two natural units, plain Semberija and mountain Majevica and three municipalities, Bijeljina, Ugljevik and Lopare. It belongs to the southern part and the rim of the Pannonian basin and is characterized by the heterogeneity of the relief. From a geomorphological point of view, the researched area can be divided into three parts. These are: the lowland part, the mountain (foothill or transition) part and the mountain part (figure 1). On the whole, it slopes towards the northeast, with the Majevica mountain descending, reducing the altitude to the Semberija plain, which is slightly inclined towards the river mouth of the rivers Drina and Sava. The whole area is intersected by smaller rivers [1].

Deciduous forests have the greatest distribution in the researched area. The presence of forests increases with elevation (figure 2). In the entire researched area, the largest area is covered by forest

communities of Quercus petraea and Quercus cerris and Quercus robur and Carpinus betulus, There are also large expanses communities of Fagus and Quercus petraea forests [1].

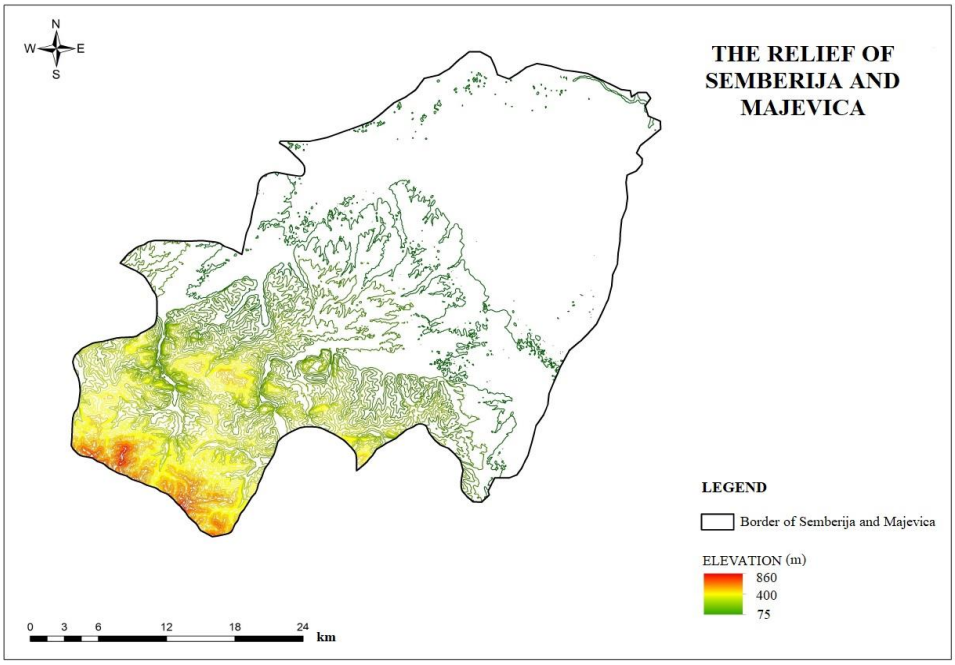

Figure 1. The relief of researched area

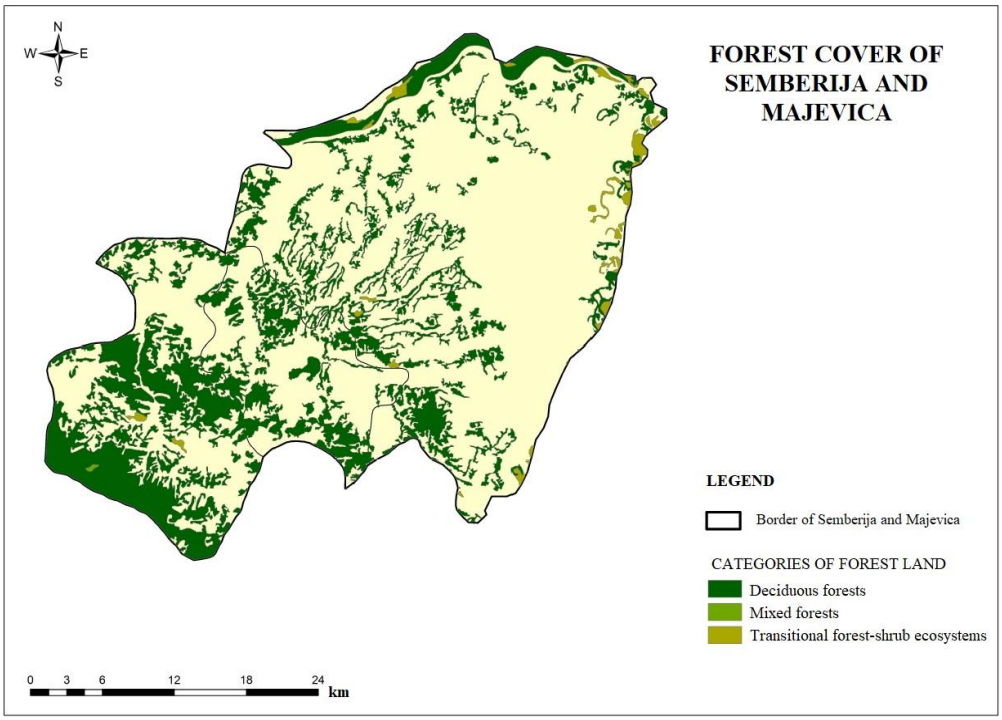

Figure 2. Forest cover of researched area

The researched area belongs to a moderately continental climate, with the presence of a Pannonian (steppe) climate in the part of Semberija. It is characterized by four seasons with equal presence. The main features are hot summers, with maximum temperatures that can sometimes exceed 40°C and cold winters, with temperatures sometimes falling below – 15°C. During the spring, the temperatures rise sharply, while during the autumn they gradually and suddenly drop. The area of Majevica also belongs to a moderately continental climate, with milder summers and slightly harsher winters, with more of snowfall [1].

Despite the most favorable climatic conditions that are present in this area during the spring and autumn months, the number of tourists for all forms of tourism is the highest during the summer months [10,11,12,13,14].

METHODOLOGY

Research included tourist objects and localities that are part of the observed types of tourism: cultural and heritage tourism, spa tourism, recreational tourism. All three types of tourism were observed as eco tourism that have minimal effect on the environment, or can have minimal effect on the environment if used sustainably.

Cultural and heritage tourism type of tourism includes the most visited cultural and historical objects, to which we mostly associate religious objects and historical monuments. The interest of religious buildings, in addition to their spiritual and historical significance, is reflected in the presence of all three faiths, Orthodoxy, Catholicism and Islam, at a short distance, which makes this area very rare in the world. Religious tourism has experienced great growth in the last ten years [1]. Besides religious tourism, for this type we relate also tourist movements motivated by cultural and artistic resources, values and content. Some of the most visited objects and localities of this type of tourism on the researched area are Monastery Tavna (figures 3) and Monastery of Sveta Petka.

Spa tourism in the researched area is linked to Dvorovi Spa (figure 4). The basic form of this type of tourism is reflected in the recreation and health role. The geoecological evaluation carried out for the purposes of the doctoral dissertation on the topic Geoecological problem of Semberija and Majevica in the Republic of Srpska [1] showed that the entire researched area is favorable for the development of health, i.e. spa and recreational tourism.

This type of tourism represents ecologically acceptable tourism that has minimal consequences for the environment and surroundings. Banja Dvorovi has geothermal water that is sodium-calcium hydro carbonate chloride, which makes it possible to treat a wide range of diseases in this institution [15].

Figures 3 and 4. Monastery Tavna (left) and Spa Dvorovi (right)

Recreational tourism includes all types of nature visited tourism, with the basic characteristics of walking or hiking. This type of tourism is relatively new in the researched area and is becoming increasingly popular. In the last 10 years a large number of people have joined various associations that carry out recreational types of tourism, such as walking, hiking, cycling, camping etc. In terms of location, this type of tourism is characteristic for forest areas, so the walking paths, viewpoints and other locations that are visited are mostly at higher altitudes.

Objects and localities that were included in this research are: Orthodox objects, Islamic objects, other cultural objects such as monuments, lakes, waterfalls, spa, caves, viewpoints, camps, picnic areas, restaurants, ethno village and mountain lodge. Location of all objects and places of above described types of tourism in the research area, are observed in the terms of their position relating natural elements, especially water and forest. Their evaluation grade was given based on data from Statistical bulletins from 2015 to 2019 [10,11,12,13,14] and also on subjective effect of the authors and their longterm observation of tourism development on the researched area of Semberija and Majevica, in all three municipalities. The grade included the presence of natural and artificial elements as their surroundings.

RESULTS

On figure 5 are shown the locations of the most visited touristic places on the researched area of Semberija and Majevica. In the tables 1, 2 and 3 are given the lists of all places shown in figure 5, with the evaluation of their visiting rating, from 1 to 5 (1 being the least visited and 5 being the most visited) and the description of surrounding area and closeness to the natural elements.

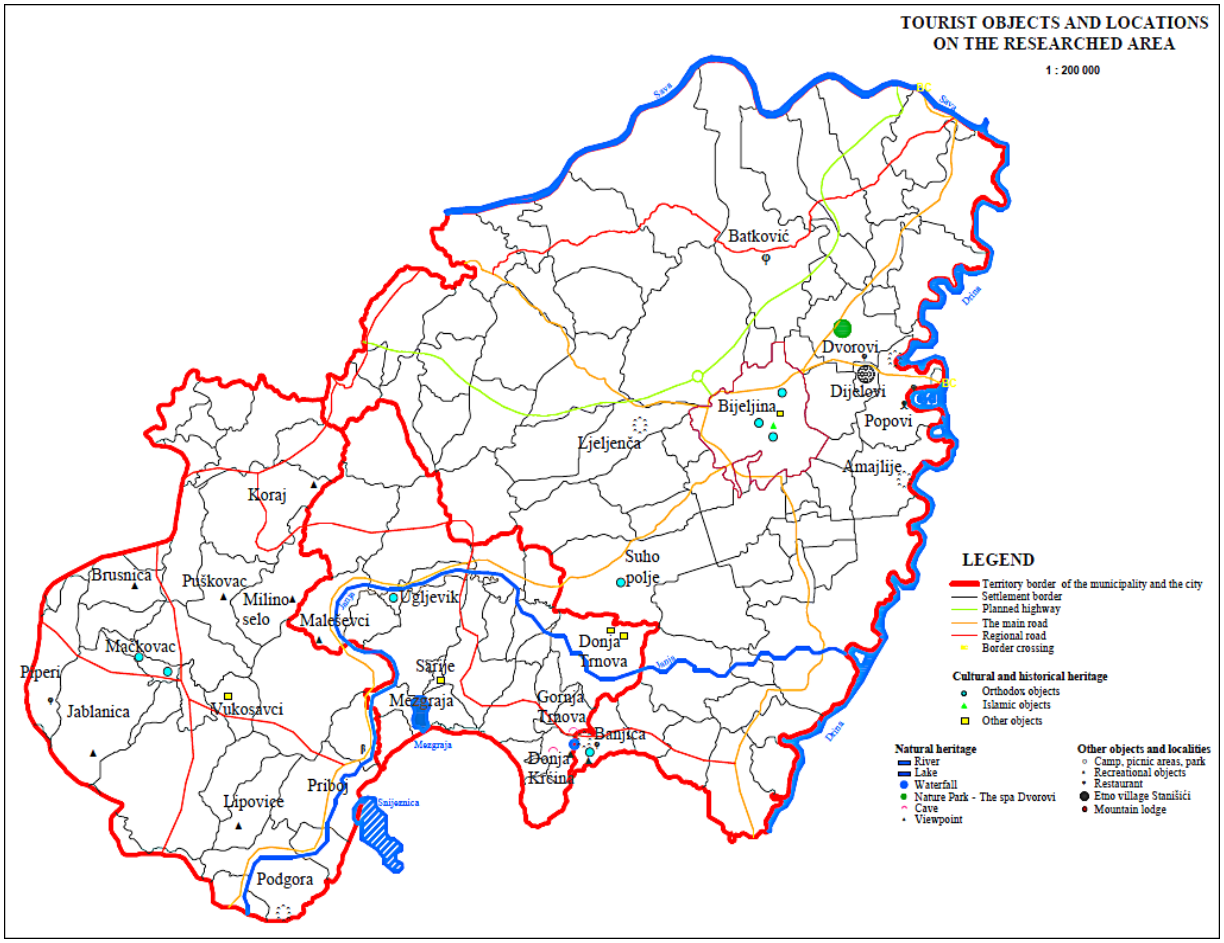

Figure 5. Touristic objects and localities on the researched area

Table 1. List of observed touristic objects and places in the Bijeljina municipality

No	Name	Location (settlement)	Surooundings (natural or artificial)	Visitation grade
1	Eco camp Amajlije	Amajlije	natural/artificial	4
2	Tavna monestery	Banjica	natural	5
3	Starine Novaka lodging	Banjica	natural	4

4	Banjica waterfall	Banjica	natural	3
5	Viewpoint	Banjica	natural	3
6	Eco camp Tavna	Banjica	natural	3
7	Imperia tavern - a small museum of antiquities	Batković	artificial	1
8	Saint Georgije church	Bijeljina	artificial	5
9	Saint Petka monastery	Bijeljina	artificial	5
10	Saint Vasilije Ostroški monastery	Bijeljina	artificial	5
11	Atik mosque	Bijeljina	artificial	5
12	Church of the Immaculate Heart of Mary	Bijeljina	artificial	4
13	Dvorovi spa	Dvorovi	artificial	5
14	Semberski salas	Dvorovi	artificial	5
15	Etno village Stanišići	Dijelovi	artificial	5
16	Picnic area	Ljeljenča	natural/artificial	4
17	Ranch Tanasić	Popovi	natural	4
18	Drinska ruža restaurant	Popovi	natural/artificial	2
19	Eco visitor center The lakes	Popovi	artificial	2
20	Monastery of the Holy Cross	Suho Polje	natural/artificial	2

Table 2. List of observed touristic objects and places in the Ugljevik municipality

No	**Name**	**Location (settlement)**	**Surooundings (natural or artificial)**	**Visitation grade**
1	Novak cave	Gornja Trnova	natural	3
2	Hollow rock cave	Donja Krćina	natural	2
3	Viewpoint Orlović	Donja Krćina	natural	2
4	Memorial complex	Donja Trnova	natural/artificial	4
5	Memorial house Liberation	Donja Trnova	natural/artificial	4
6	Viewpoint Brezovaca	Maleševci	natural	1
7	Mezgraja lake	Mezgraja	natural/artificial	4
8	Jablan city	Sarije	natural	1
9	Russian orthodox church Aleksandar Nevski	Ugljevik	artificial	3

Table 3. List of observed touristic objects and places in the Ugljevik municipality

No	**Name**	**Location (settlement)**	**Surooundings (natural or artificial)**	**Visitation grade**
1	Viewpoint Volujak	Brusnica	natural	1
2	Memorial park Vukosavci	Vukosavci	natural	3
3	Viewpoint Međednik	Jablamica	natural	1
4	Viewpoint Čitluk	Koraj	natural	1
5	Viewpoint Vratilovo	Lipovice	natural	1
6	Church of the Nativity of the Blessed Virgin Mary	Mačkovac	natural/artificial	3
7	Church of Venerable Sisoje Great	Mačkovac	natural/artificial	3
8	Viewpoint Molitvište	Milino selo	natural	1
9	Etno resort Marusa	Piperi	natural	1
10	Eco picnic area Viva natura Busija	Podgora	natural	3
11	Lake Sniježnica	Priboj	natural/artificial	5
12	Viewpoint Udrigovo	Puškovac	natural	1

In total were observed 41 objects and location on the researched area of Semberija and Majevica, 20 in the area of Bijeljina municipality, 9 in the area of Ugljevik municipality and 12 in the area of Lopare municipality. Their evaluation was based on the visitation, and was graded from one (1 – least visited) to five (5 – most visited). Evaluation of visitation of observed objects and locations for the purpose of development of eco tourism, depending on their surroundings, showed different results. Grade five (most visited) was given to 9 places, 8 from which are on the area of Bijeljina municipality. This can be associated with the most urban part of the researched area that has dense and developed traffic network. Therefore, observed objects and locations are easily accessible.

Grade four was given to seven places, five on area of Bijeljina municipality and two on the area of Ugljevik municipality. Surroundings of most of the locations with this grade are natural and artificial. Grade three was given to nine places, three in the area of Bijeljina municipality, two in the area of Ugljevik municipality and four in the area of Lopare municipality. Different types of objects and locations were given this grade.

Grade two was given to five places, three in the area of Bijeljina municipality and two in the area of Ugljevik municipality. Surroundings of all places are natural or the combination of natural and artificial. The lowest grade, one, was given to ten places, one in the area of Bijeljina municipality, two in the area of Ugljevik municipality and seven in the area of Lopare municipality. 7 out of 10 places are viewpoints that are difficult to access.

Closeness to water elements has a great role in the development of touristic objects in all three types of researched tourism. This is notable in all parts of researched area, in the plain and on the mountain, and in all three observed municipalities. Even if the viewpoints do not benefit from the water elements, they are definitely an important asset as the areas close to water elements have the greatest visitation.

Observed by the types of researched tourism, cultural and heritage tourism show little to none connection between natural or artificial surroundings and visitation grade. This can be seen in comparison of Tavna monastery that is completely in natural surroundings and far away from the city and Saint Petka monastery that is in artificial surrounding near the city and the main traffic road. Both have high evaluation, grade five, for visitations. The same goes to other cultural and heritage places, whose visitations mostly depend from the content and less from their surroundings. This type of tourism does not depend from natural or artificial elements.

Spa tourism is related to only one location, Spa Dvorovi. Its surroundings are mostly artificial. Its location had a great impact in the past on the development of this area and transit tourism. Even though spa tourism is one of the main types of tourism in the researched area when we talk about eco tourism, its surroundings and elements are all artificial. Its natural component is based on geothermal energy and its use in health and recreational purposes. Spa Dvorovi is also relatively close to the city center and to the most visited complex in the researched area, Ethno village Stanisici.

Objects and places that belong to recreational tourism record the least visitations, due to their remote locations, high altitudes and a lack of any type of passable roads. They do benefit from natural elements, especially forest presence that gives a silence and peaceful areas suitable for walks, cycling and other types of recreation. However, lack of infrastructure has a great impact on the lack of visits. On Majevica mountain the relief often suddenly changes from cultivated land on slopes to thick, impassable forests. This type of tourism depends from natural elements, but needs adequate infrastructure in order to be passable.

CONCLUSION

Eco tourism largely depends from natural elements. It is seen that way due to the importance of effects that generally tourism has on environment. However, research on the area of Semberija and Majevica showed that tourism is largely dependent from artificial elements, especially infrastructure. Natural elements are important as they represent the peace oasis that is necessary for researched types

of tourism – cultural and heritage, spa and recreational, but they are not sufficient for the object or location to be visited.

Recreational tourism is the one that has the greatest potential from natural surroundings, especially forest and water elements. Those are mainly paths, viewpoints and some objects such as Jablan city. All of them were evaluated with the lowest grades, two and one, mostly due to the lack of artificial elements.

Therefore, natural elements, especially forest has no impact on the development of eco tourism, in obserer types of tourism. Artificial elements, like railroads, are necessary for the development of these areas and also tourism locations. Also other artificial elements, such as catering facilities are necessary for the area to be attracted for visiting.

Received March 2023, accepted March 2023)

REFERENCES

[1] Đurić, D (2021). Geoecological problems of Semberija and Majevica in the Republic of Srpska. Doctoral dissertation, University of Belgrade, Faculty of Geography. Belgrade, Serbia
[2] Ateljević, A. M. (2019). Sustainable tourism in Bosnia and Herzegovina – analysis of the situation based on comparative indicators of the European Commission. Economic ideas and practice, 32, 75 – 88.
[3] Group of authors (2012). Bijeljina Municipality Tourism Development Strategy, The city of Bijeljina *[Serbian language]*
[4] Law on Spas (Official Gazette of RS, No. 20/18)
[5] Law on Tourism (Official Gazette of RS, No. 45/17)
[6] Law on Hospitality (Official Gazette of RS, No. 45/17)
[7] Law on Tourist Tax (Official Gazette of RS, No. 78/11, 106/15)
[8] www.turizamrs.com
[9] Vasileva, V. (2017). The place of Balkan countries in world tourism. Socio brains, 29, 33 – 43
[10] Statistical bulletin - Tourism, No. 11. Republic Institute of Statistics, Republic of Srpska, Banja Luka (2015) *[Serbian language]*
[11] Statistical bulletin - Tourism, No. 12. Republic Institute of Statistics, Republic of Srpska, Banja Luka (2016) *[Serbian language]*
[12] Statistical Bulletin - Tourism, No. 13. Republic Institute of Statistics, Republic of Srpska, Banja Luka (2017) *[Serbian language]*
[13] Statistical bulletin – Tourism 2018. Republic Institute of Statistics, Republic of Srpska, Banja Luka (2018) *[Serbian language]*
[14] Statistical bulletin – Tourism 2019. Republic Institute of Statistics, Republic of Srpska, Banja Luka (2019) *[Serbian language]*
[15] https://www.banja-dvorovi.com

Original scientific article
http://dx.doi.org/10.59456/afts.2023.1528.077L

THERMAL COMFORT IN BELGRADE, SERBIA: UTCI-BASED SEASONAL AND ANNUAL ANALYSIS FOR THE PERIOD 1991-2020

Lukić Milica[1], Đurić Dijana[2]

[1]*University of Belgrade - Faculty of Geography, Belgrade, Serbia, email: micalukic92@yahoo.com*
[2]*University of Novi Sad - Faculty of Civil Engineering, Subotica, Serbia*

ABSTRACT

The main goal of this research is to examine thermal comfort in the central area of Belgrade (Serbia), over a period of 30 years (1991-2020). The Universal Thermal Climate Index (UTCI) was used as a measure for evaluating outdoor thermal comfort (OTC). The obtained results were considered separately for each season, as well as at the annual level. The analysis was carried out on the basis of an extensive database, which included hourly values (7h, 14h, 21h CET) of meteorological parameters, as well as their average daily, minimum, and maximum values.

The obtained values of UTCIs show a positive growth trend during all four seasons. A significant increase in the annual values of UTCIs was also recorded. Four of five years with the highest average UTCIs were recorded in the last decade of the survey, more precisely in the period 2015-2020. The years that stand out for the frequency of record spring, autumn and winter UTCIs values are 2017, 2018, 2019 and 2020. On an annual level, minimum UTCI value has rising trend of 0.099°C/year, while at maximum UTCI value, that trend is 0.081°C/year.

Key words: *UTCI, Belgrade, outdoor thermal comfort, seasonal analysis*

INTRODUCTION

The impact of climate change on the quality of life and the sustainability of urban environments has been the subject of scientific research for decades. It is clear that human society is in a very challenging period, where every new IPCC report only further emphasizes the danger of the climate crisis, while in practice hardly anything is really done to mitigate the impact of climate change. Developing countries that are trying to make up for their economic development deficit (like Serbia) are particularly at risk. The pressure of the global economy, markets and capital is leading to an explosion in the construction and expansion of cities. Climatic and morphological transformations of urban areas take place in parallel. A similar scenario is unfolding in the Serbian capital (city of Belgrade).

The urbanization of Belgrade has received a special acceleration in recent years. According to Mitić-Radulović et al., construction in Belgrade has significantly intensified in recent years: 30% of all construction works in Serbia in 2020 were performed in Belgrade. In the period 2016-2020 number of apartments built per year increased by 70%. In the same time, the annual value of construction work increased by 105%, and the number of square meters of high-rise buildings built per year increased by

350% [1,2,3]. The transformation of Belgrade's landscape further enhanced the impact of climate change [3].

Although the link between urban planning, microclimate, and outdoor thermal comfort (OTC) has been scientifically proven (e.g. studies conducted for Valladolid (Spain), Nanjing (China), Sao Paolo (Brasil), Cairo (Egypt), Hanover (Germany), Sydney (Australia), Bursa (Turkey), etc.) [4,5,6,7,8,9,10], such practice is not represented in the local context. In the planning of the urban development of Belgrade, consideration of OTC as one of the significant indicators is still not represented, unlike some other European metropolises where different concepts of bioclimatic urban design are applied.

Given that the average summer temperature at Belgrade increases at the rate of 0.1316◦C/year [11], local urban planners must take into account changes in the local microclimate and thermal comfort if they want to develop the city in a way that is ready to respond to the challenges of the coming climate crisis.

The aim of this research is to show how the Belgrade's microclimate and OTC have changed during three decades (1991-2020), during which the morphology of the city also changed significantly, and during which we recorded some of the warmest years since meteorological measurements have been made in Serbia (according to Republic Hydrometeorological Service of Serbia). The analysis of thirty-year thermal comfort using the bioclimatic index Universal Thermal Climate Index (UTCI) will give a useful insight into the current situation, as well as indications of what changes we can expect in the future. The results of this work may be of importance for the improvement of the domestic practice of urban planning.

STUDY AREA

Belgrade, the capital of Serbia, is located in the area of South-Eastern Europe (Balkan Peninsula), and belongs to the region of the Western Balkans countries [12]. City lies on the Sava and Danube river bank, near the Mountain Avala (511m) [13,14]. According to the Köppen-Geiger climate classification, Belgrade's area belongs to the Cfa type which is characterized by the humid subtropical climate [14,15,16]. Geographically speaking, the region of Southeast Europe has been recording an evident increase in average annual temperatures for years. This has been confirmed by numerous scientific studies, and the same growth tendencies are recorded in this region. As Milovanović et al. and Tošić et al. have stated: the mean annual temperature in Belgrade for the 1961–2010 period was 12.3°C, while during the 2000–2017 period that value was 13.4°C [17,18]. The average air temperature in the first decade of the 20th century was 11.3°C, while in the last decade, it was 12.5°C [12]. In addition, Belgrade is characterized by the existence of an urban heat island [12,16].

METHODOLOGY

Universal Thermal Climate Index (UTCI)

Within the project of the International Society of Biometeorology (ISB) and framework of the European COST Action 730, the UTCI has been made available as an operational procedure by which to assess the outdoor thermal environment from the point of view of the core fields of human biometeorology [19]. By searching databases containing scientific papers from the most representative and reputable scientific journals, we can simply conclude that this index stands out as one of the most commonly used in the evaluation of outdoor thermal comfort.

Błażejczyk et al. in their research titled "An introduction to the Universal Thermal Climate Index (UTCI)", have defined UTCI (°C) as "the air temperature of the reference condition causing the same model response as actual conditions"[20]. UTCI was obtained from the "Fiala multi-node model", developed by Fiala et al. [21-23]. As this index is an indicator of thermal comfort, it considers both

meteorological and physiological parameters describing thermal comfort through the assessment of human energy balance [20,22,24].

This model includes 10 different categories of thermal stress, which are presented in Table 1. The UTCI is calculated as follows: UTCI = f (t, f, v10m, Tmrt)

Where: t = air temperature (°C), f = relative humidity (%), v10m = wind speed (m/s), Tmrt = mean radiant temperature (°C). Tmrt was calculated using the BioKlima 2.6 software [25].

Table 1. UTCI scale and corresponding physiological responses [16,20-22]

UTCI (ºC)	Stress category	Physiological responses
UTCI > 46	Extreme heat stress	Increase in rectal temperature time gradient. Steep decrease in total net heat loss. Averaged sweat rate >650 gh^{-1}, steep increase.
38 < UTCI < 46	Very strong heat stress	Low core–skin temperature gradient. Increase in rectal temperature at 30 min.
32 < UTCI < 38	Strong heat stress	Averaged sweat rate >200 gh^{-1}. Increase in rectal temperature at 120 min. Instantaneous change in skin temperature.
26 < UTCI < 32	Moderate heat stress	Change of slopes in sweat rate and rectal and skin (mean, face, hand) temperature. Occurrence of sweating at 30 min. Steep increase in skin wettedness.
9 < UTCI < 26	No thermal stress	Averaged sweat rate >100 gh^{-1}. Plateau in rectal temperature time gradient.
0 < UTCI < 9	Slight cold stress	Local minimum of hand skin temperature.
-13 < UTCI < 0	Moderate cold stress	Vasoconstriction. Face skin temperature at 30 min <15°C (pain).
-27 < UTCI < -13	Strong cold stress	Numbness. Increase in core–skin temperature gradient.
-40 < UTCI < -27	Very strong cold stress	Frostbite, numbness, shivering. Steeper decrease in rectal temperature.
UTCI < -40	Extreme cold stress	Frostbite. Decrease in rectal temperature time gradient.

Data set and software used in the study

Determination of UTCIs was conducted based on an hourly (07:00, 14:00, 21:00 CET) and "day by day" meteorological data set. Apart from the hourly values, average daily (avg.), minimum (min), and maximum (max) values of meteorological parameters were also used. The data set was extracted from the Republic Hydrometeorological Service of Serbia (RHSS), ie. from the Meteorological Yearbooks 1991-2020 [26]. Meteorological data were collected on the Meteorological Observatory Belgrade (44°48′ N, 20°28′ E, 132 m), located in the most densely populated part of Belgrade, called Vračar. The data collected in such conditions best describe the thermal comfort of the central city core [16].

Meteorological parameters which were used are: air temperature (t), relative humidity (f), wind speed (v10m) at 10m above the ground, total cloud cover (N or cloudiness) and air pressure (p). The UTCI was calculated by the BioKlima 2.6 software [25], developed by Prof. K. Błażejczyk, PhD.

For the purposes of seasonal analysis of thermal comfort, the obtained data are grouped into four seasons: spring (March, April, May), summer (June, July, August), autumn (September, October, November) and winter (December, January, February) in accordance with the Meteorological division of the seasons. After that, the results were processed and presented on the annual basis.

RESULTS AND DISCUSSION

The results are presented individually for all four seasons, as well as on an annual basis. Outdoor thermal comfort was estimated through six different UTCIs: UTCI07h (morning data values at 07:00 CET), UTCI14h (midday data values at 14:00 CET), UTCI21h (evening data values at 21:00 CET), UTCIsr (average daily values), UTCImax (maximum daily temperature was used) and UTCImin (maximum daily temperature was used).

Frequencies of different cold and heat stress are shown on the Figure 1-4, while trends are shown on Figures 1,2,3,4,5.

Thermal comfort in Belgrade: spring 1991-2020

The results of this study confirm the results of previously conducted scientific research on the topic of the urban bioclimate and thermal comfort of Belgrade. Regarding OTC, spring is rated as the most favorable part of the year for being outdoors [12,16,17]. Figure 1. shows frequencies of different cold and heat stress (according to the UCTI scale) in the Belgrade center. From left to right, results are shown for UTCI07h, UTCI14h, UTCI21h, UTCIsr (average), UTCImax, and UTCImin.

The prevalent category of spring OTC in Belgrade is the one marked as "no thermal stress" (NTS, Figure 1, green color), where the value of UTCI is in range from 9°C to 26°C. The pleasant feeling of being outdoors is mainly present during the morning hours (UTCI07h).

The NTS category takes a 60.5% share in the total number of days for UTCI07h. For UTCI14h and UTCImax we see a greater participation of next heat stress categories: MHS (moderate heat stress, 26<UTCI<32) and SHS (strong heat stress, 32<UTCI<38).

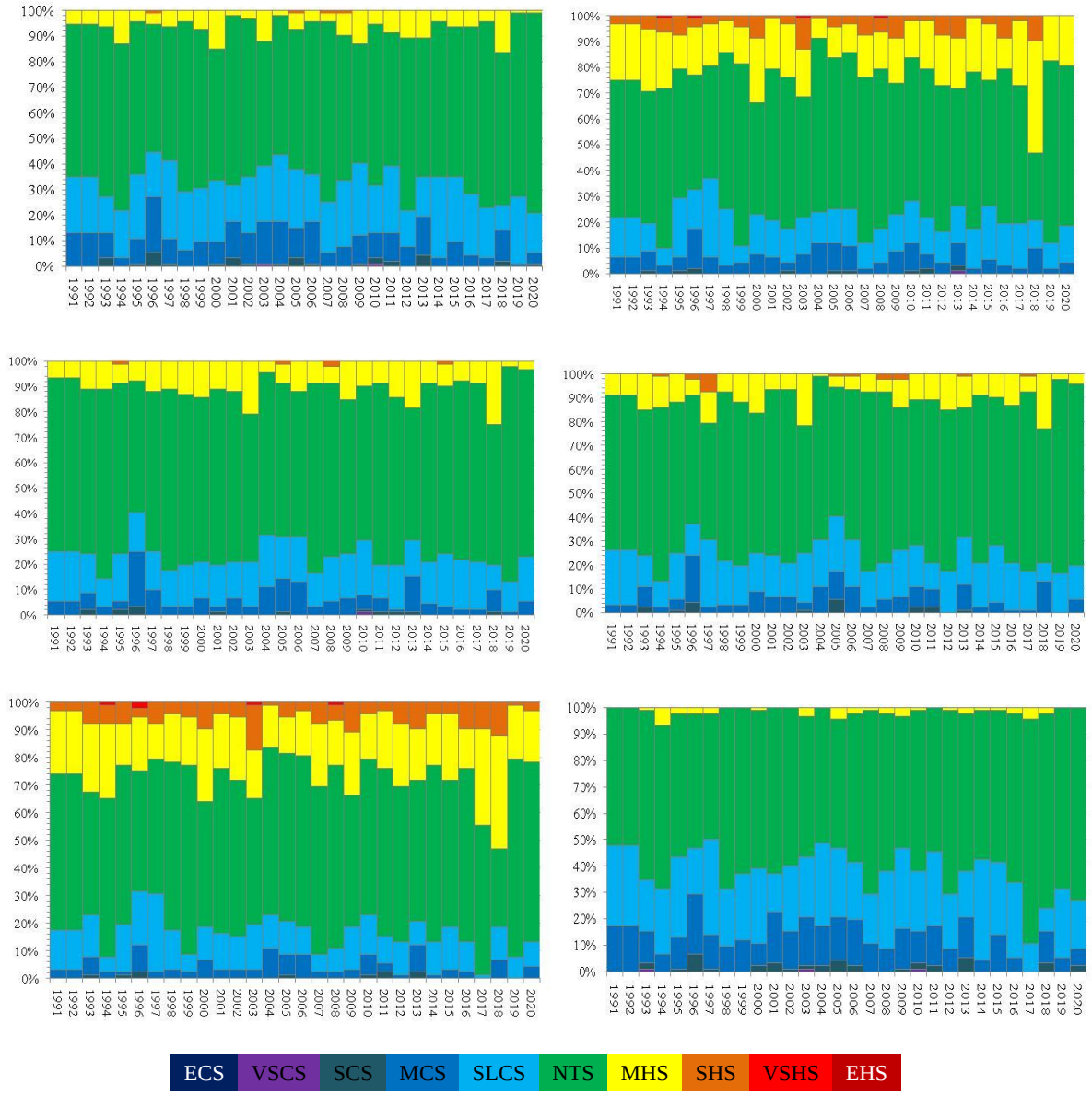

Figure 1. Frequencies of different cold and heat stress in Belgrade center; UTCI 07h, UTCI 14h, UTCI 21h, UTCIsr (average), UTCImax, and UTCImin during **spring**, over a period of 30 (1991-2020)

In Figure 2, we can clearly see that each of the spring UTCIs records a positive trend. The most pronounced positive trend has UTCImin (light blue color), where that trend is 0.101°C/year or 1.01°C/decade. It is followed by UTCImax (red color), where the recorded trend amounts to 0.083°C/year. The maximum spring UTCI value was registered in 2017 (UTCImax = 24.49°C).

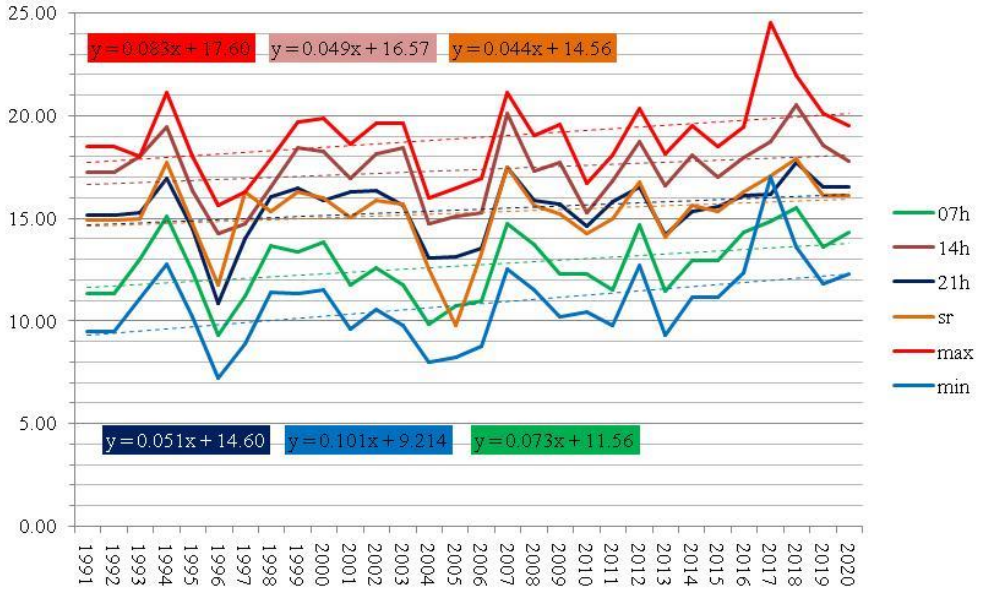

Figure 2. Average spring UTCI at: 7h, 14h, 21h CET, average daily value UTCI (sr), minimum UTCI (min) and maximum UTCI (max), Belgrade 1991-2020

Thermal comfort in Belgrade: summer 1991-2020

Figure 3. shows frequencies of different cold and heat stress during summer 1991-2020 in Belgrade. From left to right, results are shown for all six UTCIs again. It was once again confirmed that summer is the most unfavorable part of the year in terms of OTC, when the most pronounced temperature extremes (high temperatures, heat waves) occur [1213,14,16,17,18,24].

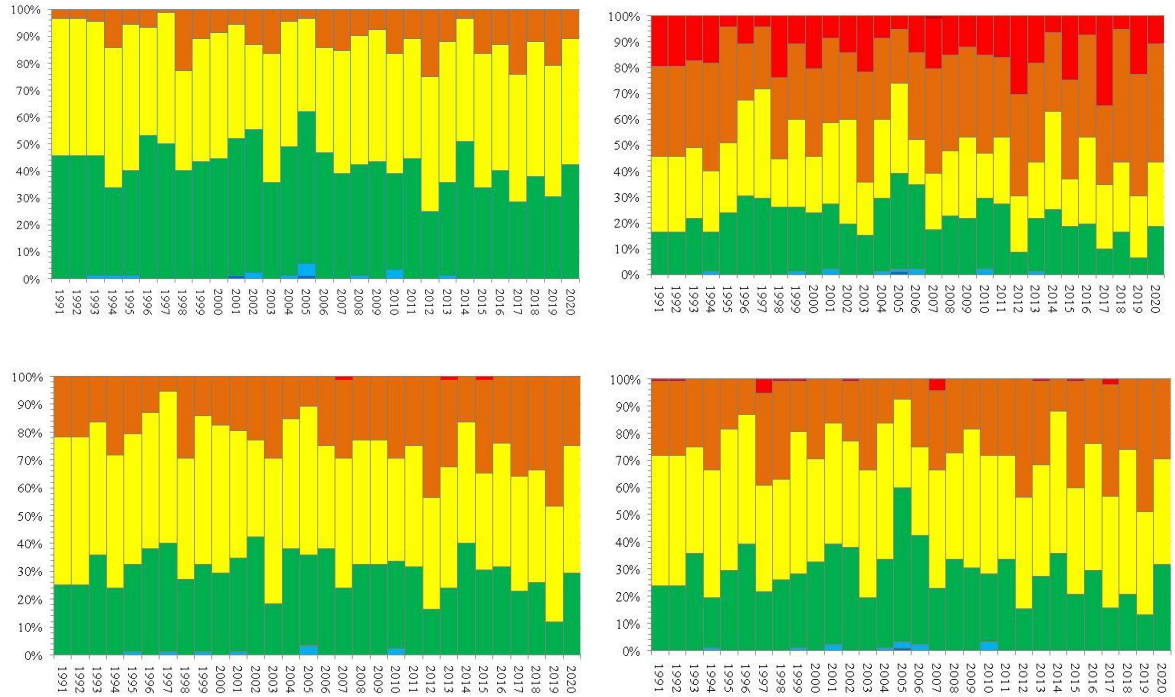

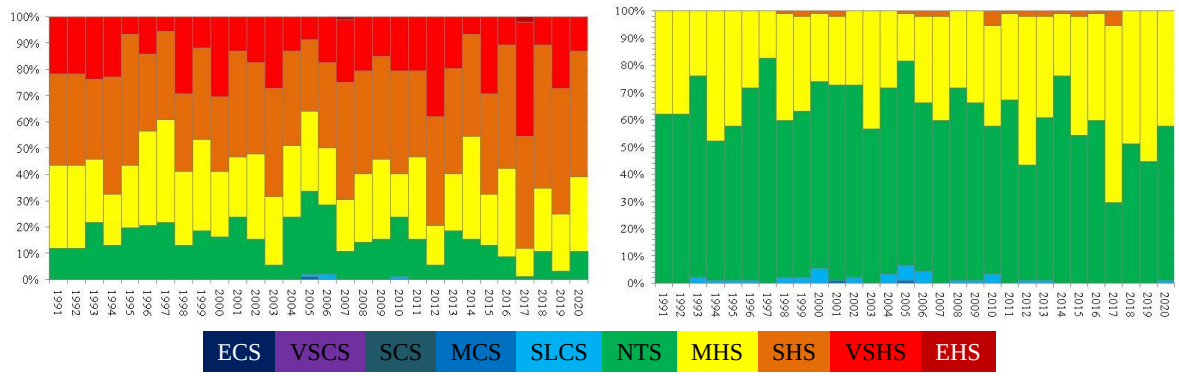

Figure 3. Frequencies of different cold and heat stress in Belgrade center; UTCI 07h, UTCI 14h, UTCI 21h, UTCIsr (average), UTCImax, and UTCImin during summer, over a period of 30 (1991-2020)

If we look at the three decades of the researched period separately (1991-2000; 2001-2010 and 2011-2020) on Figure 3. we can clearly see that the number of days in higher categories of thermal stress (especially MHS, SHS and VSHS) increases from decade to decade (regardless of which of the 6 different UTCIs we are considering). UTC14h records the largest share of days when OTC could be described as "strong heat stress" with 35% such days during 30 years. For UTCImax and SHS that share amounts to 38.5%. Frequency of MHS category for UTCI14h is 27.4%, and for UTCImax is 26.4%. VSHS category (very strong heat stress, 38<UTCI<46) covers 19.5% of the total number of days for UTCImax, and 15.4% for UTCI14h.

The increase in summer air temperatures affects the increase in the value of the UTCI index, which was confirmed by research. A positive trend is noted for all summer UTCIs (Figure 4). Again, the most pronounced positive trend has UTCImin (light blue color), and it is 0.081°C/year. In second place is UTCImax (red color), with an increasing trend of 0.068°C/year. The maximum summer UTCI was 37.22°C, and it was registered in 2017.

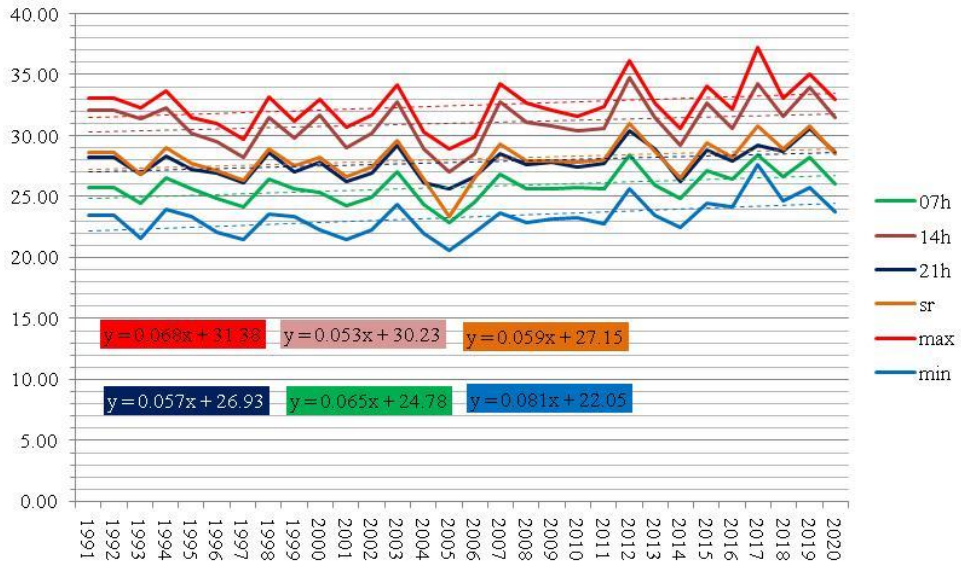

Figure 4. Average summer UTCI at: 7h, 14h, 21h CET, average daily value UTCI (sr), minimum UTCI (min) and maximum UTCI (max), Belgrade 1991-2020

Thermal comfort in Belgrade: autumn 1991-2020

Thermal comfort during the autumn months is most similar to the spring, but still with a clear difference, due to the greater number of days with cold stress: SLCS (slight cold stress) and MCS (moderate cold stress). However, as the years go by, the number of days in the categories belonging to

cold stress decreases, while the number of days with higher values of thermal stress increases (Figure 5). This applies to all 6 sub-indices (UTCI07h, UTCI14h, UTCI21h, UTCIsr (average), UTCImax, and UTCImin). If we look at the percentage participation, days without thermal stress dominate (NTS, green color, Figure 5). Regarding the UTCI14h and UTCImax sub-indexes, during the last decade of the researched period, an increase in days belonging to the VSHS category was recorded. This indicates an increase in UTCI values during the autumn months.

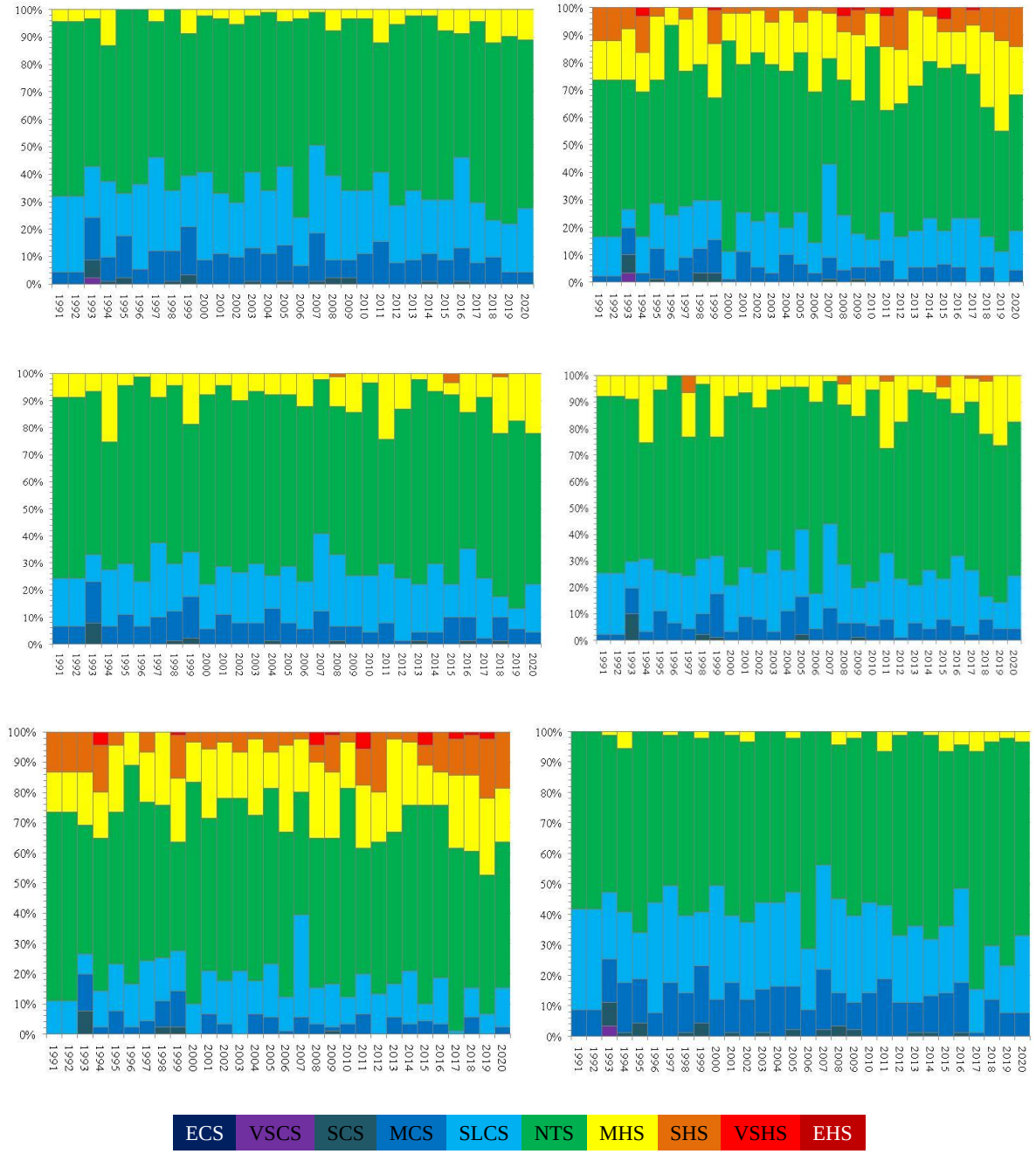

Figure 5. Frequencies of different cold and heat stress in Belgrade center; UTCI 07h, UTCI 14h, UTCI 21h, UTCIsr (average), UTCImax, and UTCImin during autumn, over a period of 30 (1991-2020)

As with the previous two seasons, very similar results are recorded when it comes to autumn. UTCImin records the highest positive trend again (0.141°C/year). During the autumn months, there is an increase in all UTCI values, especially in the morning hours (UTCI07h, trend is 0.108°C/year).

Next is UTCImax, with the rising trend of 0.104°C/year. The maximum autumn UTCI value was registered in 2019 (UTCImax = 23.54°C), Figure 6.

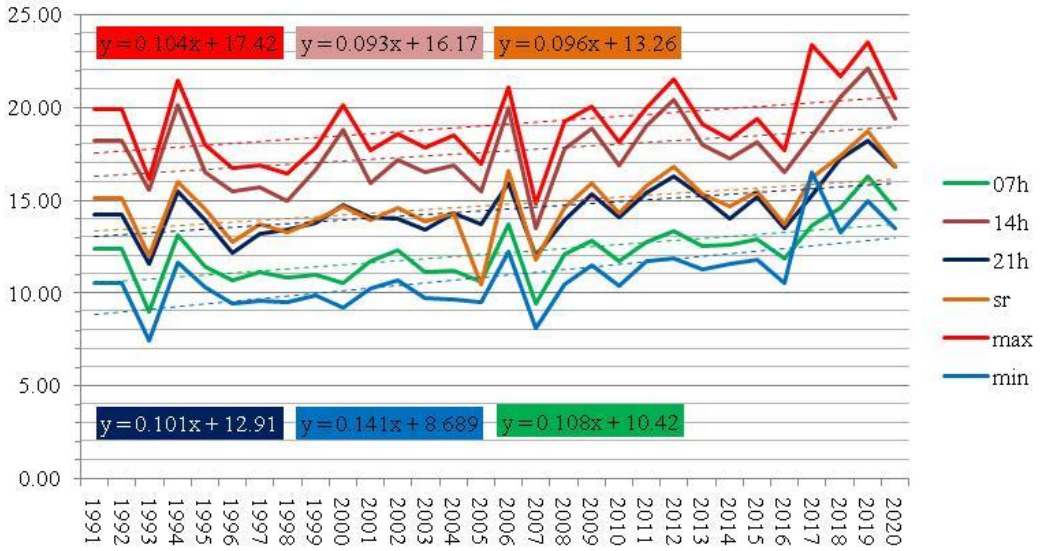

Figure 6. Average autumn UTCI at: 7h, 14h, 21h CET, average daily value UTCI (sr), minimum UTCI (min) and maximum UTCI (max), Belgrade 1991-2020

Thermal comfort in Belgrade: winter 1991-2020

If we carefully look at Figure 7, we can see that the winter in Belgrade is getting milder and warmer. The average winter air temperature in Belgrade grows at the rate of 1.95°C/100 years [27]. It directly affects the growth of UTCI values and changes in outdoor thermal comfort. When we consider OTC in the central areas of Belgrade, on Figure 8. we can clearly see that the most significant changes in this thirty-year period took place precisely during the winter months. A positive trend is noticeable in all winter UTCIs. This is especially noticeable after the winter of 2012/13. Winter UTCImin records the highest positive trend (0.070°C/year). The winter of 2019/20 proved to be the warmest (regarding OTC) in this period (1991-2020) when the highest values of almost all UTCI were measured. The maximum winter UTCI value was registered during winter 2019/20 (UTCImax = 8.40°C).

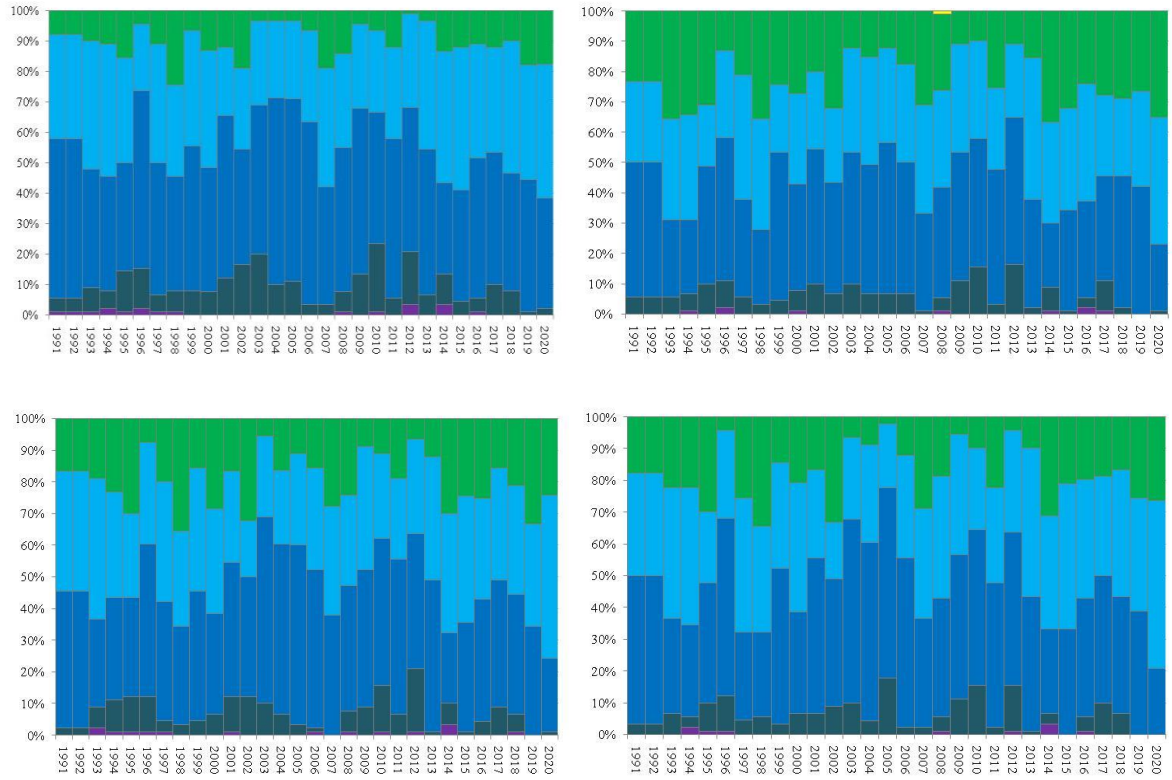

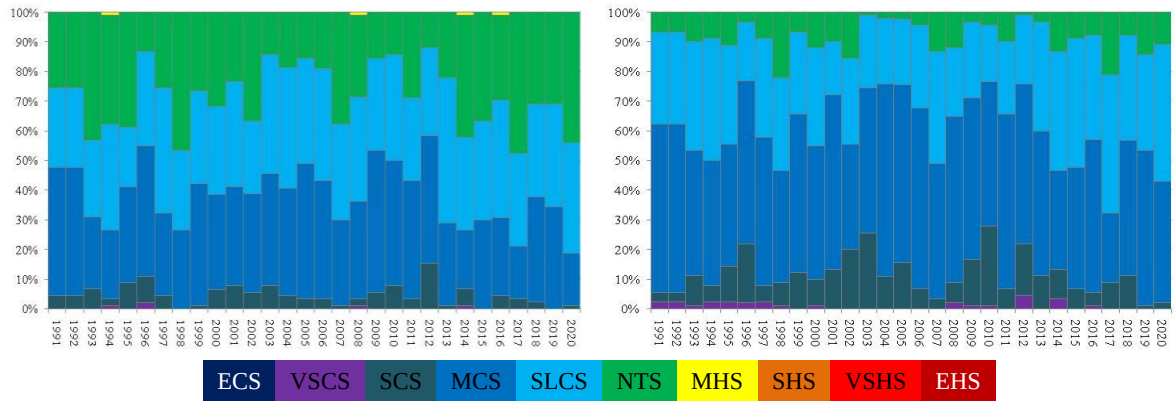

Figure 7. Frequencies of different cold and heat stress in Belgrade center; UTCI 07h, UTCI 14h, UTCI 21h, UTCIsr (average), UTCImax, and UTCImin during **winter**, over a period of 30 (1991-2020)

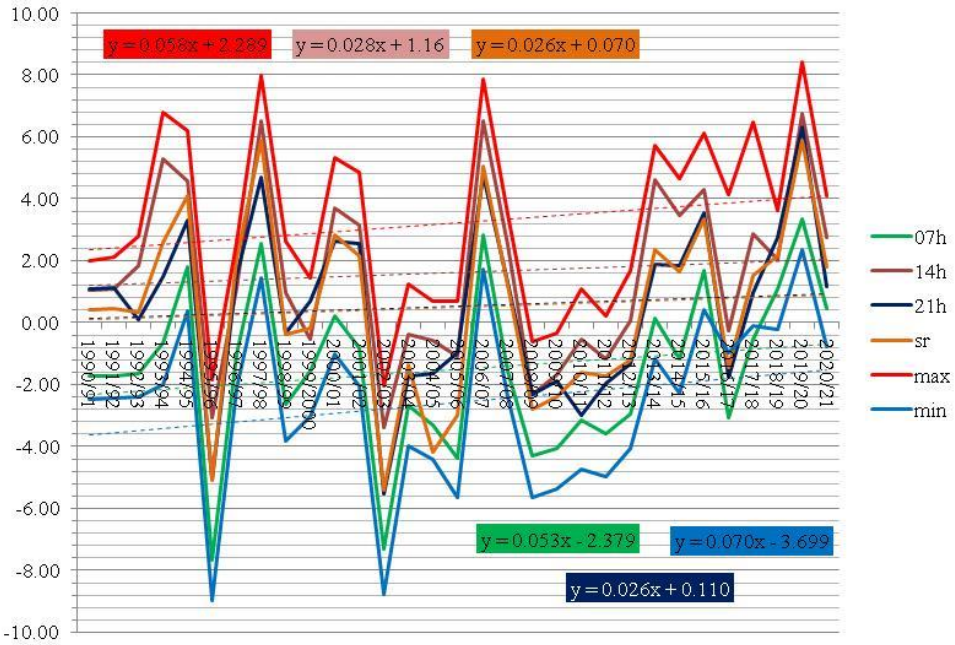

Figure 8. Average winter UTCI at: 7h, 14h, 21h CET, average daily value UTCI (sr), minimum UTCI (min) and maximum UTCI (max), Belgrade 1991-2020

Thermal comfort in Belgrade: annual analysis

Table 2. presents the average annual values of the bioclimatic index UTCI in Belgrade during the period 1991-2020. The values for each of the considered UTCIs in this study are extracted for this purpose. In this way, we get a precise insight into the mean annual values for each UTCI. We can also see when the maximum values were recorded. It is clearly observed that the highest values are recorded at the end of the third decade of the researched period, i.e. in the period 2017-2020. The highest record values were recorded in 2019 and 2017. The continuous increase in air temperature in Belgrade, which is accompanied by the increase in the UTCI value, indicates that we can expect such trends in the coming years as well.

Table 2. Average annual values UTCIs in Belgrade, 1991-2020
(five highest recorded avg. annual values are highlighted in red)

Year	**1991**	**1992**	**1993**	**1994**	**1995**	**1996**	**1997**	**1998**	**1999**	**2000**
07h	11.89	12.00	11.60	13.62	12.15	9.75	11.53	13.04	12.34	12.35
14h	16.90	17.25	17.39	19.12	16.44	14.20	15.24	17.25	16.52	17.62
21h	14.01	14.76	13.86	15.56	14.21	11.69	13.75	15.65	14.58	15.25

avg.	14.22	14.85	14.15	16.32	14.66	12.01	13.51	15.46	14.63	15.18
max	17.91	18.47	18.00	20.53	17.93	15.54	16.66	18.73	18.04	19.05
min	9.98	10.32	9.69	11.74	10.34	7.92	9.63	11.19	10.55	10.34
Year	**2001**	**2002**	**2003**	**2004**	**2005**	**2006**	**2007**	**2008**	**2009**	**2010**
07h	11.33	12.11	11.41	10.54	10.17	11.78	13.06	12.56	11.84	11.21
14h	15.62	17.21	16.66	15.19	14.20	16.26	17.65	17.22	16.53	15.06
21h	14.01	14.73	13.77	13.14	12.88	14.00	15.32	14.69	14.51	13.26
avg.	13.81	14.84	14.12	13.06	9.56	14.14	15.46	14.86	14.35	13.32
max	17.33	18.61	18.02	16.64	15.75	17.62	18.93	18.70	18.03	16.44
min	9.40	10.23	9.55	8.76	8.40	9.99	11.12	10.65	10.03	9.37
Year	**2011**	**2012**	**2013**	**2014**	**2015**	**2016**	**2017**	**2018**	**2019**	**2020**
07h	12.26	12.72	12.22	12.61	13.39	13.10	13.81	14.15	14.94	14.39
14h	17.09	17.74	17.12	17.21	18.14	16.86	18.29	18.79	19.52	18.64
21h	14.68	14.83	14.67	14.47	15.54	14.93	15.10	16.29	17.37	16.64
avg.	14.93	15.23	14.78	14.75	15.84	14.91	16.05	16.44	17.26	16.59
max	18.43	19.05	18.43	18.45	19.46	18.39	23.30	20.20	20.94	20.12
min	10.51	10.88	10.44	10.99	11.75	11.36	15.75	12.54	13.20	12.81

Figure 9. shows the annual trend for each UTCI and each year of the researched period (1991-2020). As expected, the highest positive trend was recorded with the UTCImin index (trend is 0.099°C/year). Next is UTCImax with a positive trend of 0.081°C/year, followed by UTCI07h (0.073°C/year). The lowest rising rate (but still not negligible) amounts to 0.054°C/year for UTCI14h.

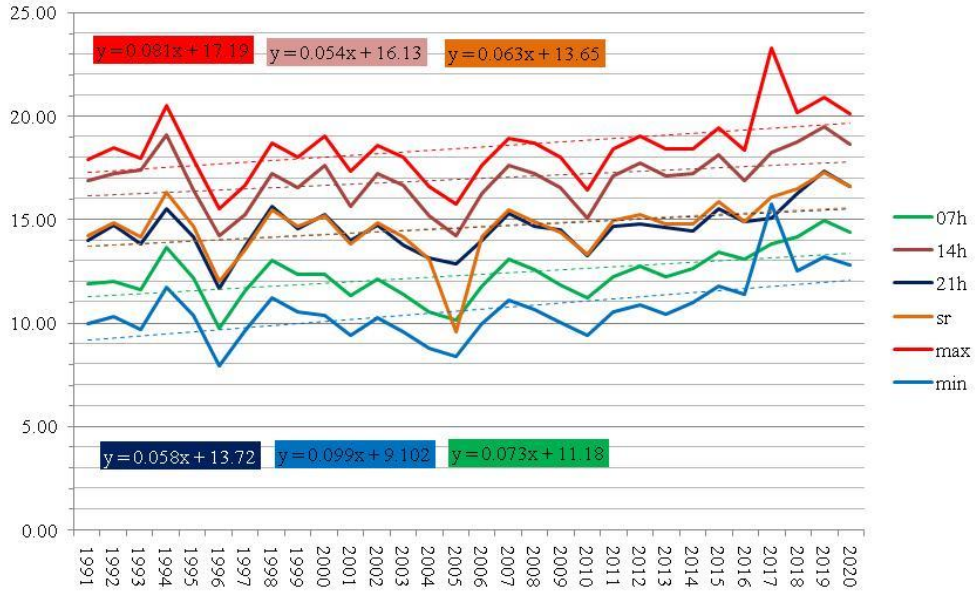

Figure 9. Average **annual** UTCI at: 7h, 14h, 21h CET, average daily value UTCI (sr), minimum UTCI (min) and maximum UTCI (max), Belgrade, 1991-2020

CONCLUSION

The aim of this research was to analyze thermal comfort outdoors in the central area of Belgrade, over a period of 30 years (1991-2020). The obtained results were considered on a seasonal and annual level, and the UTCI bioclimatic index was used for the analysis, which proved to be one of the most optimal and most frequently used in modern scientific research.

Belgrade has changed tremendously in recent decades. Urbanization is pronounced, and the morphological structure of the city has taken on entirely new contours. At the same time, due to the reduced share of green areas (only 2.83% of public green areas in the central part of the city), and the increasing dominance of artificial materials used in construction (concrete, asphalt, steel), Belgrade's urban heat island is becoming more pronounced. Parallel, the impact of climate change as a global phenomenon on the microclimate of the city is obvious. Average summer temperature in Belgrade increases at the rate of 0.1316◦C/year, while the average winter air temperature grows at the rate of 1.95°C/100 years. In such changed conditions, it is highly important to take OTC into account when planning the city. The results of this research show that changes are present and constant, and everything indicates that they will continue in the same direction.

All six considered sub-indices show a positive rising trend. On an annual level, UTCImin has rising trend of 0.099°C/year, while UTCImax has trend of 0.081°C/year. For spring 1991-2020, the most pronounced positive trend has UTCImin (0.101°C/year) and UTCImax (0.083°C/year). For summer 1991-2020, the most pronounced positive trend has UTCImin (0.081°C/year) and UTCImax (0.068°C/year). The biggest changes were recorded during the autumn months. Autumn UTCImin records the highest positive trend of all: 0.141°C/year, which is actually the highest rate of growth in this thirty-year period. Winter in Belgrade is getting milder and warmer, and the winter of 2019/20 proved to be the warmest (regarding OTC) during the period 1991-2020. Four of five years with the highest average UTCIs were recorded in the last decade of the survey, more precisely in the period 2015-2020 (especially 2017, 2018, 2019 and 2020).

Acknowledgements: The study was supported by the Ministry of Education, Science and Technological Development of the Republic of Serbia (Contract number 451-03-68/2022-14/200091).

Received March 2023, accepted March 2023)

LITERATURE

[1] Mitić-Radulović, A., Lukić, M., Simić, A. (2022a). Ecological index as an instrument of Belgrade's adaptation to climate change. Collection of works "Local self-government in planning and arrangement of space and settlement". Belgrade: Association of Spatial Planners of Serbia, Faculty of Geography, p. 123-130. *[Serbian language]*

[2] Mitić-Radulović, A., Simić, A., Ljubić, S. (2022b). Possibilities of applying the ecological index in the planning of Belgrade. Belgrade: Center for Expertise and Urban Studies - CEUS. *[Serbian language]*

[3] *Lukić, M., Lukić, A. (2022). Outdoor thermal comfort as an indicator of the "Belgrade Green City" concept - advantages and applications. Proceedings of the 4th International Conference on Urban Planning – ICUP 2022. Niš: University of Niš - Faculty of Civil Engineering and Architecture, pp 173-180, ISBN 978-86-88601-74-0*

[4] Madeco Alves, F. et al. (2022). The use of Envi-Met for the Assessment of Nature-Based Solutions' Potential Benefits in Industrial Parks - A Case Study of Argales Industrial Park (Valladolid, Spain). Infrastructures 7, 85, https://doi.org/10.3390/infrastructures7060085

[5] Rui, L., Buccolieri, R., Gao, Z. et al. (2019). Study of the effect of green quantity and structure on thermal comfort and air quality in an urban-like residential district by ENVI-met modelling. Build. Simul, 12, pp 183–194, https://doi.org/10.1007/s12273-018-0498-9

[6] Carfan, A. Galvani, E., Nery J. (2012). Study of thermal comfort in the City of São Paulo using ENVI - met model. Investigaciones geográficas, 78.

[7] Fahmy, M., Sharples, S. (2009). On the development of an urban passive thermal comfort system in Cairo, Egypt. Building and Environment, 44(9), pp 1907-1916, https://doi.org/10.1016/j.buildenv.2009.01.010

[8] Forouzandeh, A. (2021). Prediction of surface temperature of building surrounding envelopes using holistic microclimate ENVI-met model. Sustainable Cities and Society, 70, 102878, https://doi.org/10.1016/j.scs.2021.102878

[9] Abdollahzadeh, N., Biloria, N. (2021). Outdoor thermal comfort: Analyzing the impact of urban configurations on the thermal performance of street canyons in the humid subtropical climate of Sydney. Frontiers of Architectural Research, 10, pp 394–409, https://doi.org/10.1016/j.foar.2020.11.006

[10] Cetin, M. (2019). The effect of urban planning on urban formations determining bioclimatic comfort area's effect using satellitia imagines on air quality: a case study of Bursa city. Air Quality, Atmosphere & Health, 12, pp 1237–12, doi:10.26650/PB/PS12.2019.002.040

[11] Unkašević, M. Vujović, D., Tošić, I. (2005). Trends in extreme summer temperatures at Belgrade. Theor. Appl. Clim, 82, pp 199–205.

[12] Pecelj, M., Matzarakis, A., Vujadinović, M., Radovanović, M., Vagić, N.; Đurić, D., Cvetković, M. (2021). Temporal Analysis of Urban-Suburban PET, mPET and UTCI Indices in Belgrade (Serbia). Atmosphere, 12(7), 916, https://doi.org/10.3390/atmos12070916

[13] *Lukić, M., Milovanović, J. (2020). UTCI based assessment of urban outdoor thermal comfort in Belgrade, Serbia. Proceedings of the SINTEZA 2020 - International Scientific Conference on Information Technology and Data Related Research. Belgrade: Singidunum University, pp 70-77, https://doi.org/10.15308/Sinteza-2020-70-77,ISBN 978-86-7912-735-8*

[14] Lukić, M. (2019). An analysis of the influence of air temperature and humidity on outdoor thermal comfort in Belgrade (Serbia) using a simple heat index. Archives for Technical Sciences, No. 21 (1), pp 75-84, https://doi.org/10.7251/afts.2019.1121.075L

[15] Kottek, M., Grieser, J., Beck, C., Rudolf, B., Rubel, F. (2006). World map of the Köppen–Geiger climate classification updated. Meteorol. Z., 15(3), 259–263, https://doi.org/10.1127/0941-2948/2006/0130

[16] Lukić, M., Filipović, D., Pecelj, M., Crnogorac, Lj., Lukić, B., Divjak, L., Lukić, A., Vučićević, A. (2021). Assessment of Outdoor Thermal Comfort in Serbia's Urban Environments during Different Seasons. Atmosphere, 12, 1084, ISSN: 2073-4433, https://doi.org/10.3390/atmos12081084

[17] Milovanović, B., Radovanović, M., Schneider, Ch. (2020). Seasonal distribution of urban heat island intensity in Belgrade (Serbia). J. Geogr. Inst. Jovan Cvijić SASA, 70 (2), 163-170, https://doi.org/10.2298/IJGI2002163M

[18] Tošić, I., Mladjan, D., Gavrilov, M., Živanović, S., Radaković, M., Putniković, S., Petrović, P., Krstić Mistridželović, I., Marković, S. (2019). Potential influence of meteorological variables on forest fire risk in Serbia during the period 2000-2017. Open Geosci., 11, 414-425, https://doi.org/10.1515/geo-2019-0033

[19] Bröde, P.; Krüger, L.E.; Fiala, D. UTCI: validation and practical application to the assessment of urban outdoor thermal comfort. Geog. Pol 2013, 86 (1), 11-20. http://dx.doi.org./10.7163/GPol.2013.2

[20] Błażejczyk, K., Jendritzky, G., Brode, P., Fiala, D., Havenith, G., Epstein, Y., Psikuta, A., Kampmann, B. (2013). An introduction to the Universal Thermal Climate Index. Geogr. Pol 2013, 86 (1), 5-10, http://dx.doi.org./10.7163/GPol.2013.1

[21] *Bröde, P., Fiala, D., Błażejczyk., K., Holmér, I., Jendritzki, G., Kampmann, B., Tinz, B., Havenith, G. (2012). Deriving the operational procedure for the Universal Thermal Climte Index (UTCI) J. Biometeorol, 56 (3), 481-494.* https://doi.org/10.1007/s00484-011-0454-1

[22] *Błażejczyk, K., Kuchcik, M., Błażejczyk, A., Milewski, P., Szmyd, J. (2014). Assessment of urban thermal stress by UTCI – experimental and modelling studies: an example from Poland. Die Erde, 145 (1-2), 16-33,* https://doi.org/10.12854/erde-145-3

[23] *Blażejczyk, K., Epstein, Y., Jendritzky, G., Staiger, H., Tinz, B. (2012). Comparison of UTCI to selected thermal indices. Int. J. Biometeorol, 56 (3), 515-535,* https://doi.org/10.1007/s00484-011-0453-2

[24] *Pecelj, M., Lukić, M., Filipović, D., Protić, B., Bogdanović, U. (2020). Analysis of the Universal Thermal Climate Index during heat waves in Serbia. Nat. Hazards Earth Syst. Sci., 20, 2021–2036,* https://doi.org/10.5194/nhess-20-2021-2020

[25] *Institute of Geography and Spatial Organization Polish Academy of Science. Available online:* https://www.igipz.pan.pl/Bioklima-zgik.html *(accessed on 22nd February 2023)*

[26] Republic Hydrometeorological Service of Serbia (RHSS). Available online: http://www.hidmet.gov.rs/latin/meteorologija/klimatologija_godisnjaci.php (accessed on 03rd February 2023).

[27] Đorđević, S. (2008). Temperature and Precipitation Trends in Belgrade and Indicators of Changing Extremes for Serbia. Geog. Pannon., 12(2), 62-68, https://doi.org/10.5937/GeoPan0802062D